FHWA-ID-EIS-12-01-F

Weather Technical Report

Final Environmental Impact Statement

US-95 Thorncreek Road to Moscow

Project No. DHP-NH-4110(156);Key No 09294

Project # DHP-NH-4110 (156)
Key # 9294
Thorncreek Road to Moscow

Weather Analysis and Climate Study for US Highway 95, Thorncreek Road to Moscow, Four Proposed Alternatives: No-Build, W-4, C-3 and E-2

June 5, 2014

Prepared by
Russell J. Qualls, Ph.D., P.E.

Table of Contents

1 Introduction

This project was commissioned by the Idaho Transportation Department (ITD) in order to characterize spatial variation of aspects of climatic conditions within a three mile wide, and six mile long study area south of Moscow, Idaho, which is traversed by U.S. Highway 95 (hereafter, the "Study Area"), as shown in Figure 1.1 US95 Proximity Map. The study area is being evaluated with regard to possible realignment alternatives for US Highway 95, from Thorncreek Road to Moscow, in order to improve its drivability and safety. The primary variables of concern are precipitation, wind, fog, and air temperature as it relates to production of road ice and frost.

This report is a compilation and synthesis of several previous reports (Blackketter et al., 2006; Qualls and Zhao, 2005; Qualls, 2006; Qualls, 2012) and includes new data and analysis. The analysis has benefited from the input of citizens and organizations with an interest in this project. It describes on-site measurements and analysis which were carried out, and how the measurements relate to and describe variability across the study area. Satellite images provide high resolution views of the characteristic spatial distribution of snow in and around the study area. Measurements from a nearby long-term climatological station are used to place the on-site measurements in the context of the region's normal climate. Principles of physics, thermodynamics, and comparisons with similar processes and areas from scientific literature are presented to describe many of the observed climate and weather characteristics.

Study Objective

1. To characterize the general climate of the region using nearby long-term climatological measurements, 2. to characterize spatial and temporal variability of important weather and climate elements across the study area using on-site weather data, satellite images, and principles of physics, thermodynamics, and other published studies, and 3. to describe the relationship of this variability to relative safety of roadway alignment alternatives or groupings of roadway alternatives.

Executive Summary

- Spatial variability of weather exists across the study area.
- Weather-related accidents are predominantly associated with frozen surface conditions (i.e., snow/ice/slush).
- Most often when frozen surface conditions exist, they occur across the entire study area.
- Very few accidents are associated with wind and fog.
- The spatial distribution of weather-related accidents on the existing US95 from Thorncreek Road to Moscow is predominantly associated with the spatial distribution of road characteristics such as tight radii curves located downslope on hills, and ingress/egress associated with road junctions and driveways, rather than due to spatial distribution of weather.
- All proposed new alignments (i.e., W-4, C-3 and E-2) are designed in accordance with current AASHTO (American Association of State Highway Transportation Officials) standards, which are much safer than the existing US95.
- Because road characteristics, rather than the spatial distribution of weather, dominate the distribution of accidents, the prescribed AASHTO safety analysis of each of the proposed alternatives (Arnzen, 2013) should be taken at face value for the comparison of the accident safety of the proposed alternatives.

Figure 1.1 US95 Proximity Map

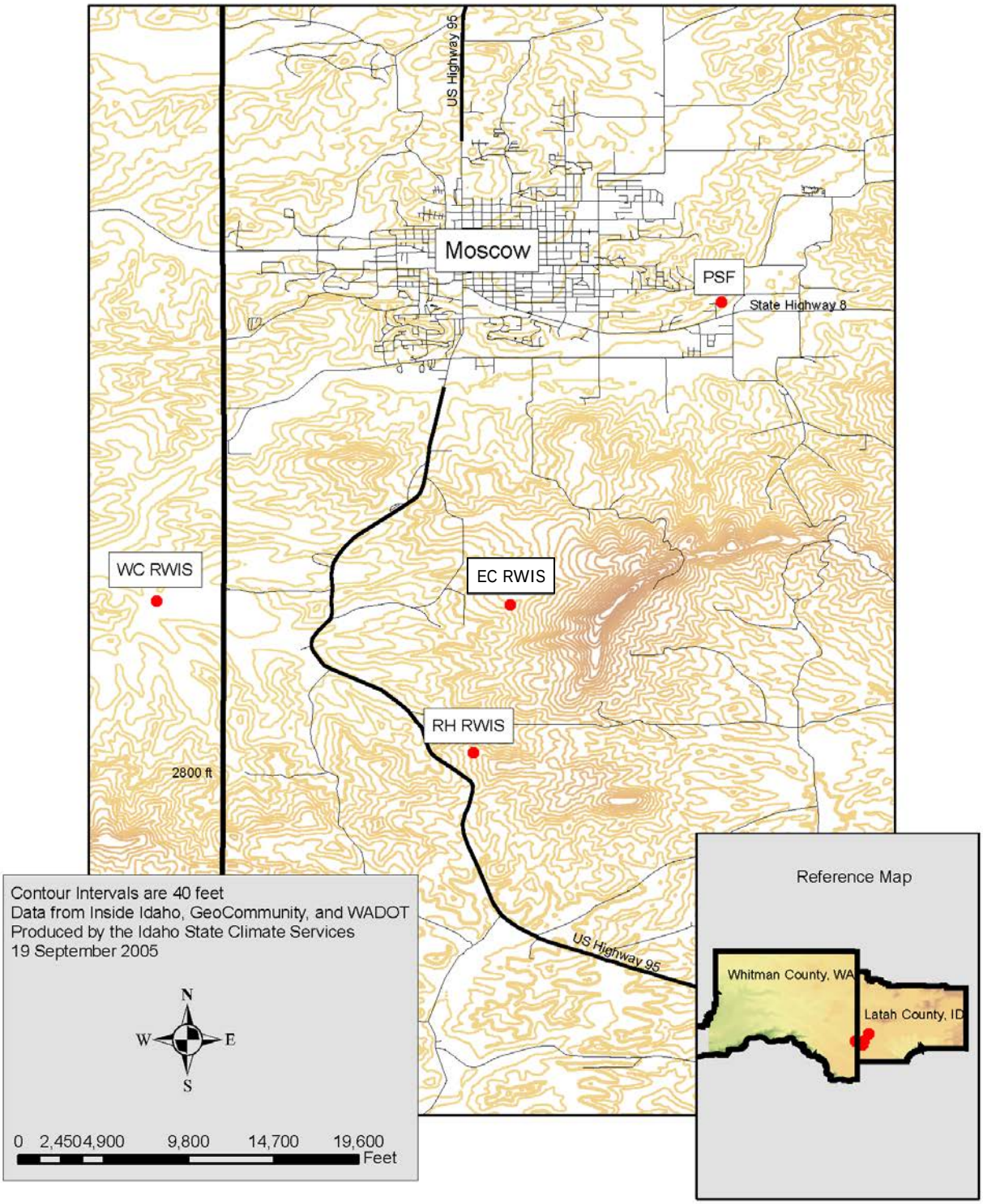

General Climate of Region

Northern Idaho, including Moscow, Idaho and surrounding areas, has a maritime, dry-summer climate (e.g, Abramovich et al, 1998). The area containing the existing US Highway 95 from Thorncreek Road to Moscow, and all of the proposed alternatives, is subject to this climate. Thus, it is unnecessary to establish the climate of the region or of any alternative roadway as though no prior knowledge existed; there is a lengthy history of climate information available as a reference for the region, such as data from the University of Idaho Plant Sciences Farm (PSF) located approximately one mile from the study area which extends back to 1892. Given the general climate of the region, what is needed is knowledge about the distinctions or variations among subareas of the study area. Therefore, the original study (Qualls and Zhao, 2005) and the follow on reports and studies had the objective, "to collect, and analyze weather data from within three anticipated climate regimes within the study area, *to compare and contrast the three areas* (Italics added)…"

These distinctions and variations among subareas are governed by physics, thermodynamics and similarity laws. Some of these are absolutes (e.g, dry adiabatic temperature lapse rate), and others include one or more parameters in their equations which may differ among the subareas (e.g., surface roughness for the wind speed profile). Even without prior knowledge of the value of these parameters, field measurements provide confirmation and insight about the nature of the relevant processes, and allow spatial comparisons to be made. A sampling of measurements over a limited time-frame that covers a relevant range of a meteorological variable, therefore, can be used to establish relationships among different subareas within the study area for that variable. Examples include proportionality relationships for wind speed, altitudinal gradients for precipitation, and altitude and cold air drainage relationships for temperature differences. Once established, these relationships can be used in their own right, or can be used in conjunction with nearby climatological data (e.g., from the University of Idaho Plant Sciences Farm climate station) to extend the record within the study area over the period of record of the nearby climate station.

Site Selection

Three climate regimes with generally continuous variation among them were anticipated based on orographic features present within and around the study area. The factors considered to be important were: a) elevation, and b) proximity to Paradise Ridge. Elevation was anticipated to influence the study area by means of adiabatic cooling of air with increasing elevation under neutral or unstable atmospheric conditions, such as experienced during windy conditions or on sunny days with strong convection, which was anticipated to increase precipitation with increasing elevation. Conversely, under stable atmospheric conditions, often experienced at night especially during periods of low wind speeds, elevation gradients can guide cold air drainage into low-lying areas producing an inversion with much colder temperatures in those low-lying areas compared to higher-elevation surrounding areas.

Figure 1.2 Study Area Map

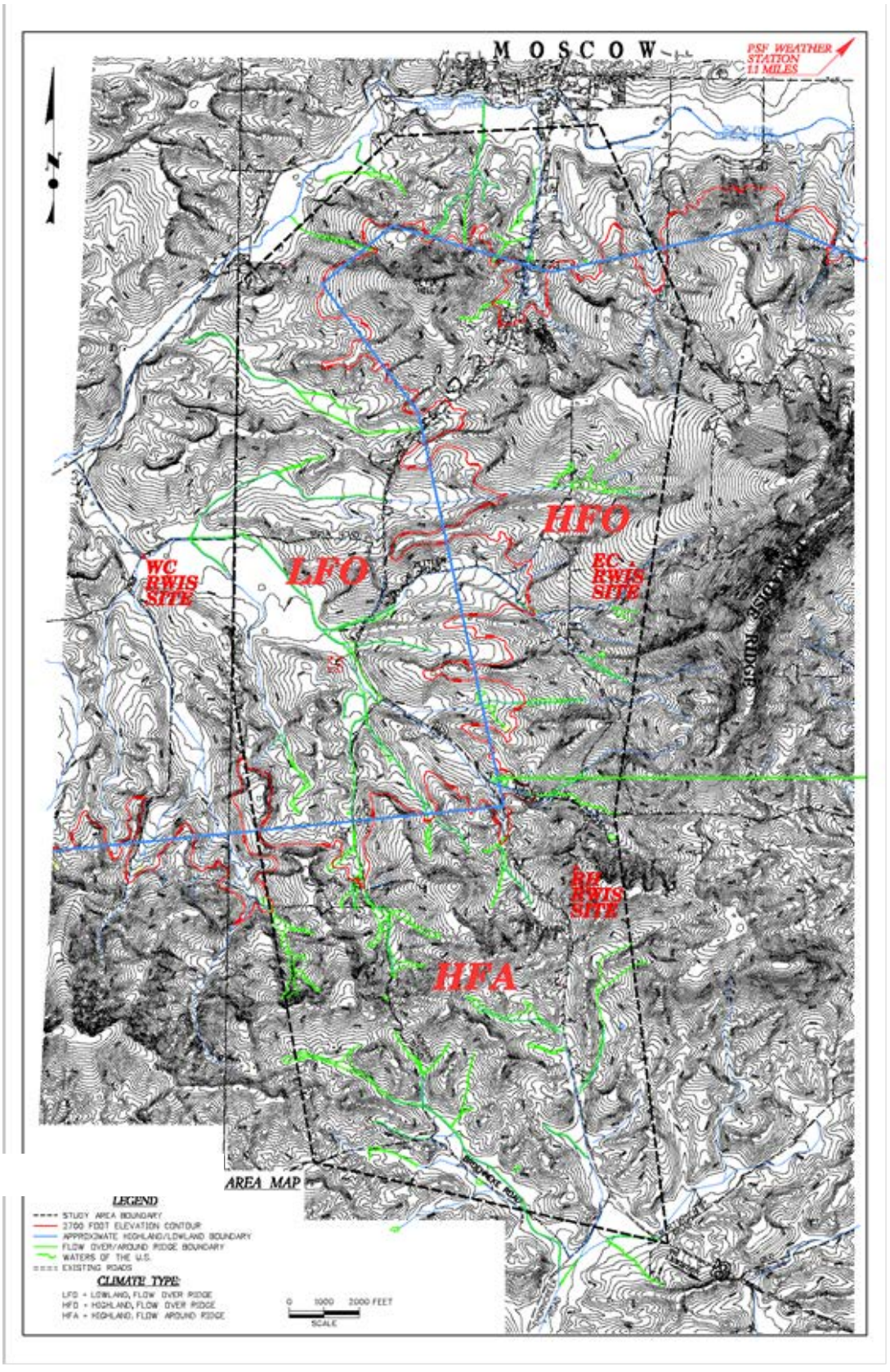

The topography of the region is shown in Figure 1.2 Study Area Map. Elevations within the study region range from a low of approximately 2540 feet above mean sea level (amsl) to a high of approximately 3000 feet amsl or slightly higher. For the most part, the southern third of the study area was dominated by elevations above approximately 2800 feet, and every possible alignment must attain an elevation above 2900 feet while traversing the southern third of the study area. Similarly the eastern corridor of the study area lies on rising ground, reaching a maximum elevation slightly above 3000 feet amsl, and remaining generally above 2800 feet amsl. The western corridor has some higher elevations exceeding 3000 feet amsl in the South, and also has a hill reaching 3000 feet amsl in the North, but drops below 2600 feet amsl in its central portion.

For the purposes of this study, lowland sites were considered to be areas lying below about 2600 feet amsl, and highland sites were considered to be areas above approximately 2800 feet amsl. In order to distinguish between lowland and highland sites, the 2700 foot amsl elevation contour has been highlighted in red on the Study Area Map, and then approximated by a series of line segments in blue. In order to capture the climate effects at the elevation extremes, it was determined that weather stations would be installed below 2600 feet and at or above 2900 feet.

In addition to these effects associated with absolute elevation of points within the study region, it was anticipated that proximity to Paradise Ridge could impose additional effects. Paradise Ridge lies outside and to the east of the study region. It runs roughly northeast to southwest, and reaches a maximum elevation of about 3703 feet amsl. Portions of the study region in the path of air flow moving over the top of Paradise Ridge experience different climate effects from portions of the study region whose air flow passes around Paradise Ridge, even for sites with the same elevation. This is due to the fact that air forced up over Paradise Ridge would cool as it was elevated, causing more water vapor to condense from the air. As a result, one might observe greater precipitation depths for sites whose airflow moved over Paradise Ridge, as opposed to sites whose airflow was able to move around Paradise Ridge.

The predominant air flow in the region is in the East-West direction. Given the extent of Paradise Ridge, this meant that the northern two-thirds of the study area was dominated by flow over Paradise Ridge, and the southern third of the study region generally experienced air flow which moved around the southern end of Paradise Ridge. The approximate demarcation between the flow-over versus flow-around portions of the study area is indicated by an east-west green line just to the south of Paradise ridge, as shown In Figure 1.2. The flow-over/flow-around demarcation continues westward from the green line along the blue-line-approximation to the 2700 foot elevation contour.

In the context of the study region, these two factors were combined into a matrix to stratify the study area to determine the number of sampling areas required, as shown on the next page.

The matrix indicates that three climate areas should be sampled. These are a "Lowland, Flow-Over Ridge" (LFO) area, a "Highland, Flow-Over Ridge" (HFO) area, and a "Highland, Flow-Around Ridge" (HFA) area. These regions are labeled on the Study Area Map. Accordingly, one climate station was established in each of the three climate regions of the study area. In the LFO area, a station was placed adjacent to Snow Road, west of the existing Highway 95. In the HFO area, a station was placed east of the existing Highway 95 on a bench butting up against the base of Paradise Ridge. Finally, an HFA station was located in the southern portion of the study area, slightly east of the existing Highway 95. The first two stations we refer to as the West Corridor (WC) Site and the East Corridor (EC) Site, respectively, in accordance with their position with respect to Highway 95. The third site in the south was located in the vicinity of Reisenauer Hill, near an existing cellular telephone tower, and we refer to it as the Reisenauer Hill (RH) Site. These stations are shown on the Study Area Map and a description of each of these sites is given below. A Central Corridor is referenced in this report, which runs in a north-south direction generally encompassing the existing US95 and the C alternatives. The West Corridor encompasses the W alternatives, and the East Corridor encompasses the East alternatives. These corridors are used to describe variations of weather and climate within the study area, and therefore do not have precise boundaries. Weather measurements were collected at the EC, WC and RH sites as point measurements. Weather and climate within the Central Corridor is determined either by interpolation between the WC and EC measurement sites, or by spatially and temporally distributed satellite observations. Existing and proposed alternatives represent lines through the corridors. Except in some cases with spatial data from satellites and historical accident records on the existing US95, no attempt is made in this report to specify weather or climate conditions exactly on a particular existing or potential roadway alignment, but rather the conditions within the general corridors are discussed.

	Highland	Lowland
Air Flow Over Paradise Ridge	√	√
Air Flow Around Paradise Ridge	√	None

Site Descriptions

West Corridor Site

The WC site is located in the LFO region of the study area, 30 feet south of Snow Road, with a latitude of N 46° 40' 38", a longitude of W 117° 03' 00" and an elevation of 2520 feet amsl. The tower was placed slightly west of the western edge of the study area for logistical reasons, and is slightly north of the middle of the study area in the north-south direction. It is part of a broad drainage valley flowing from the southeast from within the study area, and is no more than ten feet below the elevation of the drainage valley within the western edge of the study area. Thus, it is representative of low elevation drainage valleys within the study area. The surrounding terrain is flat in

the vicinity of the tower. One upstream tributary to the drainage channel flowing past the WC site, lies adjacent to the Eastern Corridor site, creating continuity of water and air flow between the two sites. About 100 feet to the east-northeast there is a large storage shed, and about 60 feet to the northwest there is a row of trees. Both of these obstructions could influence wind speeds when wind is coming from those directions, but would not influence any of the other variables measured including precipitation, visibility (fog), and temperature. The WC site represents the “lowland, air-flow-over-ridge” condition.

East Corridor Site

The EC site lies in the HFO area, on a southwesterly facing bench, on the eastern edge of the study area, slightly north of the middle of the study area in the north-south direction. It has a latitude of N 46° 40' 36'', a longitude of W 116° 59' 39'' and an elevation of 2950 feet amsl. Within a few hundred feet to the east of the tower, but outside the study area, there begins an abrupt ascent up Paradise Ridge. The two highest peaks of the ridge lie approximately one mile outside of the study area, nearly due east of the tower. Placement of the tower at this location maximizes the measurement of effects on climate of air flow over the Ridge. This is a “highland, air-flow-over-ridge” site. There are no obstructions to the tower to the north, west or south, but a few hundred feet to the east lies the upslope, which also has a number of large trees. Since the tower sits on a topographic bench, but near the beginning of the ascent up the ridge, wind speeds tend to be lower than measured at the other two tower sites.

Reisenauer Hill Site

The RH site lies in the southern HFA portion of the study area and is representative of the southern one-third to two-fifths of the study area. It has a latitude of N 46° 39' 12', a longitude of W 117° 00' 00'' and an elevation of 2990 feet amsl. It sits on a west-facing slope, with an approximately uniform slope to both the east and west, approximately 250 feet south of the Reisenauer Hill cellular telephone tower. It has the greatest wind exposure of the three tower sites, but is similar to much of the southern two-fifths of the study area. This is a highland site whose dominant air flow pattern moves around the south end of Paradise Ridge.

2 Data and Instrumentation

2.1 Weather Data

On-site measurements were collected with NTCIP compliant Road Weather Information System-Environmental Sensing Stations (RWIS-ESS) purchased from Vaisala, Inc. Measurements at all three stations ran from January 1, 2005 and through July 21, 2006, and are included in this report. Data was transmitted using CDMA cellular technology from each of the three sites to an ITD server located in Pocatello, Idaho. The ITD server polled and downloaded data from the three stations approximately every five minutes, however, the actual time of polling, and hence the time corresponding to each data value and the interval between pollings of a given station, varied depending on access waiting times, and download durations from sensors polled previously.

For consistency between the data sets, we resampled all data by interpolation from the recorded data sets to a common five minute time increment corresponding to 0, 5, 10, 15, 20, etc. minutes after each hour (e.g., interpolated values at each station corresponding to 1:00, 1:05, 1:10, 1:15, 1:20, etc.)

On-Site Measurements

The following on-site measurements were collected: Instantaneous, and 24-hour maximum and minimum air temperature (°F, °C), relative humidity (%), average and gust wind speeds/directions(mph, m/s; °), incoming shortwave radiation (W m^{-2}), precipitation type (no precipitation, slight, moderate or heavy rain, snow, or frozen precipitation), precipitation rate (in/h, mm/h) and accumulation (in, mm), snow depth (in, cm), and visibility distance (33 – 6560 feet, 10-2000 m). Wind speed/direction and incoming solar radiation on a horizontal plane were measured at 33 feet height; air temperature, relative humidity, precipitation, visibility distance, and snow depth were measured at approximately 6.5 feet height. Wet bulb and dewpoint temperatures have been calculated from the temperature and humidity data. Specific details of instrumentation is provided in Appendix A.

University of Idaho Plant Sciences Farm

Long-term daily climate data (1890's to present) are available from the University of Idaho Plant Sciences Farm (PSF), located about 1.1 miles northeast of the study area. Data of interest to this study include daily snowfall (SNOW), snowdepth (SNWD), precipitation (PRCP; water equivalent depth of all types of precipitation), 24-hour maximum air temperature, minimum air temperature, and air temperature at time of observation.

Satellite Remote Sensing

Satellite images provide a view of complete spatial coverage of an area at a moment in time. Images collected on different days provide information through time. Landsat 7 Enhanced Thematic Mapper (ETM+) data (2002-2012) and Terra MODIS data (2001-2012) were processed. Landsat has a spatial resolution of 30 meters, and a temporal resolution of 16 days. MODIS has a spatial resolution of 500 meters and a daily temporal resolution. Landsat images are presented in this report owing to Landsat's much higher spatial resolution than the MODIS instrument aboard the Terra satellite. Landsat Images after 2002 have diagonal blacked-out stripes resulting from partial equipment failure; nevertheless, the spatial distribution of snow is clearly visible.

2.2 Existing US95 Horizontal and Vertical Alignment

The horizontal and vertical alignments of the existing US95 within the study area are shown in Figure 2.1, which is based off of "As-Built" plans for the existing US95 from Thorncreek Road to Palouse River Drive provided by ITD. The horizontal axis is marked off in stations representing horizontal driving distance along the centerline of US95. Station 1010 on the far left (south end of existing study area) corresponds approximately to milepost (MP) 337.8, about 0.8 miles south of the summit of Reisenauer Hill, and Station 1343 is near Palouse River Drive, close to MP 344. Each unit increment of station number (e.g. 1100 to 1101) represents 100 feet of horizontal distance along the US95 centerline. Each major (numbered) vertical gridline increment represents 5000 feet (e.g., from 1100 to 1150), and each minor gridline increment represents 1000 feet (e.g., from 1100 to 1110).

Specific road features are labeled. These include the summits of Reisenauer and Clyde Hills, and junctions with Eid, Jacksha, Zeitler, and Snow Roads, and Palouse River Drive. In addition, High Accident Locations (HALs) as designated by ITD and reported in the project DEIS (2012) are shown.

The elevation of the centerline of US95 is shown by the dashed line, and values above mean sea level are given on the left-hand vertical axis. The summits of Reisenauer and Clyde Hills and the locations of road junctions are shown.

The solid line in Figure 2.1 represents "relative horizontal curvature", RC, as scaled by the right-hand vertical axis. Sharper or tighter curves have larger values in absolute value, with ±1 being the sharpest curves. An RC value of zero (midway up the right-hand RC scale which ranges between +1 and -1) indicates a straight roadway with no horizontal curvature. Positive RC values indicate curves which turn clockwise while driving from south to north; and negative RC values are curves which turn counterclockwise from south to north. The length in the horizontal direction of an RC value of a specific magnitude corresponds to the horizontal length of the curve along the curve centerline, that is, the driving distance of the curve.

Relative horizontal curvature, RC is calculated as follows. Each horizontal road curve on US95 in the study area has a radius of curvature, R. The shorter the radius, the tighter or sharper the curve. RC quantifies the radius of each curve relative to the tightest curve in the study area, which has a radius of R_o=955 feet, and is located between stations 1078.8 and 1085.8, partway down the north slope of Reisenauer Hill. Each curve is inversely normalized relative to R_o by dividing R_o by the radius R of each curve (i.e., RC=R_o/R). For example, a curve with radius R=2000 ft has a relative curvature of RC=955/2000=0.48. In Figure 2.1, all curves have RC values between ±1.

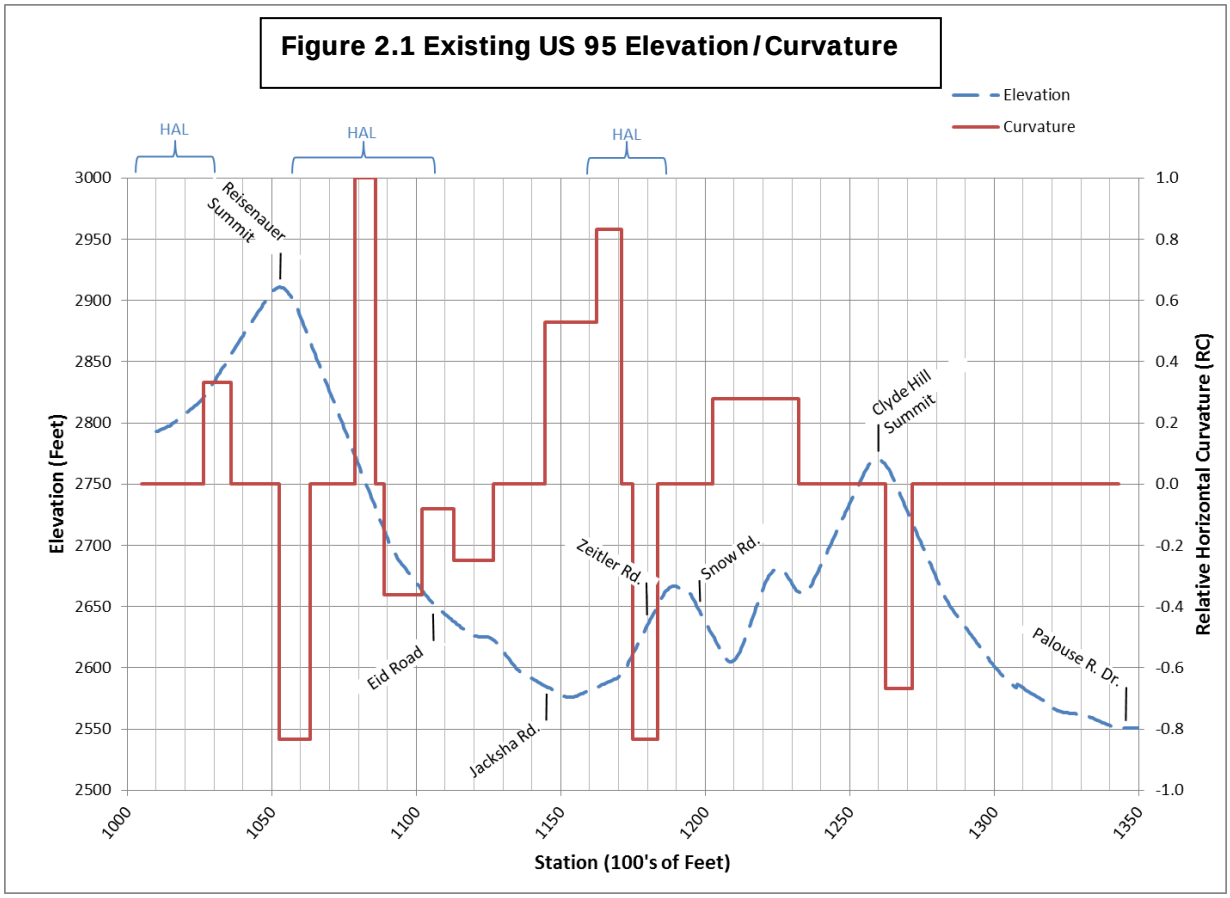

Figure 2.1 As-Built Elevation and curvature of existing US95 within the study area from 0.8 miles south of the summit of Reisenauer Hill to Palouse River Drive. See text for description. The left side of the graph is South, and the right is North. ITD-designated High Accident Locations (HALs) are identified along their corresponding station range at the top of the graph.

2.3 Vehicle Accident Data

ITD provided vehicle accident data collected by law enforcement personnel for US95 between Thorncreek Road and Palouse River Drive at the south end of Moscow for the

decade from 2001 through 2010. The data set contained, among other things, information on vehicle type(s), date, time, location, weather, surface condition (e.g., wet, snow, ice, etc.), event description, relationship to junctions, contributing circumstances, injuries and fatalities. During this decade, along US HWY 95 from 0.8 miles south of the summit of Reisenauer Hill to Palouse River Drive, 242 separate vehicle incidents occurred, involving 314 vehicles.

Figure 2.2 plots cumulative vehicles involved in accidents on US95 beginning at the south end of the study area, and adding in accidents where they occur spatially moving northward along US95 through the study area. The uppermost dash-dotted line includes all accidents within the study area during 2001-2010. Other lines indicate spatial association of accidents with the factors of horizontal curves (long-dashed line), weather/surface conditions (solid line), non-weather accidents (dotted line), and junctions such as roads and driveways (short-dashed line). High Accident Locations (HALs) as designated by ITD and reported in the project Draft EIS (DEIS, 2012) are shown. These are the three highest HALs in ITD District 2, and rank in the top 13 of Idaho State HALs (DEIS, 2012).

Particular portions of US95 exhibit higher concentrations of accidents than others, as indicated by the slope of each line. More steeply sloped lines indicate higher concentrations, and shallow slopes indicate lower concentrations of accidents. Large vertical step changes indicate multiple accidents occurred at a given location; flat horizontal lines indicate an absence of accidents over range of distance spanned by the flat line.

Several short segments within the study area in Figure 2.2 exhibit no or few accidents. With reference to both Figures 2.1 and 2.2, these include the approximate station ranges from 1048-1058 (Reisenauer Summit), 1132-1140 (approaching Jacksha road from south; straight road, shallow slope, nearing nadir road elevation between Reisenauer and Clyde Hill summits), 1185-1197 (summit between Zeitler and Snow Roads), 1208-1223 (short steep slope, gentle curve, nadir between Snow Road and Clyde Hill Summit), 1261-1271 (Clyde Hill Summit), and 1312-1328 (straight road, gentle slope, nearing lowpoint in approach to Moscow). Notably, the vicinities of the Clyde Hill summit, the Zeitler/Snow Road summit and even more so the Reisenauer Hill summit show low concentrations of accidents. Both Reisenauer and Clyde Hills have sharp curves beginning near their summits which experience few accidents, especially on the uphill side of the curve.

Accidents for which weather or surface conditions were listed in the reported accident data as snow, ice, slush, wet, rain, sleet/hail, fog, or severe side winds are shown by the solid black line in Figure 2.2. The two ovals superimposed on the weather accident line indicate the two regions with highest accident concentrations associated with weather conditions, and both overlap with HALs. Referring back to Figure 2.1, the left oval between stations 1058 and 1090 denotes a region of increasing accident

concentration corresponding to the descent of Reisenauer Hill. The two sudden increases in numbers of accidents occurring approximately at stations 1080 and 1085 are collocated with the beginning and ending of the sharpest curve in the study area (RC=+1 in Figure 2.1) midway down Reisenauer Hill. Preceding this curve, there is a gradual increase in the concentration of accidents beginning just downhill to the north of the Reisenauer Hill summit and continuing north down the north slope of Reisenauer Hill. Following the sharp RC=1 curve, the concentration of accidents as indicated by the slope of the weather accident line reduces suddenly and become more similar to the rate of accident occurrence along US95 throughout most of the study area. The highest concentrations of accidents within this HAL occur at mid-elevations (2710-2760 feet) with respect to the range of elevations experienced by US95 within the study area.

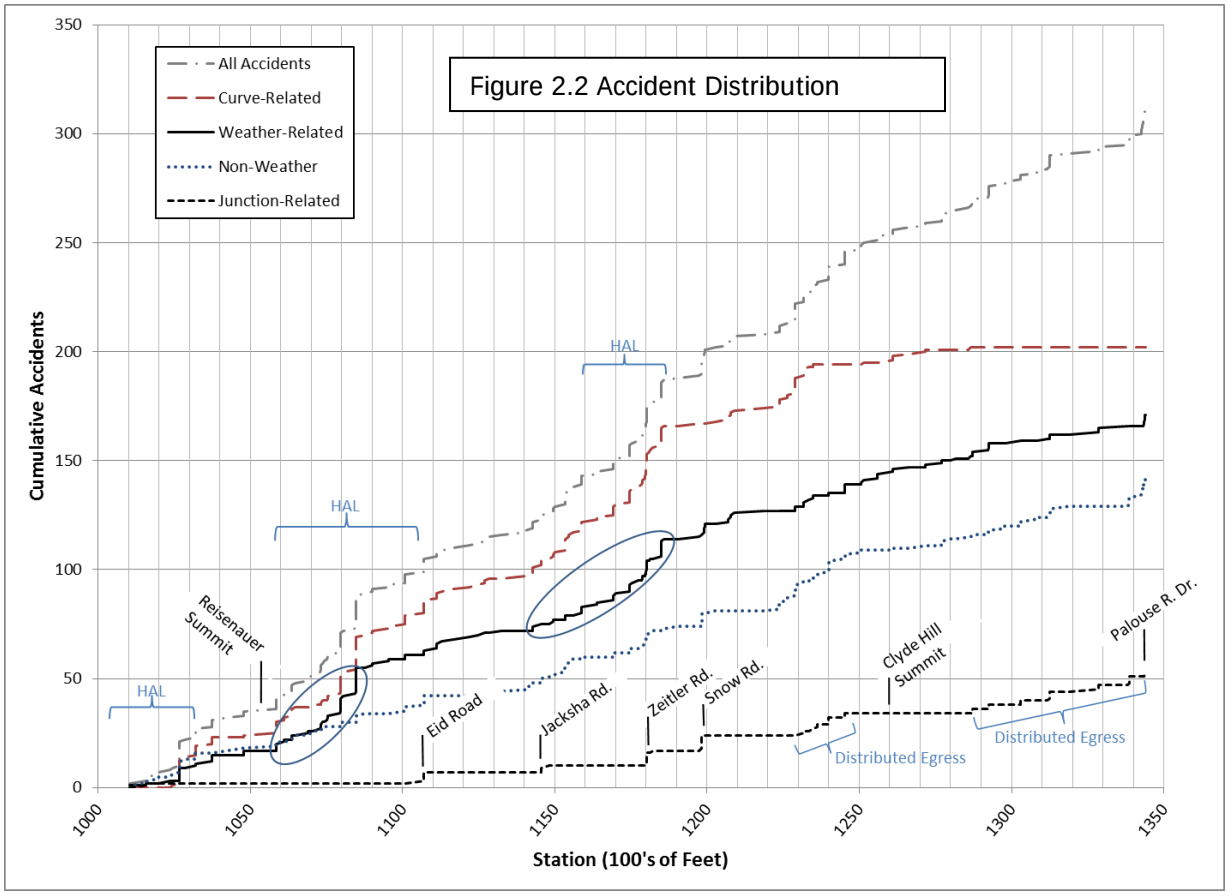

Figure 2.2 Cumulative accidents from south to north along US95 in the study area associated with various factors given by the legend, from 2001 through 2010. The left side of the graph is South, and the right is North. The solid line indicates inclement weather-related accidents, including surface conditions, and the ovals show areas of increased concentrations of accidents (steeper slope of the line). ITD-designated High Accident Locations (HALs) are identified along their corresponding station range.

The second oval on the weather-related accident curve between stations 1140 and 1190 in Figure 2.2 shows an increasing concentration of accidents moving from south to north (left to right). Point concentrations of accidents denoted by step increases in the cumulative numbers of accidents, are collocated with beginnings and endings of curves, including a pair of sharp reverse curves, and the junction with Zeitler Road within this section (see Figure 2.1 for curve locations). The highest concentrations of accidents within this oval occur along a south-sloped roadway section between stations 1170 and 1184. Note that this HAL/Oval occurs in a low elevation region of the study area but still on a steep slope with sharp curves, a distance down the slope.

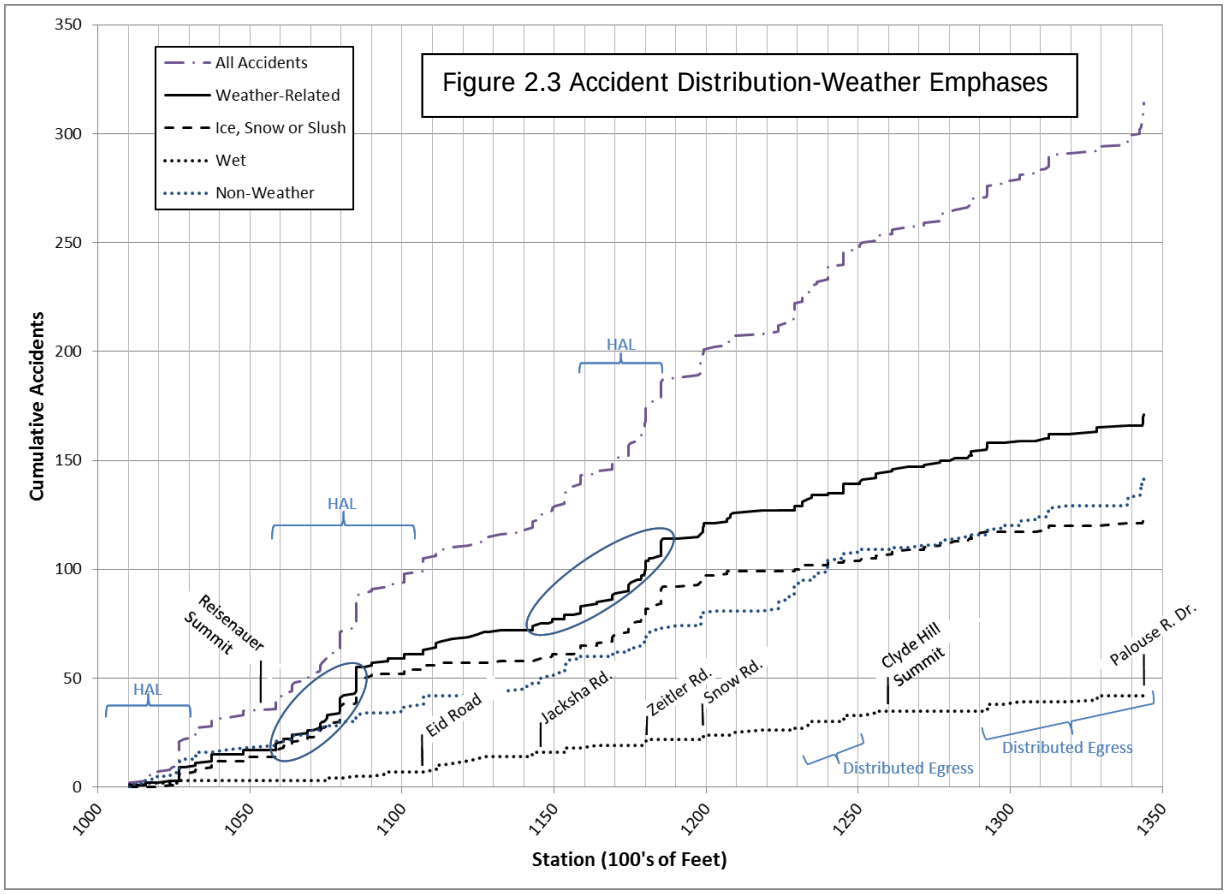

Figure 2.3 Similar to Figure 2.2, but emphasizing distinction between accidents with solid (Ice, snow, slush) versus liquid (wet) surface water conditions. Ice/snow/slush conditions show concentrations of accidents collocated with downslope horizontal road curves. The wet conditions are more characteristic of the non-weather conditions, which exhibits greater collocation of accidents with junctions.

There is also a concentrated region of accidents between stations 1020 and 1030 within an ITD listed HAL. The highest point concentrations of accidents in or near this HAL occur at the beginning and end of the curve between stations 1026 and 1036, which is well below the summit of Reisenauer Hill, but to the south (see Figure 2.1). In this

vicinity, the existing US95 no-build alternative, and the three alternatives W-4, C-3 and E-2 are collocated, but W-4, C-3 and E-2 would become median-divided highways.

Non-weather related accidents (Figure 2.2 dotted line) all listed the surface condition as dry, and the weather condition as clear or cloudy. This line exhibits a more uniform rate of accident occurrence along US95 than the weather related cumulative accident line, with the most pronounced point increases in accidents collocated with junctions (e.g., Eid, Zeitler and Snow Roads, as well as the distributed egress regions associated with driveways and commercial access). This can be seen by comparing the non-weather cumulative accident line with the junction-related accident line (short-dashed line), which only includes accidents listed as junction related by law enforcement personnel on accident reports. Unlike the weather-related accident line, the non-weather accident line does not exhibit a pronounced collocation of high accident concentrations with curves.

Solid (ice/snow/slush) and liquid (wet) surface conditions correspond to different accident associations as shown in Figure 2.3. Ice/snow/slush surface accidents are most pronounced on curves, but also occur at junctions. Wet surface accidents exhibit stronger collocation with junctions and exhibit little collocation with sharp curves. The wet surface condition associated accidents are more similar to the non-weather accident distribution than to the ice/snow/slush accident distribution. Furthermore, about 74% of all weather-related accidents are associated with ice/snow/slush surface conditions, whereas about 24% are associated with wet conditions.

From 2001-2010, four accidents were reported during foggy conditions on US95 between Thorncreek Road and Moscow. One of these was due to tire defect, and occurred south of Reisenauer Hill at station 1010.4, elevation 2790', before any of the proposed alternatives deviate from the existing US95 No-build alternative. The other three fog accidents occurred while negotiating tight radii curves on portions of the existing US95, at low elevations. The first accident was at station 1084, elevation (Z) 2740 feet, RC=+1 (see Figure 2.1). This accident was on the tight radius curve midway down Reisenauer Hill. The other two fog accidents occurred in different years at station 1174.5 where Z=2610 ft, RC=-0.83. These were at the sharp reverse curves below Zeitler Road, and both listed ice as a surface condition, None of the accidents during foggy conditions occurred at high elevations (i.e., near the top of Reisenauer Hill), but rather in mid- to low elevations of the study area.

Between 2001 and 2010 over the existing US Highway 95 within the study area, three accidents, one involving two vehicles, included severe cross winds as a contributing factor. None of these were semi-trucks. One was at station 1079.5, elevation 2770 feet with a surface condition of slush. This was on the sharp curve midway down Reisenauer Hill (see Figure 2.1). Two vehicles were involved in a single accident at station 1207.9, elevation 2605 feet, and a third vehicle was involved in an accident at station 1250.54, elevation 2735 feet. These last two accidents (three vehicles)

occurred between Snow Road and Clyde Hill summit. All of these wind-related accidents occurred at mid- to low-elevations within the study area.

This information about accident distribution may be summarized as follows:

- Weather-related accidents can and do occur along the existing US95 irrespective of elevation. HALs occur at high, intermediate and low elevations.
- Frozen-surface (Ice/snow/slush) weather-related accidents are concentrated on curves, especially sharp ones, which are located some distance downslope.
- Summits exhibit low accident concentrations, even with sharp curves located at their apex.
- Dry surface (i.e., non-weather related) as well as wet (but not frozen) surface conditions exhibit concentrations of accidents primarily associated with junctions or distributed egress areas .
- Few accidents are associated with fog and high wind speeds.

3 Precipitation

Precipitation, especially as snow, is of significant interest in this project in terms of its impact on driving safety for each of the roadway alignment alternatives. For the decade beginning in 2001 and ending in 2010, 250 accidents were reported on the existing portion of US Highway 95 within the study area. Of these, approximately 44% involved road conditions with "snow", "ice", or "slush". If "wet" road conditions are also included, the percentage is greater than 56% of the total accidents. Seventy-five percent of these wet or frozen road condition accidents occurred in association with road curvature, with high concentrations on short radii curves (i.e., sharp curves), especially when those curves were located on slopes of 2.5% or more. As a result, the spatial distribution of precipitation, especially as snow, and corresponding roadway alignment alternatives are discussed below.

Multiple aspects of precipitation and snowcover are presented in the following, including a visual representation of snowcover using satellite images, on-site measurements of snowfall and snow depth within the study area, the topographic influence on rain and snow accumulation, and the topographic/energy balance influence on snowmelt.

3.1 Spatial Distribution of Snowcover from Satellite Images

Landsat satellite images of the study area and the surrounding region provide an excellent picture of the spatial distribution of snow. Examples of these images from the period 2002 through 2012 are provided, which provide the range of common occurrences with regards to snow in the study area as described in the key satellite findings below. In the images, North is at the top, the City of Moscow lies roughly in the top center, Paradise Ridge lies just right of center (trees on north side of the ridge are a large, dark green patch) and US Hwy 95 runs north-south from Moscow down the center of the image. Cyan (blue) is snow, and green, brown, and red represent vegetation or bare ground. The key satellite findings are:

1. When there is six to eight inches depth or more at the UI Plant Sciences Farm (PSF), either accrued as a single, large snowfall event, accrued in small increments over multiple days, or while melting down to 6-8 inches from greater depths at PSF, the satellite images show continuous spatial coverage of the study area and surrounding region by snow (See Figure 3.1).
2. When the snow depth at PSF drops below about six inches during melting, exposed earth and vegetation patches begin to emerge within the middle portion (i.e., between the north and south ends) of the E-2 and C-3 alternative alignments. The emergence of these exposed patches is strongly controlled by the orientation of hill slopes, beginning on south-facing slopes, which have much greater exposure to the sun than do north-facing slopes. This is discussed in greater detail in section 3.4. The patch quickly spreads westward, and then

begins to melt off north-facing slopes in the middle area defined above and including west of US 95 (See Figure 3.2).

3. Snow consistently persists longer south and east of the ridgeline of Paradise Ridge, including the ridgeline as it passes Reisenauer Hill, which during the winter months is usually the downwind or lee side of the ridgeline. Snow also persists down the north-facing slope of Reisenauer Hill, particularly from the existing US 95 toward the west. Additionally, snow persists on the north end of the study area on north-facing slopes north of Clyde Hill and the east-west powerlines of the eastern alignment, though it does not persist there for as long as on either the north face or the south side of Reisenauer Hill (See Figures 3.3 and 3.4).
4. Regional coverage snowfall of a few inches can provide relatively complete coverage of the study area, and it begins to melt off following the pattern described in 2 and 3 above (See Figure 3.5).

Figure 3.1 Landsat Image December 7, 2005

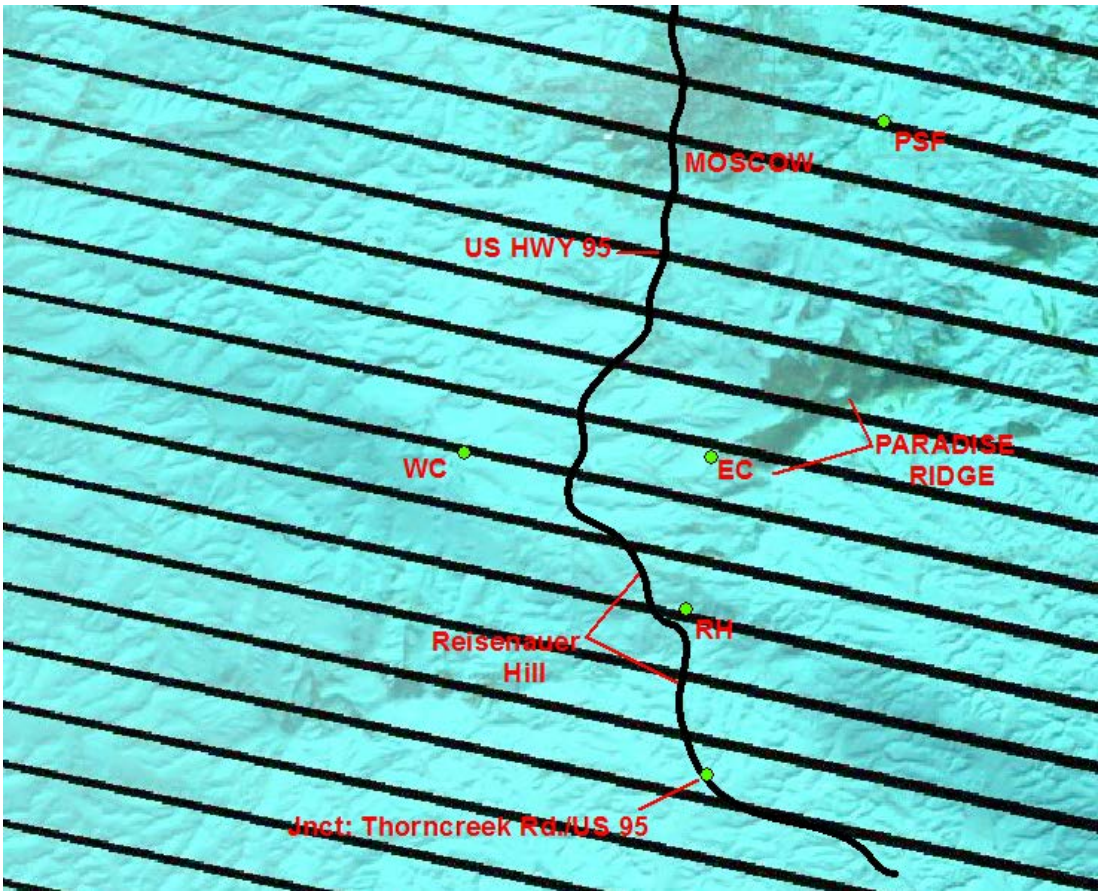

Figure 3.1 December 7, 2005. Complete snow coverage. Cyan (blue) is snow, and green, brown, and red represent vegetation or bare ground. Weather stations located at Plant Sciences Farm, Reisenauer Hill, and on the Western and Eastern Corridors are designated PSF, RH, WC and EC, respectively. Landsat Images after 2002 have diagonal blacked-out stripes resulting from partial equipment failure; nevertheless, the spatial distribution of snow is clearly visible.

Figure 3.2 Landsat Image February 13, 2004

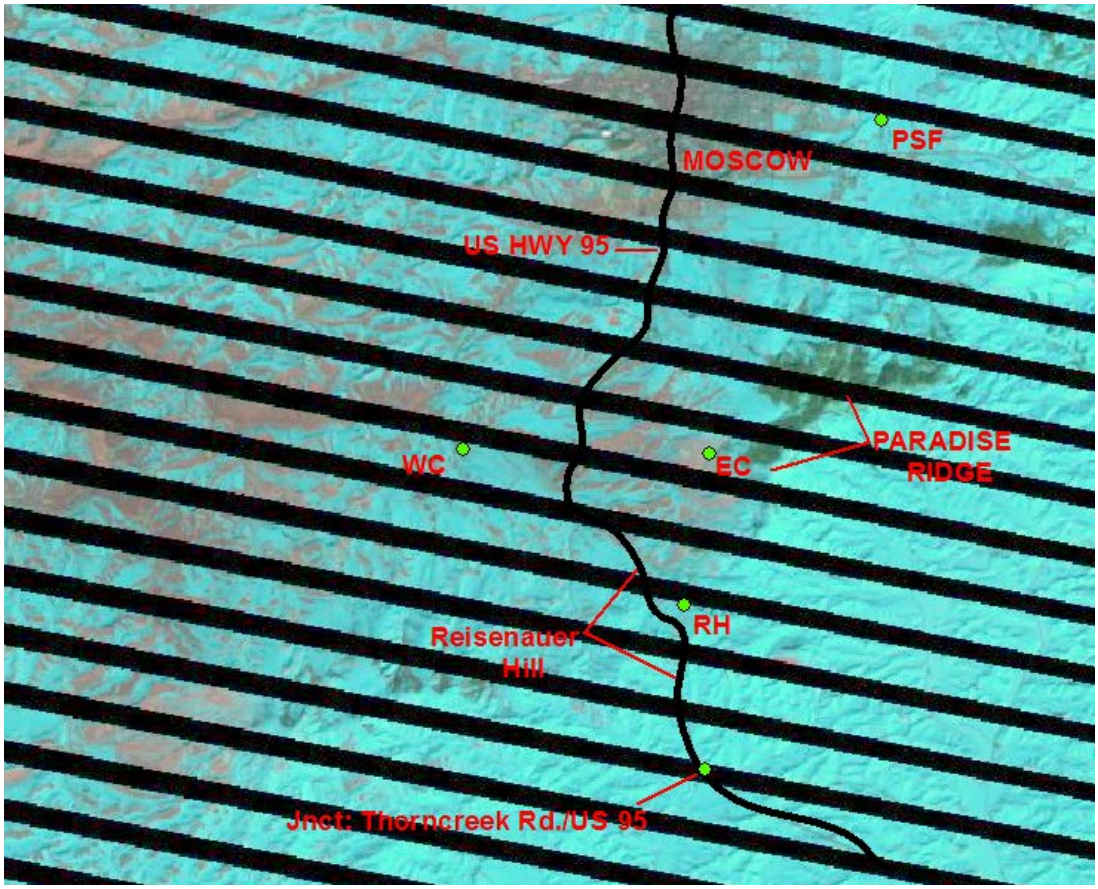

Figure 3.2 February 13, 2004. Middle portion of E-2 and C-3 beginning to melt. Cyan (blue) is snow, and green, brown, and red represent vegetation or bare ground. Weather stations located at Plant Sciences Farm, Reisenauer Hill, and on the Western and Eastern Corridors are designated PSF, RH, WC and EC, respectively. Landsat Images after 2002 have diagonal blacked-out stripes resulting from partial equipment failure; nevertheless, the spatial distribution of snow is clearly visible.

Figure 3.3 Landsat Image February 14, 2002

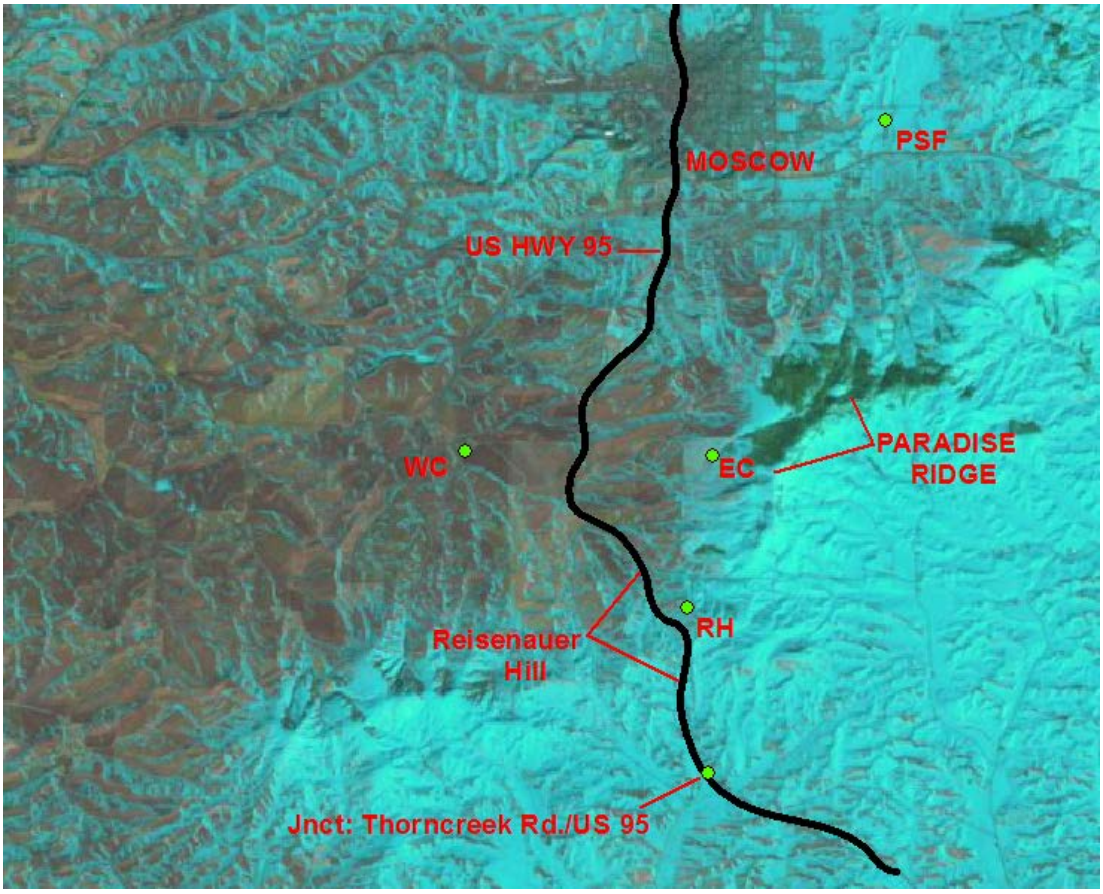

Figure 3.3 February 14, 2002. Persistence of snow on Reisenauer Hill and its north face. Modest persistence on north face of hill at north end of E-2, C-3 and existing US Highway 95. Cyan (blue) is snow, and green, brown, and red represent vegetation or bare ground. Weather stations located at Plant Sciences Farm, Reisenauer Hill, and on the Western and Eastern Corridors are designated PSF, RH, WC and EC, respectively.

Figure 3.4 Landsat Image January 24, 2006

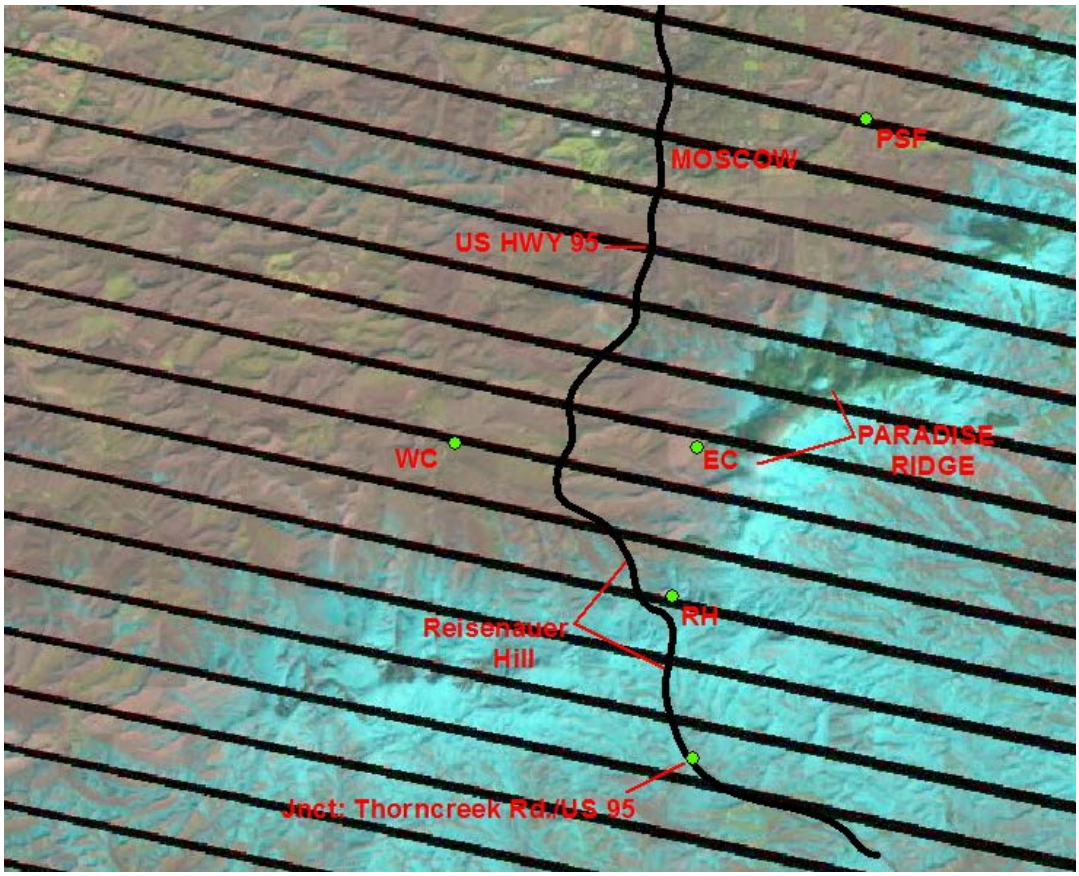

Figure 3.4 January 24, 2006. Persistence of snow on Reisenauer Hill and its north face. Modest persistence on north face of hill at north end of E-2. Cyan (blue) is snow, and green, brown, and red represent vegetation or bare ground. Weather stations located at Plant Sciences Farm, Reisenauer Hill, and on the Western and Eastern Corridors are designated PSF, RH, WC and EC, respectively. Landsat Images after 2002 have diagonal blacked-out stripes resulting from partial equipment failure; nevertheless, the spatial distribution of snow is clearly visible.

Figure 3.5 Landsat Image December 15, 2008

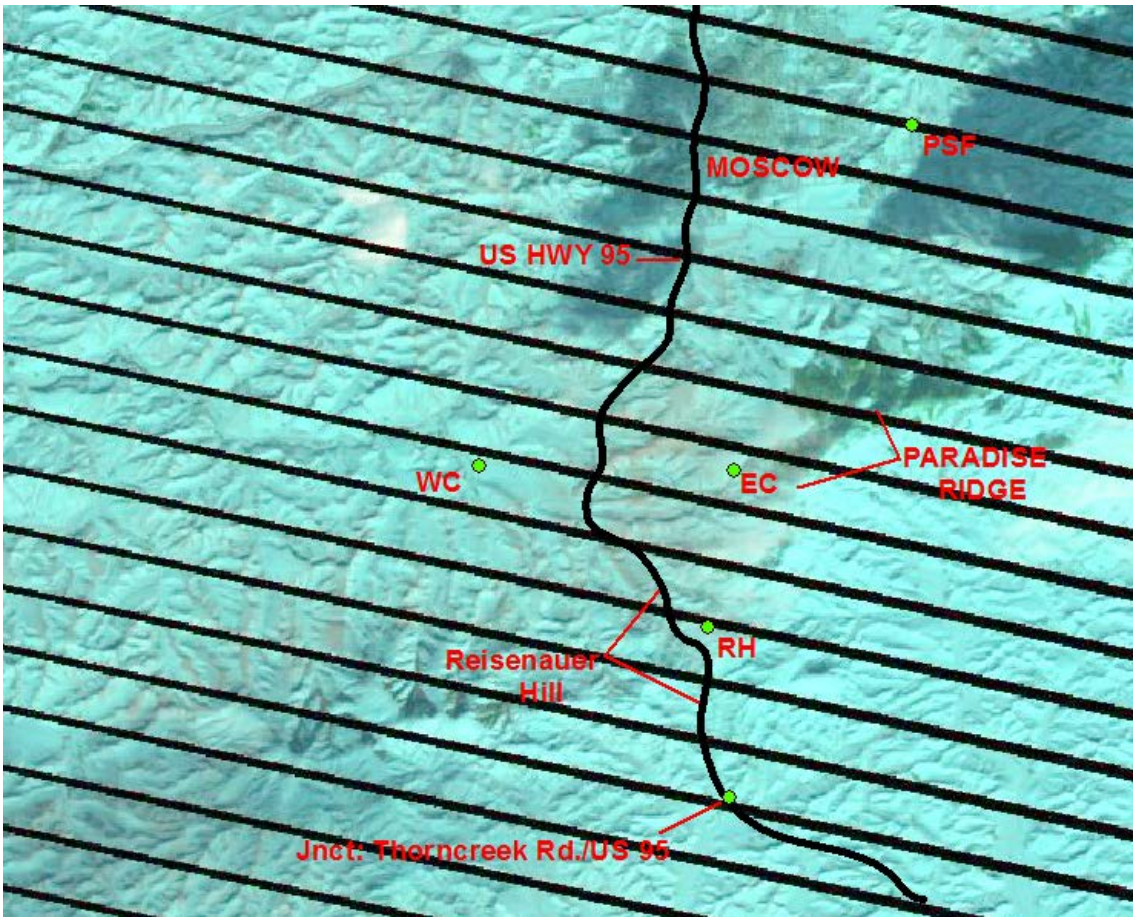

Figure 3.5 December 15, 2008. Snow beginning to melt off south-facing slopes in middle portion of E-2 and C-3 (pink-tinged areas) following regional snowfall measured at PSF of 1" on December 13 and 2" on December 14, preceded by bare ground. Cyan (blue) is snow, and green, brown, and red (pink) represent vegetation or bare ground. Weather stations located at Plant Sciences Farm, Reisenauer Hill, and on the Western and Eastern Corridors are designated PSF, RH, WC and EC, respectively. Landsat Images after 2002 have diagonal blacked-out stripes resulting from partial equipment failure; nevertheless, the spatial distribution of snow is clearly visible.

3.2 On-Site Weather Station Snowfall and Depth Measurements

On-site measurements of snowfall (i.e., precipitation type identified as light, moderate or heavy snow falling) and snow depth measurements at the WC, EC and RH stations corroborate the findings of the satellite snowcover images. These on-site measurements may be summarized as follows:

Snowfall is observed at PSF and WC on about 80% of the days at which it occurs at RH and EC. These account for the most common scenario that when snow accumulation occurs within the study area, the entire area shows accumulation. Between the EC and RH weather stations, the number of days of snowfall and whether or not ground accumulation occurs are nearly identical. The total number of days of snowfall include those when snow falls for any duration, sometimes even only for a few minutes or a half hour. Many of these days, have little or no ground accumulation of snow. Most of the difference in number of days of snow between PSF and WC on the one hand, and EC and RH on the other, correspond to days when no ground snow accumulation occurs. That is, the approximately 20% of snowfall days at EC and RH on which no snow is observed at WC and PSF largely correspond to days at EC and RH when the duration of snowfall is short and or light enough that no ground accumulation occurs. Under these circumstances weather would have little impact on driving safety for any of the alternative roadway alignments.

A small fraction of the 20% actually have ground accumulations of snow at the EC and RH weather stations when there is none at WC. As noted above, days of ground accumulations of snow at RH and EC closely correspond to one another. When this occurs, the depth at the upper stations varies from a light dusting to usually not more than a few inches. These result in an altitudinal gradient of snow accumulation in which snow gradually becomes thinner and disappears during the descent from the elevations of RH and EC.

When significant snowfall events occur, snow is present at all three weather stations. For example, on December 5, 2005 (see Figure 3.1 satellite image), snow depths at the measurement sites were RH 9.5 inches, WC 8.5 inches, EC 6.3 inches, and PSF 9 inches. These depths were the result of a cumulative total of 13.7 inches of snow, measured at PSF, having fallen from November 29-December 4, 2005. This event persisted into late December, melting off from EC on December 21st, and lasting through December 22nd at PSF, WC and RH. These are not significantly different durations of snow among the measurement stations. Snowfall events of this magnitude initially pose accident risk everywhere across the eastern, western and central alignment corridors, which is best mitigated by alignment design characteristics, as discussed in the ITD safety study (Arnzen, 2013).

3.3 Topographic Effects on Rain and Snow Accumulation

Precipitation in the region surrounding the study area is predominantly controlled by the fall-winter-spring maritime climate (Abramovich et al, 1998) and topography (Molnau, 1995). The maritime influence has spatial scales much larger than the study area, so the following concentrates on topographic influences leading to spatial variability within the study area. Qualls and Zhao (2005) present the results of precipitation measurements at the weather stations RH, EC, and WC.

As an airmass is lifted, whether due to topography (orographic lifting), convection (convective lifting) or collision of large weather systems (frontal lifting), it cools. Cooler air has a lower capacity to hold moisture, and thus as moist air cools, its relative humidity increases toward saturation. If the airmass reaches saturation, condensation occurs forming fine water droplets and clouds. Given condensation nuclei onto which condensate can coalesce and enough time, droplets can form of sufficient size that gravity overcomes the upward drag force of the lifting airmass, and precipitation occurs (Chow et al., 1988).

The orographic influence spans a wide range of scales from 100's of miles down to scales on the order of a mile. The large-scale topographic influence begins with annual average precipitation amounts ranging across much of central Washington between 8 and 12 inches, increasing gradually to about 20-24 inches on the portion of the Idaho-Washington border adjacent to Latah and Benewah Counties, and the lower quarter of Kootenai County. Precipitation then continues to increase moving eastward into the Clearwater and Bitterroot ranges, fairly uniformly exceeding 60 inches along the eastern trajectory by the Idaho-Montana border, and reaching mean annual maximums greater than 70 inches on numerous localized peaks (Molnau, 1995).

Across eastern Washington, isohyets (contours of uniform precipitation) run roughly north-south, parallel to the Washington-Idaho border. The exception to this is the influence of the Wallowa Mountains in northeastern Oregon (increased precipitation), and the Snake River flowing from Idaho into Washington (decreased precipitation) (PRISM, 2012).

Owing to the combined effects of the Snake and Clearwater River drainages in the south, and Moscow Mountain to the North of Moscow, isohyets run approximately east-west, or perpendicular to the Washington-Idaho border between Moscow and Lewiston. From Moscow south to the top of the escarpment dropping down to the Clearwater River in Lewiston, Idaho, 1961-1990 mean annual precipitation decreases from more than 25 inches in Moscow to about 16 inches at the top of the escarpment (Molnau, 1995; note: 1961-1990 mean annual precipitation values at University of Idaho Plant Sciences Farm are about 1.5 inches lower than the corresponding 1981-2010 normals, however, much of this difference occurs during non-snow months, so that the 1961-1990 mean annual snowfall is greater than that from 1981-2010). Thus, precipitation decreases from North to South, from Moscow to the top of the escarpment above the Clearwater River. The 20-inch contour runs approximately through Genesee, Idaho, thus, linear interpolation from the Idaho mean annual precipitation map would give a 1960-1991 mean annual precipitation of 23.5 inches in the vicinity of the study area.

Competing with the general decrease of precipitation depth from Moscow toward Genesee, is the relatively small-scale proturbance of Paradise Ridge. In this context, Paradise Ridge is considered small-scale relative to Moscow Mountain and even moreso

to the Clearwater Range. For comparison, the elevation of several local features are given below, including the elevation of these features measured relative to US Highway 95 at Palouse River Drive (PRD), at the north end of the study area, and the percent elevation gain of the feature relative to the elevation difference of Moscow Mountain and PRD.

Feature	Elevation (ft amsl)	Elevation above PRD (ft)	Elevation above PRD (%)
Palouse River Drive (PRD)	2550	0	0
WC	2550	0	0
EC	2950	400	16
RH	2990	440	18
Paradise Ridge	3702	1152	47
Moscow Mountain	4983	2443	100

Altitudinal gradients of precipitation have been studied for many years. As reported in Barry (1992), the most comprehensive global survey of altitudinal precipitation gradients was conducted by Lauscher (1976). For mid-latitudes on average there is a gradient of 0.36 inches per 100 feet of elevation gain up to nearly 5000 feet, and 0.58 inches per 100 feet above 5000 feet, although there is considerable variability.

These altitudinal gradient concepts apply most directly to long ascending slopes in the downwind direction. For hills running perpendicular to the mean wind direction, but with limited downwind extent, the location of the precipitation maximum varies depending on the downwind length of the hill, and is dependent upon a number of atmospheric factors (Smith, 1982). For hills with half-lengths (i.e., from beginning of slope to peak) less than 12.5 miles, the precipitation maximum occurs at the summit or on the lee side of the hill due to wind drift of the forming precipitation Carruthers and Choularton, 1983). Paradise Ridge's downwind extent is certainly much less than this, so its precipitation maximum is likely to occur at the summit or on the lee side (downwind). This accumulation and retention of snow on the lee side of Paradise Ridge and South of Reisenauer Hill is clearly visible in the satellite images of the spatial distribution of snow. Furthermore, it does not extend far in the direction perpendicular to the wind, so atmospheric flow around the north or south may lessen its orographic effect.

The peak of Moscow Mountain receives on average 40 inches of precipitation per year, and Moscow received 25 inches on average. For the elevation difference of 2443 feet, this amounts to a gradient of 0.61 inches per hundred feet, which is larger but of the same order of magnitude as the mid-latitude average. Interpolating this gradient to the peak of Paradise Ridge would yield about 30.5 inches per year at the peak using 1961-1990 averages (23.5 inches per year at 2550 feet amsl within the study area). The elevations of the proposed alignments and the RH, EC and WC weather stations are much lower than the peak of Paradise Ridge. Applying the altitudinal gradient from

Moscow Mountain to these stations gives mean annual values in inches per year of 26 (EC and RH), and 23.5 (WC), or about 2.5 inches difference between WC and EC.

The fraction of precipitation which occurs as snow has also been observed to have an altitudinal gradient owing to the altitudinal temperature lapse rate. The global relationship for solid precipitation as a percentage of total precipitation (S) is given by Barry (1992) as:

$$S = 50 - 5\,T$$

where T is the mean monthly temperature in degrees C. The constant 50 varies from location to location as does the coefficient 5. Taking these values as parameters and using regression with monthly data from PSF yields the relationship:

$$S = 30 - 5\,T$$

Applying this on a monthly basis to the study area using 1980-2010 mean monthly temperatures from PSF and assuming an average monthly temperature difference of -1.78 °F (-0.99 °C) based on the average temperature lapse rate between WC and EC gives a mean annual snow depth difference slightly lower than 7 inches. The temperature difference used excludes all times when WC is colder than EC, and thus creates an upward bias in the difference in temperature between EC and WC; the actual mean monthly temperature difference between them would be smaller, so 7 inches is biased high.

This analysis can also be carried out based simply on mean annual fraction of precipitation that occurs as snow. Based upon 1961-1990 statistics, about 21% of mean annual precipitation at PSF occurred as snowfall, 5.35 inches snow water equivalent (SWE, depth of liquid water in melted snow). For the more recent 1981-2010 climate normal when the mean annual precipitation was 27.07 inches, about 18% of mean annual precipitation occurs as snowfall, or 4.92 inches SWE. The percentage decrease in snowfall is both due to a slight decrease in snowfall, and to an increase in mean annual precipitation during warmer spring and fall months for the latter climate normals. Using the higher 21% of annual precipitation occurring as snow to the estimated 2.5 inch mean annual precipitation difference between WC and EC, and assuming a typical snow density of 10% gives an annual snow depth difference of 5 inches (snow depth on ground, not SWE). The annual snowfall for the Central Corridor would be expected to lie between the values at WC and EC.

Based on the temperature analysis for the study area showing limited time when EC is below freezing and WC is above freezing, most of this snow depth difference would occur as a difference in depth of snow falling simultaneously across the study area, thus all potential alternatives would be affected by snow and reduced traction conditions, just with different depths of snow. This would be particularly true for the large snowfall

events. However, some of this snow depth difference would occur as snow which falls exclusively on the higher elevation EC, and some would fall on both EC and CC but not WC. These latter two circumstances would generally correspond to light snowfall, although even light snowfall will often affect the entire study area. More importantly, RH is at approximately the same elevation as EC, thus the increased snow depth analysis above applies equally to RH. Since all road alternatives must pass Reisenauer Hill at the same elevation as the EC alternatives, the snow depth gradient would affect all alternatives. Therefore, the most significant distinguishing factor among proposed alternatives is their respective alignment configurations more so than spatial variability of weather. Quantification of the relative safety of the alternative alignments is presented in the ITD safety study (Arnzen, 2013).

3.4 Topographic and Energy Balance Influence on Snowmelt

The depth of snow in a location is determined by the balance of past deposition and melting. Deposition of snow depends on depth of precipitation at a given location, and a sufficiently cold temperature to cause the precipitation to fall as snow rather than rain. In high topographic relief areas, including the Moscow, Idaho area, the depth of precipitation tends to increase with elevation, and the temperature tends to decrease, as discussed in the previous section. In fact the increase of precipitation is largely governed by the altitudinal decrease of temperature, which causes increased condensation and cloud formation in air masses, and hence more precipitation at higher elevations than at lower. Over large elevation differences, such as between the City of Moscow (2600 feet), and the top of Moscow Mountain (4983 feet), which differ by nearly 2400 feet of elevation, this difference is significant. As described later, the temperature differences based on the saturated or dry adiabatic lapse rates between the City of Moscow and Moscow Mountain are 7.9 °F to 14.4 °F, respectively. As an example, based on snow measurements at the Moscow Mountain SNOTEL site, this was sufficient so that on March 29, 2006, there was a temperature difference between Moscow Mountain and PSF of 9.1 °F, and 56.4 inches of snow on the ground or 21.6 inches of snow water equivalent near the top of Moscow Mountain, while there was no snow on the ground at PSF, EC, RH, or WC.

Although Qualls and Zhao (2005) reported a precipitation difference between the Eastern Corridor and the Western Corridor, presumably due to the elevation difference, and the close proximity of the bench of the EC site to Paradise Ridge, the temperature differences are not sufficiently large to sustain long-lasting differences in accumulated snow between the EC and WC sites. Certainly there are times when it snows on the EC bench, but does not snow in the City of Moscow, or at the WC site, and sometimes the snow persists on the EC Bench when it does not at lower elevations. As noted earlier, the small difference between the temperatures at EC and WC and the infrequency with which WC and EC reside on opposite sides of the required temperature to allow snow at the upper site and rain at the lower reduces the frequency at which this might be

expected to occur. In order to get a good idea of the frequency of persistent snow at EC when there is none at WC, one must consider the causes of snowmelt.

Melting, or snow ablation, is primarily caused by a flux of energy into the snow pack. There are three primary sources of energy for snow melt: solar irradiance from sunshine, heat released by the condensation of water vapor onto the snow surface, and heat absorbed from warm winds blowing over the snow also known as convection (Linacre, 1992). Convective melting can be calculated as,

$$M_c = 0.19u(T_a - T_s)$$

where M_c is the melting rate in mm/day liquid water equivalent, u is the wind speed at two meters height above ground in m/s, T_a is the daily average air temperature and T_s is the temperature of the snow surface both in °C. T_s may be taken as 0°C, especially during melting conditions, and dropped from the equation. If the air temperature is colder than the temperature of the snow, no melt occurs. If we want to consider the difference in melting rates between the WC site and the EC site, we can use the difference in the air temperature of the two sites, which has a mean daytime value of about 1.78 °F, or 0.99 °C, and the mean site wind speed, adjusted to 2 meters height, which is 6 m/s. This produces a difference of 1.1 mm/day, or roughly about 0.04 inches greater melt per day at WC due to convection than at EC. Note that frequently the temperature difference does not persist through the night, and often changes sign, so that EC is warmer than WC, 1.1 mm/day difference is probably an overestimate.

Similarly, condensation melting can be calculated as,

$$M_d = 0.6u\frac{\Delta}{\gamma}(T_d - T_s)$$

where M_d is the condensation melting in mm/day liquid water equivalent, Δ is the slope of the saturation vapor pressure curve at the surface of the snow which has a value of about 0.5 hPa/°C, γ is called the psychrometric constant and has a value of about 0.6 hPa/°C, T_d is the daily average dewpoint temperature in °C, and all the other input variables are the same as for convection melting. The coefficients in the equations for convective and condensation melt account for unit conversions, the effects of the latent heats of fusion and of sublimation, and effects of turbulent energy exchange between the air and the surface. Different values of the coefficients appear in the literature, however, whatever values are used in a particular equation should be similar when compared between the different sites As with convection melting, we can determine the difference of melt which would be expected between EC and WC. The differences in dewpoint temperature between WC and EC are close to the difference between the air temperatures, namely, 1 °C. This produces a difference in melt rate of 3.6 mm/day or one-eighth of an inch per day. Generally the temperatures are colder at the RH site in the southern climate regime of the study area. Consequently, convective and condensation melting there would be less than occurs at the EC site.

The final important source of energy is net radiation, or the balance of the incoming and outgoing components of solar and terrestrial radiation, given by,

$$Q_n = (1-\alpha)R_s - R_{nl}$$

where Q_n is the net radiation in W/m^2, R_s is the incoming solar radiation, in W/m^2, α is the albedo or fraction of incoming solar radiation that is reflected by the surface and which ranges from about 0.9 for fresh new snow, to about 0.4 for old dirty snow, and R_{nl} is the net outgoing longwave radiation, in W/m^2. If Q_n, R_s, and R_{nl} are taken as 24-hour averages, or are integrated over 24 hours, the net radiation input to the snowpack in W m^{-2} can be converted to snowmelt in mm/day by multiplying Q_n by 0.254.

Net longwave outgoing radiation consists of the longwave radiation emitted by the surface minus the incoming longwave sky radiation, plus the reflected fraction of the incoming longwave sky radiation.

$$R_{nl} = \varepsilon_s \sigma T_s^4 - \varepsilon_s \varepsilon_{sky} \sigma T_a^4$$

where ε_s is the surface emissivity taken as 0.97, σ is the Stefan-Boltzmann constant (=5.6697 x 10^{-8} W m^{-2}K^{-4}), ε_{sky} is the sky emissivity taken as 0.97 for heavily overcast conditions and as 0.76 for clear sky conditions, T_s is the snow surface temperature, taken as 0°C during melting, and T_a is the air temperature at 6 feet above the ground. As a result, since all three sites, EC, WC and RH are exposed to the same sky conditions, their incoming longwave radiation components would be very close to one another in magnitude. Similarly, when snow is present at all three sites, the surface temperature would be close to 0 °C at all three sites so their values of emitted radiation would also be close to one another. In general, net longwave radiation results in a loss of energy from the surface when the sky is clear, and may result in a net gain of energy by the surface when the sky is cloudy if the air temperature is above about 1 or 2°C.

Solar radiation was measured at each of the climate stations in the study area. Comparison between the measurements at the three sites showed that their five-month averages only differed by about 3 W m^{-2}, which is smaller than the stated accuracy of the instruments. Daily peak values in the 350 W m^{-2} range in early January, in the 600 W m^{-2} range by March, and above 900 W m^{-2}in late May were observed. These corresponded to daily 24-hour mean values of around 75 W m^{-2} in early January, 175 W m^{-2} in early March, and nearly 350 W m^{-2} by the end of May. In comparison to these numbers, the 3 W m^{-2} difference between the radiation measured at the stations is negligible.

One can model snowmelt caused by the three dominant melting factors, convection, condensation, and radiation using the equations given above. Given a starting point snow depth, one can model the snowmelt, or ablation, subtract the ablation from the starting depth to estimate the current depth of snow on the ground. This modeled depth can be compared with measured snow depth to determine how accurately the model represents the melting events at a given site, and can be used as a useful tool to

compare rates of melting and or persistence of snow at different points in the study area.

Figure 3.6 Snow depth

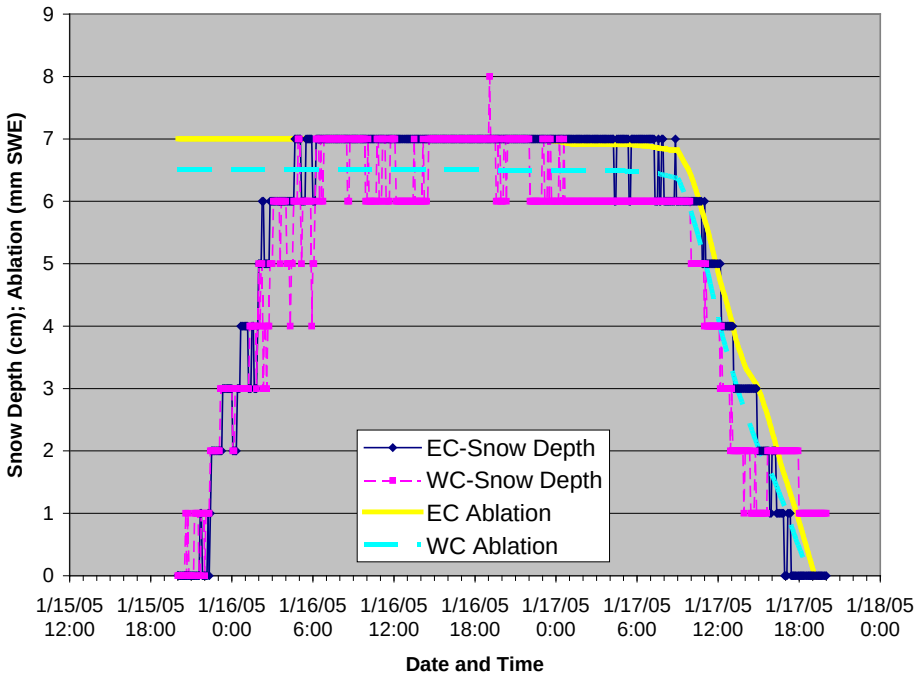

Figure 3.6. Comparison of snow depth measurements with modeled ablation.

Figure 3.6 illustrates the use of this snowmelt model at the EC and WC climate sites, compared to snow depths measured with sonic snow depth sensors, for a snowfall and ablation event which occurred on January 15, 16, and 17, 2005. The snow depths are reported in units of centimeters, which can be divided by 2.54 to get inches. The sonic snow depth measurement at the WC and EC sites reported 6.5 cm (2.56 in) and 7 cm (2.76 in) of snow accumulation, respectively, reported as actual depth of snow on the white snow collection board. Independent precipitation depth measurements as snow water equivalent, SWE, (i.e., the liquid depth of water the snow would contain if it were melted) at the two sites indicate that during this snowfall event 6.51 mm and 6.66 mm of SWE fell at WC and EC, respectively. Comparisons of precipitation depth measurements in SWE units of mm with snow depth in cm during this same snow event, indicate that the density of the snow was approximately 10% (100 kg m^{-3}) at WC and 9.5% (95 kg m^{-3}) at EC, compared to the density of liquid water, both of which fall in the middle of the normal range for new snow densities (Pomeroy and Gray, 1995). As a result, centimeters of snow depth and millimeters of liquid water ablation are just about directly comparable, that is, a reduction of 1 cm solid snow depth is approximately equal to ablation of 1 mm liquid water. However, as snow melts, the meltwater drains into the snowpack, and may cause subsidence of the snowpack at a slightly faster rate than the actual rate at which melting occurs (Kattelmann and Elder,

1993). Hence, the measured depth of snow from the sonic depth sensor might decrease slightly faster than the snow actually melts.

There are several features which can be observed from Figure 3.6. One is that the accumulated depths are similar at the two sites, and are fairly well synchronized. The snow depth sensor only changes in 1 cm steps. Some of the oscillation associated with the measurements may be associated with blowing snow during the accumulation period; as the snow piled up, wind redistribution may have caused the depth to oscillate between two adjacent measurement values. This is particularly evident at the WC site during the accumulation stage, and before the beginning of ablation. There was much less oscillation once melt began, perhaps since once the snow begins to melt, it cannot be blown around by the wind.

Secondly, the ablation calculated based on data measured independently at EC and WC also track each other fairly well. The difference between the two is primarily an artifact of the starting point of each curve corresponding to the mean depth of snow at the end of the snow event. At least for this particular snow accumulation and melt event, the variables used as input from the two sites were close enough that the simulated melt rates were very close, and the field observations of the decline in snow depth corresponded closely with the simulated values.

The fractions of total melt corresponding to convection, condensation, and net radiation were 0.25, 0.34, 0.41, respectively at WC, and 0.28, 0.28 and 0.43, respectively at EC. Prior to January 17th, no significant melting occurred since temperatures were well below freezing, and radiation was limited. During the mid-day period on January 17th, net radiation dominated the other two terms by about a factor of three, whereas in the late afternoon and early evening, condensation melt exceeded convection and radiation melting by factors of about two and five, respectively. The relative fractions of melt for each of the components were of similar values between EC and WC. That is, radiation caused about the same amount of melting at EC as at WC, and the same may be said of convection and condensation melting when comparing the two sites. Also note that the combined fractions of melt caused by condensation and convection, the two components most dependent on air temperature, humidity, and wind speed were similar between EC (0.56) and WC (0.59).

This leads to the point of the foregoing analysis. Observations from Moscow sometimes indicate that there is occurrence and/or persistence of snow on the highland bench of the Eastern Corridor and an absence of such in the Western Corridor. How can these observations be reconciled with a) the fact that predominant mechanisms of snowmelt that indicate that snowmelt should occur at relatively similar rates at both EC and WC, and b) that measurements at both sites indicate that snowfall at EC is regularly accompanied by snow at WC? This may be explained in light of the one factor that varies significantly around the study area: radiation loading as a function of slope and aspect of the land surface. The snowmelt information shown above corresponds to

measurement sites which were approximately level, and all the radiation calculations assumed a level land surface. However, the interaction of the position of the sun at a given moment, and the slope and aspect of the land surface has a tremendous impact on the amount of solar radiation absorbed by the surface. Slopes with a south-facing aspect point more directly toward the sun and receive more radiation per unit area tangent to the surface; slopes with a northern aspect tilt away from the sun and receive much less radiation.

Figure 3.7 Study Area Aspects

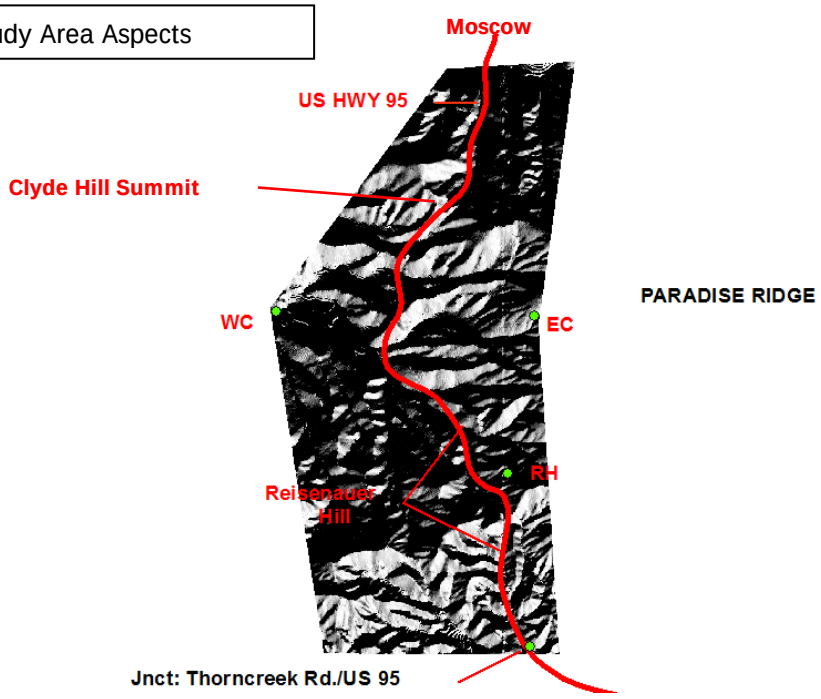

Figure 3.7 Distribution of aspects throughout the study area. Light-colored areas have generally south-facing aspects (west through south through east), and dark areas have north-facing aspects (west through north through east). WC, EC and RH are the locations of the weather stations.

The distribution of south versus north aspects throughout the study area is shown in Figure 3.7. South of Reisenauer Hill, the topography has a predominantly south-facing aspect. The descent from Reisenauer Hill has a north-facing aspect. The middle portion of the Eastern Corridor and Central Corridor east of US95 have mixture of aspects but are predominantly south-facing. The lower middle Western Corridor from Reisenauer Hill to the WC weather station is mostly north-facing; The Eastern, Central and Western Corridors in the vicinity of Clyde Hill are mostly south-facing. The north end of the Western, Eastern and Central Corridors are mostly north-facing, including the descents from E-2, C-3 and W-4. The magnitude of the slopes associated with these aspects are not differentiated in Figure 3.7.

Table 3.1 presents multiplication factors for the amount of radiation received on a sloped surface relative to a horizontal surface for two different combinations of slope and aspect and a few different dates during the winter. The multiplication factors have been adjusted to allow for diffuse radiation, and have been integrated throughout the day. The combinations of slopes and aspects presented are abundantly present in the study area.

Table 3.1. Radiation Loading Factors relative to a horizontal surface, for 16° slopes and aspect oriented either directly north or south.

Aspect	Date	Factor
South	January 1	1.79
North	January 1	0.14
South	February 1	1.56
North	February 1	0.37
South	March 1	1.35
North	March 1	0.58
South	April 1	1.21
North	April 1	0.72

The factors in the table above may be used to adjust the solar radiation flux density to the amount received by the surface with the specified slope and aspect given the radiation flux density received by a horizontal surface at the same location. For example, on January 1, the 24-hour average clear sky solar radiation on a horizontal surface is approximately 74 W m^{-2} in the study area. The 24-hour average solar radiation on a south-facing, 16° slope is 1.79 times the horizontal surface amount, or 132.5 W m^{-2}, and has 179% of the melting capability of the horizontal surface; on a north-facing, 16° slope the factor is only 0.14, so the 24-hour average solar radiation on that slope is only 10.4 W m^{-2}, or 14% of the horizontal slope radiation. If one considers the radiation loading ratio of south-facing to north-facing slopes, the differences become even more pronounced. For example, on January 1, the ratio of radiation loading on a south-facing, 16° slope to a north-facing slope is 12.8 (=1.79/0.14). That means there is 12.8 times more radiation received on a south-facing slope than on a north facing slope. This radiation difference translates proportionally into melting differences between south- and north-facing slopes. In the example given above, for an old snow with an albedo of 0.4, this radiation load would result in the snow water equivalent melting of 20 mm (0.79 inches) on a south-facing slope, 11.2 mm (0.44 inches) on a horizontal surface, and 1.6 mm (0.06 inches) on a north-facing slope. Of course, convection, conduction and longwave radiation are other melt terms, but when temperatures are below freezing these factors contribute to little or no melting, and when temperatures are above freezing, as shown in Figure 3.6 above, elevation does not make a significant difference. If anything, the north-facing slopes would tend to be colder because there is less radiation heating of the surface to heat the air directly above it, which would exacerbate the already existent difference between melting rates on north and south-facing slopes. As a result spatial variability in

melt rates are much more strongly tied to slope and aspect within the study area than they are to elevation. This supports the results found in the satellite images shown in section 3.1 (Figures 3.1-3.5), where melting begins on the south-facing slopes of the middle region of the study area (eastern and central corridors). Snow is retained in the vicinity of Reisenauer Hill owing to greater accumulations in that region.

The following photographs illustrate this north-south radiation snowmelt phenomenon within the study area. The photographs were taken on March 15, 2006 following a relatively light snowfall, which fell between 1:00 and 1:30 a.m. at all three sites in the study area. During the same time, 0.5 inches of snow fell at the UI Plant Sciences Farm, which was equal to 0.06 inches of Snow Water Equivalent, or liquid water depth. Light snows like this are more relevant to an intercomparison of EC and WC, because they show the strong dominance of radiation loading due to slope-aspect differences compared to convection or condensation snowmelt. Furthermore, if a heavy snow occurs, say 2 or more inches, at the time of occurrence generally the entire area receives snow (see Landsat image Figure 3.5), it would pose similar driving hazards across the entire study area, and before there was time for it to melt from roadways, snow would be removed by plowing. Snow removal tends to equalize the duration of snow on roadways despite longer persistence of snow in the natural environment in some areas compared to others. That is, persistence of snow on the ground in the natural environment (i.e., prior to construction of one of the alignment alternatives or on land surrounding the roadway), does not translate into persistence of snow on a completed roadway.

Photograph 3.1. View toward the northern side of the bench of the eastern corridor of the study area showing fresh snow on the north-facing slopes, March 15, 2006 (DSC_0100).

Photograph 3.1 was taken from the south side of Moscow, looking south toward the bench of the eastern corridor of the study area showing fresh snow on the north-facing slopes. Pape' Machinery, Inc. sits in the right foreground, and the buildings in the center of the photograph are on Palouse River Drive, just east of U.S. 95. The low lying ground in the center of the photograph has an elevation around 2550 feet above mean sea level, and the high area on the left side of the photograph, just at the edge of the tree line is approximately 3100 feet amsl.

Photograph 3.2 was taken near the cell tower at Reisenauer Hill looking northward, toward the south-facing side of the eastern corridor bench. This is the backside of the slope shown in photograph 3.1. No snow is visible anywhere in this photograph, because everything within view of the camera, which was pointing north, had a southern exposure. Hidden Village lies in the foreground at the bottom of the hill at an elevation of about 2750 feet amsl; the right side of the photograph goes up to an elevation of about 3100-3200 feet amsl.

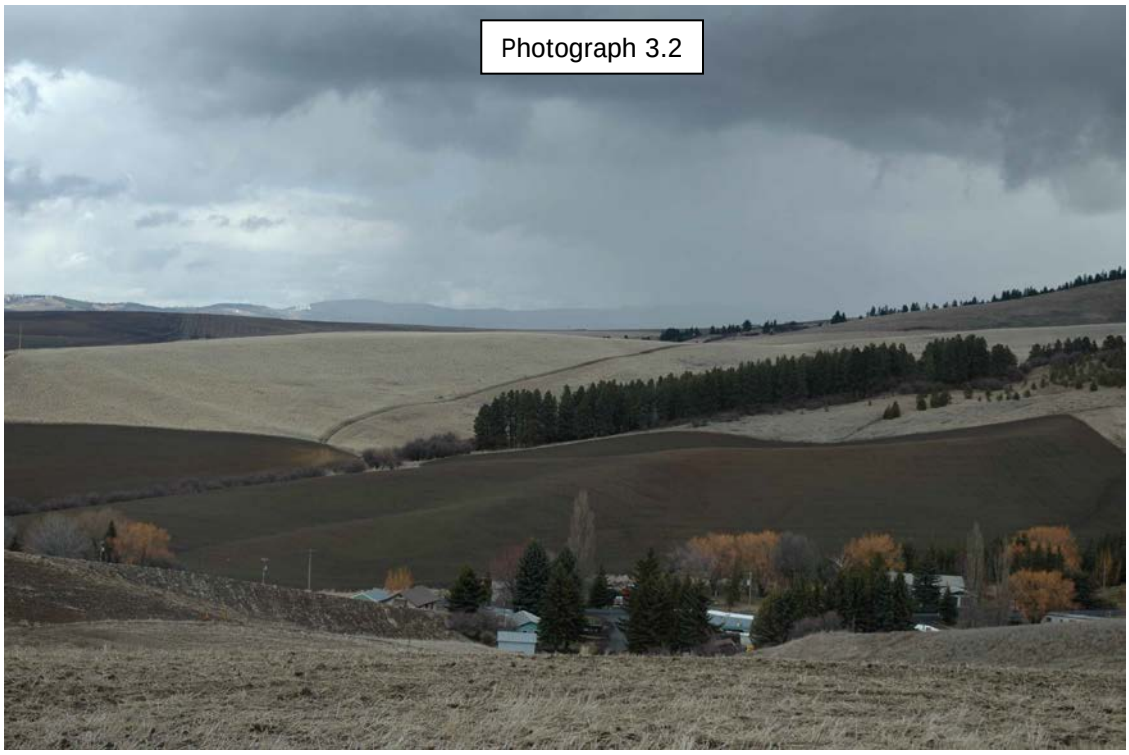

Photograph 3.2. View toward the southern side of the bench of the eastern corridor of the study area showing south-facing slopes devoid of snow March 15, 2006(DSC_0132).

The next two photographs are from the western corridor of the study area, along Snow Road. Photograph 3.3 points south, looking at north-facing slopes, and some flat ground. The snow-covered ridge running East-West across the foreground of the photograph has an elevation of about 2560 feet amsl on the right side of the photograph; the north-facing slopes in the background are also snow-covered.

Photograph 3.3. Southward looking view from Snow Road toward north facing slopes in the western corridor, and in the southern portion of the study area March 15, 2006 (DSC_0106).

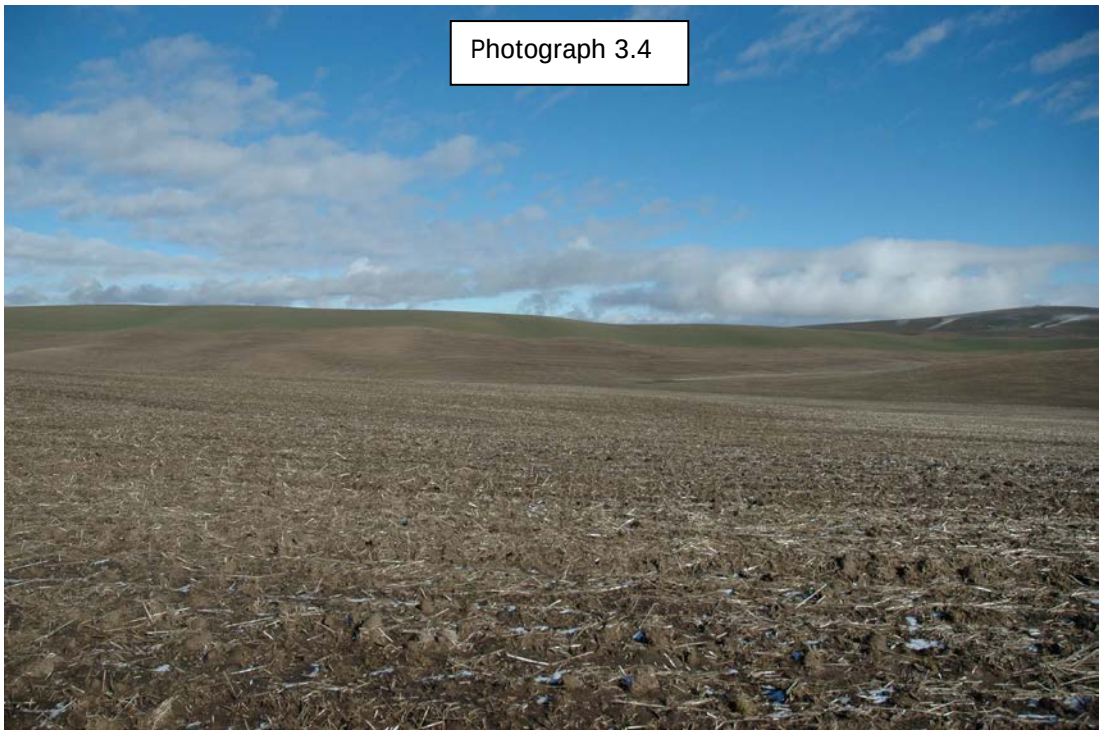

Photograph 3.4. Northward looking view from Snow Road toward south-facing slopes in the western corridor March 15, 2006 (DSC_0105).

Photograph 3.4 contrasts photograph 3.3. It was taken from the same point as 3.3, but shooting toward the north with south-facing slopes in view. The photographs were taken within the same one minute interval.

Photograph 3.5 shows an eastward looking view of the eastern corridor from Zeitler Road. Here the contrast between either flat or south-facing slopes, and slopes with a north-facing aspect is evident. The snow covered slopes face northwest. Since the photographs were taken before 10 a.m., the sun was still to the east, so that northwestern slopes had not yet been exposed to direct solar radiation. Note that flat and south-facing slopes both in the low-lying foreground, and at higher elevations in the background are free of snow.

Photograph 3.5. Eastward looking view from the beginning of Zeitler Road, right after the turn off from U.S. Highway 95 March 15, 2006 (DSC_0111).

The only view of the study area from the City of Moscow is of the slope leading up to the highland bench of the eastern corridor. The western corridor is hidden behind Clyde Hill, and the Highland Flow Around area occupying the southern one-third of the study area is hidden either by Clyde Hill or by the highland bench of the eastern corridor, depending on the viewing location. As a result of the affect of slopes and aspects on radiation loading, what one sees from Moscow is predominantly a north-facing slope. This remains snow covered for a larger percentage of time than the low

lying valley along Palouse River Drive because of the levelness of the bottom of the valley, which increases its radiation exposure, more so than because of its elevation. The south slope of the eastern corridor bench, is often free of snow because of its radiation exposure, even though it is at higher elevation. The ramification of this is that the appearance that there is frequently snow on the eastern corridor highland bench when there is none at the lower elevations is misleading; the anecdotal evidence indicates a higher frequency of snow at higher elevations compared to the lowlands than actually occurs.

Coming back to the initial concern regarding the observation of snow on Paradise Ridge and the bench of the eastern corridor, the evidence may be summarized as follows: Sometimes the snow level will occur between the high point of the eastern corridor and the low point of the western corridor, when the freezing point happens to be located between those two elevations and precipitation is occurring. However, given the thermodynamics governing the stability of the atmosphere, the temperature difference between the EC and WC sites cannot be sustained at much more than 2°F with WC warmer than EC for extended periods of time (see Temperature section below). This small temperature difference limits the window of opportunity for snow to occur on the eastern corridor highland when it rains in the lower western corridor. There is much greater opportunity for it to snow across the entire study area, or to rain across the entire study area. The snowmelt model and measurements within the study area, show that the convection, conduction and radiation melting mechanisms do not exhibit significant variation with elevation, but that radiation loading contributes significantly to spatial variation of snowmelt as a result of slope and aspect. For the same amount of initial snow cover, south-facing slopes melt earlier than north-facing slopes. Significant differences in initial snow accumulation can cause snow to persist longer in some locations even when they have higher melt potential. This occurs south of Reisenauer Hill. Due to its leeward or downwind location, it appears to receive greater snow accumulation as explained earlier from the scientific literature. This explains the longer retention of snow south and east of Reisenauer Hill, as seen in satellite images, than its southern exposure would suggest would occur. Satellite images and photographs taken within the study area support these conclusions.

4 Air Temperature

Air Temperature influences a number of phenomena relevant to this study including formation of precipitation, the form of precipitation as either rain or snow, persistence of snow or ice on the ground, and deposition of frost. Air temperature and its spatial variation are discussed below.

4.1 Lapse Rate

The decrease of atmospheric temperature with elevation, or temperature lapse rate, is familiar to most people. The temperature lapse rate with elevation is a reasonably well-understood thermodynamic phenomenon. Under well-mixed conditions, for example during windy weather or when there is strong heating of the surface by the sun to produce significant convection, the lapse rate is generally positive, where a positive lapse rate means the temperature decreases, or "lapses", with increasing elevation. The thermodynamics are developed by combining the equation of state of an ideal gas, the first law of thermodynamics, and the hydrostatic approximation which governs the rate of change of pressure with elevation (Iribarne and Godson, 1981). The full development of these goes beyond the scope of this report, but suffice it to say that if a parcel of air were to ascend up through the atmosphere, the atmospheric pressure which surrounds that parcel would decrease with elevation because there is less weight of air piled above the parcel the higher it goes. From the ideal gas law, as pressure decreases, so does temperature. As a result, a parcel of air which is raised without exchanging heat with its surroundings, has its temperature decreased with height. This process is known as adiabatic expansion for an ascending parcel of air, and adiabatic compression for a descending parcel.

The actual rate at which this lapse occurs depends on whether the parcel of air is dry (i.e., unsaturated) or saturated. In the dry case, the lapse rate is about 0.00548 °F/ft, and in the moist case, the lapse rate is about 0.003018 °F/ft (Dutton, 1986). The dry adiabatic lapse rate represents the upper limit to the absolute rate of temperature decrease of the atmospheric column with height, due to hydrostatic stability of the atmosphere (Barry, 1992). Actual environmental lapse rates may exceed this such as results from strong surface heating, but this produces unstable conditions which result in mixing and drives the lapse rate back toward the dry lapse rate (or the saturated lapse rate for a saturated atmosphere).

4.2 Temperature Comparison

For the 400 foot elevation difference between the Eastern Corridor station, EC, and the Western Corridor station, WC, these lapse rates translate into differences between WC and EC of 2.2 °F for dry air, and 1.2 °F in the saturated air case, with WC warmer than EC. The dry case represents the largest temperature difference that can be sustained; If the temperature difference gets larger than these numbers, e.g., if the temperature

at the lower station, WC is more than 2.2 °F warmer than the air at the EC station, the air parcel at WC would become less dense and therefore lighter than the air at EC. When lighter air resides below more dense air, buoyancy drives the lighter air upward, in the same way that buoyancy causes a ball which has been forced to the bottom of a swimming pool to float upward. This buoyancy causing mixing, and restores the proper temperature lapse rate in the atmospheric column. The time scale for this to occur is generally about 15 minutes.

The saturated air case is of greater interest because the temperature differences are most relevant to this study during precipitation events. When precipitation is occurring, the humidity of the air will tend toward saturation, thus the temperature difference between EC and WC will be closer to 1.2 °F than 2.2 °F. This reduces the frequency of events when it snows at EC and rains at WC.

In our measurements, there were limited cases amounting to only a few percent of the time, when WC was warmer than EC by more than the 2.2 °F prescribed by the dry air lapse rate. This can occur, for example, when the sun shines at WC, and EC is shaded by clouds, causing the surface and air to be warmed more at WC than EC. WC was warmer than EC by 3 °F or more only about 3% of the time, and 5 °F or more only 0.01% of the time throughout the entire nineteen months reported in the climate study. The average difference when WC was warmer than EC was 1.76 °F which is very near the midpoint between the dry and moist air lapse rate temperature differences. The fact that the average temperature difference between the two stations lies very close to the midpoint between a very narrow range of expected temperatures provides significant confidence in the accuracy and precision of the measurements.

Figure 4.1 plots the temperatures at EC against the corresponding temperatures measured at WC. The solid line represents the one-to-one slope along which temperatures at the two sites were equal. Points above this line have EC colder than WC. Points below the line have WC colder than EC. The vertical and horizontal dashed lines represent the freezing temperature at EC and WC, respectively.

As is apparent from Figure 4.1, there are many points with WC colder than EC, and the temperature differences are much larger when WC is colder than EC. The upper limit imposed by buoyancy constraints on the temperature lapse rate as to how much warmer WC can be than EC is clearly shown by how tightly and uniformly the points above the 1:1 line lie in proximity to the line.

It is very important to note how small the upper limit to the sustained temperature difference between the WC and EC stations is in relation to the possibility of producing sub-freezing temperatures at EC while WC is above freezing. In Figure 4.1 this situation corresponds to the region in the graph above and to the left of the intersection of the two dashed lines demarking freezing temperatures (32°F). Given the narrow, lapse rate imposed range of the temperature difference when WC is warmer than EC,

i.e., 2.2°F, both temperatures must be very near freezing in order to produce the situation where WC is above freezing and EC is below. This significantly reduces the frequency with which this occurs, and is demonstrated by how few points occupy the upper left quadrant in Figure 4.1. Of course if the stations had a much larger vertical separation, such as between the city of Moscow and the top of Moscow Mountain, the temperature difference would have the potential to be much larger, 7.9 °F to 14.4 °F, for the saturated and dry adiabatic expansion cases, respectively. In this case the opportunity for Moscow Mountain to be below freezing while the city of Moscow is above freezing is greatly increased simply owing to the greater difference in their temperatures.

Figure 4.1 Air Temperature EC and WC

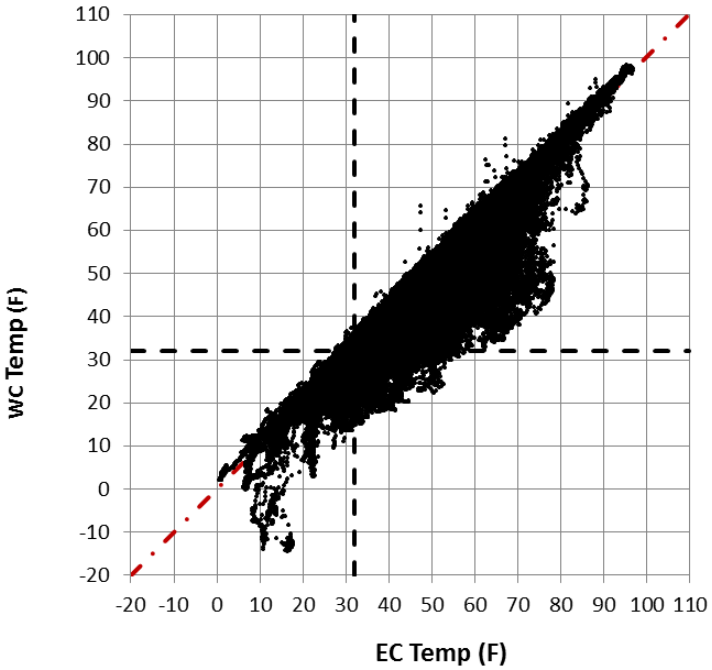

Figure 4.1. Scatterplot of air temperature at EC versus WC.

There is another opposing factor to the positive lapse rate described above. In the evening, the surface and near surface air begin to cool. If this occurs non-uniformly in space, then some air ends up being cooler than other air. By the ideal gas law, the cooler air is more dense. This dense air will sink to the ground and "flow" downhill, just as water does during a heavy rainstorm. This cold air drainage, known as a "katabatic" wind, follows the topography sinking to the lowest spot accessible from its point of origin, pools there, and produces a negative lapse rate, in which the temperature is colder at lower elevations than at higher elevations. This phenomenon does not require a large scale inversion to be in place to occur and occurs over land sloping more than

about 2°, and it will generally occur at night unless there is regional wind in excess of 11 mph present to prevent it (Linacre, 1992). It regularly happens at night, and occurred throughout the measurement period with great frequency. The magnitude of the temperature difference will be larger when clear skies exist owing to greater radiative cooling of the surface, but clear skies are not required for katabatic winds to occur.

This cold air drainage phenomenon is apparent from all the data that lie below the one-to-one sloped solid line. The area of Figure 4.1 which is of particular interest here is the lower right quadrant, which represents points where temperatures are sub-freezing at WC, and above freezing at EC. There are numerous points in this region, and the temperature differences between WC and EC are much more extreme.

Once this stratification is established, it produces very stable conditions which require an external energy input to be broken up. Thus once it is established, it often persists. The breakup can occur either by the external imposition of wind such as from the passing of a front, or by heating of the ground which warms the cold air, so that it then mixes upward with the air aloft due to buoyancy, and restores the positive lapse rate discussed above.

Cold air drainage is not subject to the same buoyancy-driven maximum temperature difference limitation as adiabatic expansion. The lower elevation site can become much colder than the upper site.

Comparing the relative frequencies with which EC was below freezing, and WC was above (upper left quadrant) and vice versa (lower right quadrant), reveals that during the study period, the data fell in the upper left quadrant about 1.9% of the time, and in the lower right quadrant about 3.8% of the time; thus WC was sub-freezing while EC was above freezing about twice as often as the converse situation. In addition, when WC was below freezing and EC was above, the average temperature difference between them was 10.9 °F, whereas when EC was below freezing and WC was above, the average temperature difference between the two was only 1.97 °F. In other words, WC gets much colder than EC. Furthermore, even if the mean temperature or the region was warmer or colder, as it might be in a different year, this would only shift the temperature data set diagonally up or down along the one-to-one line, and would not appreciably change either the numbers of hours in each category, or the relative frequency with which they occur. The region of “space” on the graph, the upper left quadrant, is simply too restrictive for there to be a large quantity of hours subject to EC below freezing with WC above. This makes the observations during the measurement period relevant as a general climate statistic applicable to other years.

The RH weather station was located at a similar elevation as EC, both of which were a few hundred feet of elevation above WC. A plot of air temperature at RH versus WC shown in Figure 4.2 bears the same characteristics as the one of EC versus WC,

namely, 1) the tight limit above the one-to-one line indicating that the air temperature at WC is constrained not to become substantially warmer than RH due to buoyancy considerations governing the dry and saturated adiabatic lapse rates, and 2) WC is often much colder than RH due to cold air drainage.

Figure 4.2 Air Temperature RH and WC

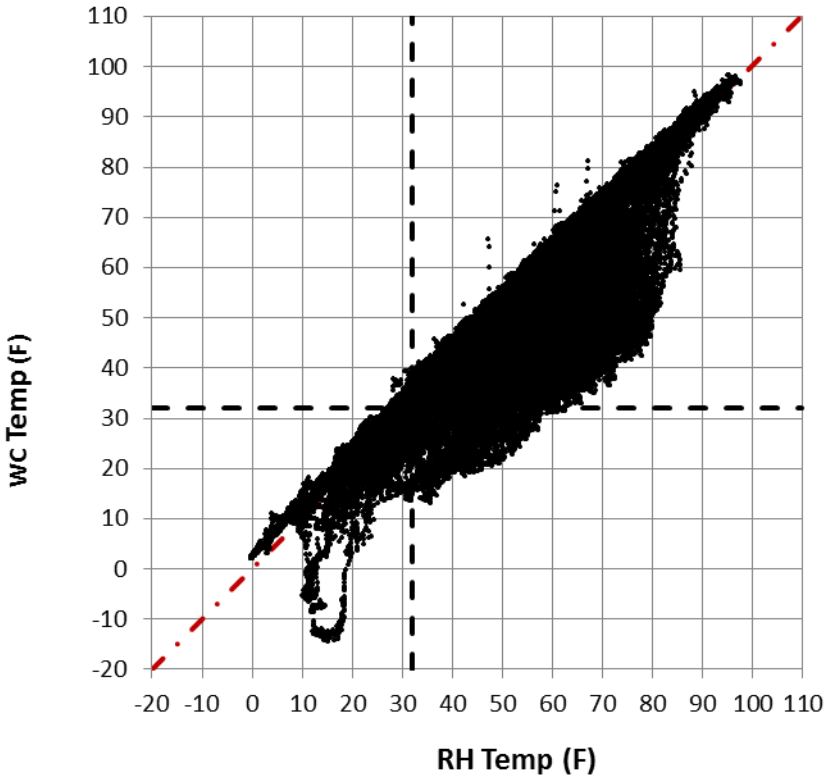

Figure 4.2 Scatterplot of air temperature at RH versus WC.

An air temperature plot of RH versus EC shown in Figure 4.3 looks very different from plots involving WC. The plot is very symmetric and much more tightly packed around the one-to-one line. This shows the similarity in temperature between the EC and RH stations which are located at similar elevations. There is some evidence of cold air drainage at EC which is not manifest at RH. EC experiences a limited amount of cold air drainage from air flowing down off of Paradise Ridge, which RH does not because RH occupies a near top-of-hill location. However, at EC this cold air drainage only manifests itself when temperatures are above about 50 °F, and does not involve sub-freezing temperatures at either EC or RH.

It is also useful to note that due to the relatively short vertical separation between all of the weather stations, that most of the time when freezing temperatures occur, it is below freezing at all three sites, so that a similar number of hours of freezing

temperatures occur at all sites. For example, during the nineteen month period of measurement, temperatures were below freezing 22.3%, 20.6% and 22.2% of the time at WC, EC and RH, respectively.

Figure 4.3 Air Temperature EC and RH

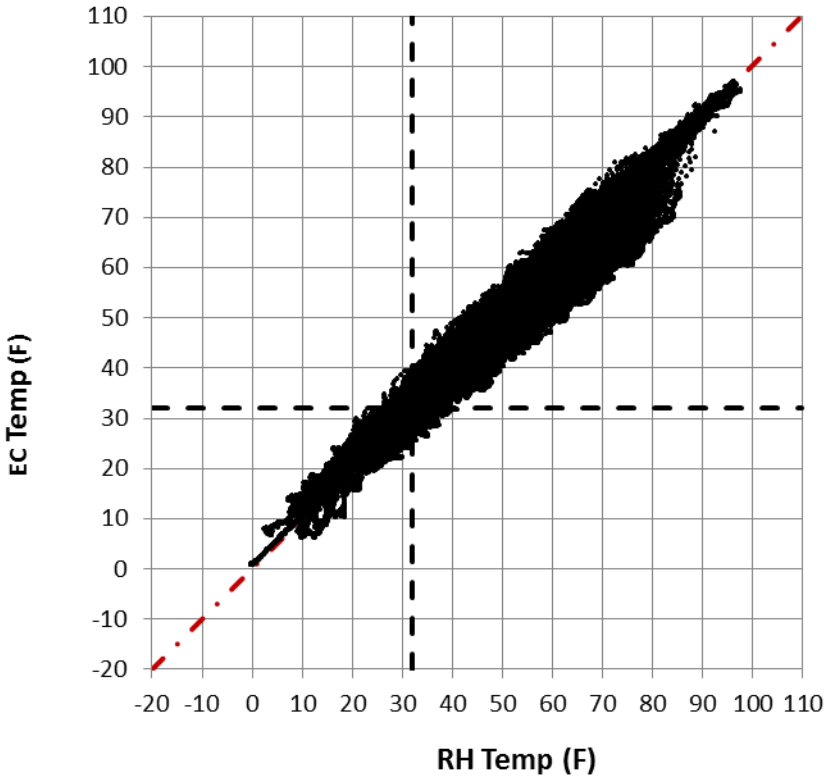

Figure 4.3 Scatterplot of air temperature at RH versus EC

The air temperature and lapse rate discussion can be summarized as follows. When the air is well-mixed either by wind or by convection such as results from heating of the land surface, one can usually expect a positive lapse rate, that is a decreasing temperature with increasing elevation. The greater the vertical distance, the greater the temperature difference. The 400 foot vertical separation between the EC and RH with respect to WC was large enough regularly to produce an average difference of 1.8 °F (calculated including only values of the temperature difference in which EC and RH were colder than WC), which closely matches the theoretically expected difference of between 1.2 and 2.2 °F. This small difference limits the frequency with which the situation occurs where EC or RH are below freezing and WC is above freezing. Cold air drainage can occur year round, generally occurs at night, and produces a stable temperature profile with cold temperatures at lower elevations. The temperature differences between the upper elevation site and lower elevation site can be much larger during these cold air drainage periods than the differences corresponding to the

case where the upper elevation site is cooler. Even though temperature differences occur among the sites, the largest fraction of the time, all sites are either above freezing or below freezing simultaneously so that the entire study area is subject to the same kind of freezing/non-freezing conditions. One important implication of this is that during winter storm conditions, one can expect similar durations of freezing temperatures across the study area.

4.3 Frost

In addition to air temperature by itself, the combination of freezing temperatures together with relative humidity values equal to 100% is considered as an indicator of frost or ice with the potential to produce slippery road surfaces. Freezing air temperatures do not provide a perfect assessment of freezing surface conditions. Greater accuracy could be obtained with either some measure of the surface skin temperature, or by means of a complete surface energy balance. However, these other measures are not perfect either, since they would provide spot measurements, and surface temperature exhibits a great deal of spatial variability. Furthermore, pavement possesses different thermal and radiative properties than vegetation or soil, and no pavement was present at any of the measurement sites. At night, there is generally a net radiative energy loss from ground surfaces, which causes the ground to be colder than the air above it; the opposite is true during the daytime when the sun is shining on the ground. Usually relative humidity values of 100% occur either at night or under cloudy conditions, which eliminate or reduces the heating of the ground surface. Therefore, freezing air temperatures provide a conservative representation of frozen ground conditions, meaning that freezing air temperatures will not overestimate the occurrence of frozen ground.

As noted earlier, the primary concern with freezing temperatures relates to icing of roadways. In this regard, freezing of dry, bare roadways does not pose a problem. Instead, the concern is with freezing of wet roadways or deposition of frost. One of the ways that this occurs is from condensation of saturated air, which forms frost at sub-freezing temperatures. In the absence of sensors to detect frost directly, we rely on the combination of sub-freezing temperatures and relative humidity values equal to 100%.

The percentages of total hours during different portions of the year which are conducive for frost or road ice formation are shown in Figure 4.4. As expected, the winter half-year has a greater potential for road ice formation than the summer half-year. During the winter, the low elevation WC site exhibits a slightly greater percentage of freezing temperatures with saturated air than either EC or RH. In the summer half-year during the measurement period, WC alone exhibits this characteristic. In both half-year periods this can be attributed to cold air drainage pooling in low lying areas and causing a modestly greater frequency of saturated air conditions in these low

lying areas. These “frost pockets” are commonly observed around the Palouse, nevertheless, the annual percentage difference among the three sites is not great.

Figure 4.4 Freezing with 100% Relative Humidity

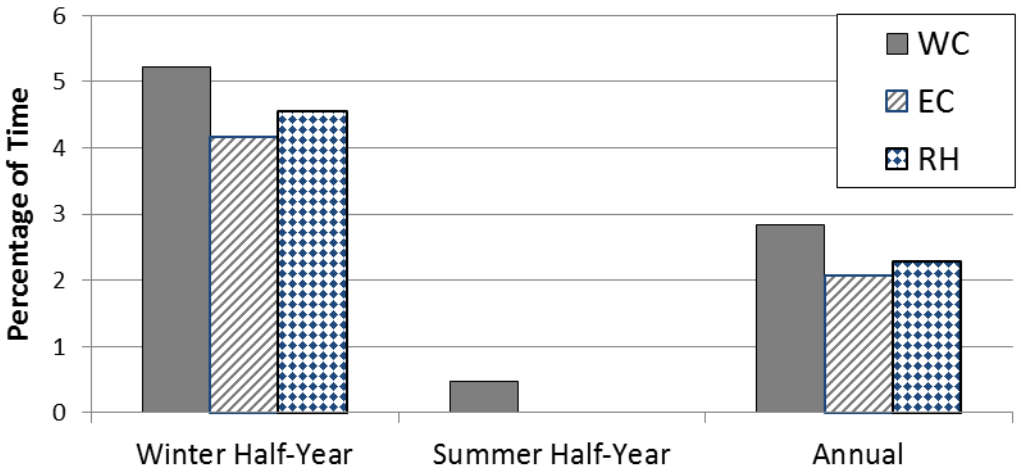

Figure 4.4. Percentage of total hours in which sub-freezing temperatures occur simultaneously with saturated air conditions during the Winter (October-March) and Summer (April-September) half years and annually as an index to frost or road ice formation potential.

5 Wind

Drivers of the Palouse regularly experience windy conditions in the winter and make adjustments, regardless of where they drive. Out of more than 300 vehicle accidents reported between 2001 and 2010 over the existing US Highway 95 between Thorncreek Road and Moscow, only 4 include wind as a contributing factor. None of these were semi-trucks.

Nevertheless, wind was measured at three stations, whose locations are shown on the Study Area Map of the Climate Report (Qualls and Zhao, 2005), and on the ITD alignment maps. These included one station in each of the three climate regimes, Highland Flow Around (HFA-RH), Highland Flow Over (HFO-EC), and Lowland Flow Over (LFO-WC), as defined in the Introduction. The stations were designated RH (Reisenauer Hill), EC (Eastern Corridor) and WC (Western Corridor). The protocol used for measurement of wind speed was to place the sensors at the top of each tower, at 30 feet above ground level, to avoid interference of the tower structure itself on the measurements, and to ensure compatible measurements at each site. The results are shown in Table 5.1 and in Figures 5.1-5.

Table 5.1 Wind Data	HFA-RH	HFO-EC	LFO-WC
Fastest Individual Gust (mph)	66.0	50.3	54.4
Fastest Individual 5-minute Average (mph)	57.9	41.6	43.4
Average of 5-minute Gusts (mph)	13.6	11.1	9.3
Average Wind Speed (mph)	11.4	8.2	7.1

The wind data collected as part of this study and summarized in the Table 5.1 contributes important information to the comparison of wind in the three climate regimes included in this study. The data were taken from the measurement period January 2005 through July 2006. Given the close proximity of all three sites, and the fact that wind storms are large scale phenomena, these data provide a very good spatial intercomparison among the three stations, RH, EC, and WC, and the major climate regimes of the study area (namely, Highland Flow Around (HFA-RH), Highland Flow Over (HFO-EC), and Lowland Flow Over (LFO-WC), as defined in the Introduction. Since wind storms are large scale phenomena relative to the size of the study area, the predominant factors that affect the relative speeds of winds observed in various parts of the study area are topographic features, most notably Paradise Ridge itself, and local roughness elements (e.g., clumps of trees serving as wind breaks). Stations were placed to capture the influence of large scale topographic features of the study area and to avoid the influence of small-scale local roughness elements (e.g., trees). This data should be interpreted as providing relative behavior of wind rather than absolute long-term averages, or anticipated maximum winds.

To illustrate the relative magnitudes of the winds in the three climate regimes, a series of figures display data of the maximum gust observed during each 5 minute interval

throughout the 2005-2006 measurement period. The data represent the fastest gust wind speed observed in each five minute period, and therefore exceed the mean for each of the corresponding five-minute periods. Figure 5.1 presents a histogram of the percent of gusts whose speeds fell within a specific range of speeds, in 5 mph increments, at each of the three sites.

The National Weather Service (NWS) issues "Wind Advisories" for sustained winds over 25 mph (http://w1.weather.gov/glossary/index.php?letter=w). At the sites measured in this study, on average gust speeds are approximately 20% larger than 10 minute wind speed averages. Therefore gust speeds of 30 mph or greater correspond to sustained wind speeds of 25 mph or greater, and would be typical of wind speeds warranting a Wind Advisory from NWS. Therefore, the following discussion focusses on gust speeds 30 mph and greater.

Figure 5.1. Wind Gust Speeds

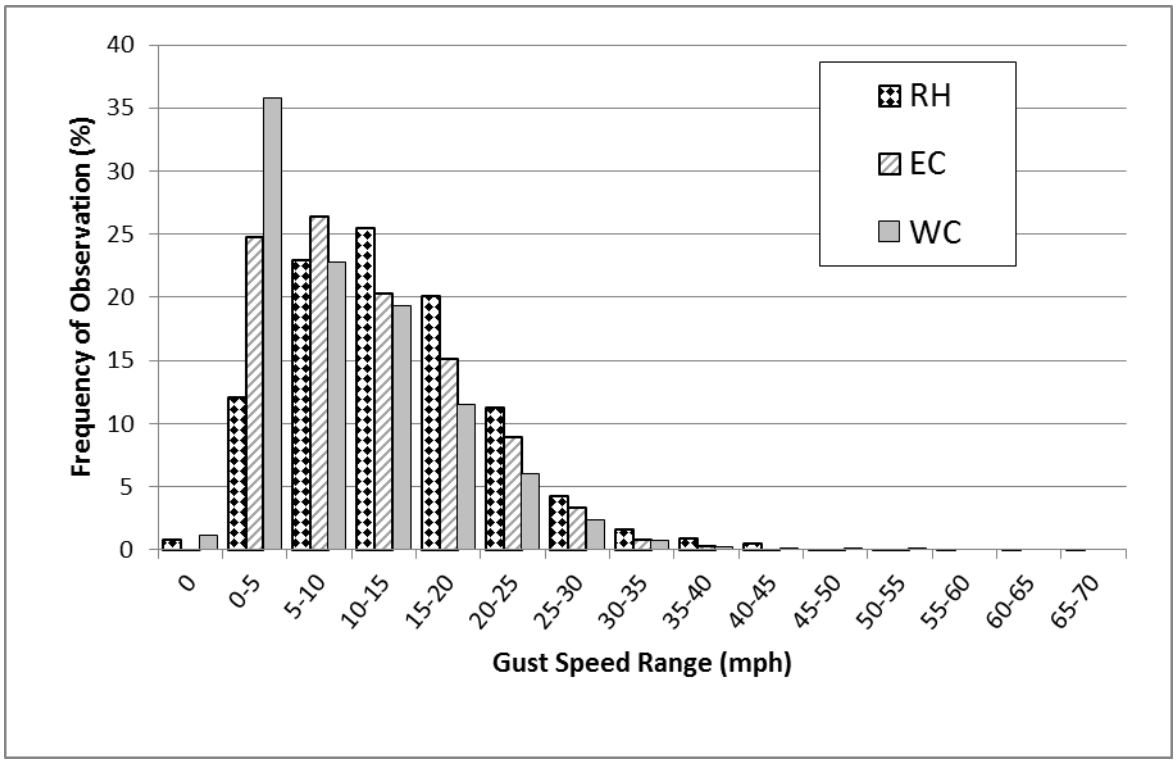

Figure 5.1. Histogram of wind gust speeds at the three measurement sites. The frequency of observation refers to the percentage of the five minute intervals during the 2005-2006 measurement period in which a gust within the specified range occurred.

The greatest percentage of gusts did not exceed 30 mph. Cumulatively, 99% or more of the gusts were slower than 30 mph at the EC and WC stations. At RH, 97% of the gusts were slower than 30 mph. However, the absolute magnitude of the gusts is not important for the present purpose. Rather, the important information to extract from this figure is the relative magnitudes of the gusts among each of the three sites. In any

given year, the bulk of the data will probably lie in the 30 mph and lower range, as it did in 2005-2006. At the upper end of this range, say from 25-30 mph, drivers need to and do exhibit greater caution, as evidenced by the low number of wind-related accidents noted above. Nevertheless, it is the upper-tail area of the histogram that is important for the purpose of this study. In order to focus on this more extreme data, it is reproduced in the Figure 5.2, with an exaggerated vertical scale, which ranges from 0 to 1.8%, and includes only the ranges of data in excess of 30 mph.

Regardless of the actual magnitudes of the data in Figure 5.2, one can see that the frequency of occurrence in each bin or range is similar for the EC and WC sites, and the frequency of occurrence in each of these "high speed" bins is larger for the measurements at RH. Furthermore, the highest gust speed at RH is 10 to 15 mph faster than at EC and WC. The differences in gust speeds among the three measurement stations may be examined in more detail by means of scatter plots of gust speeds. Figures 5.3 and 5.4 below show scatter plots of the gusts at RH versus WC and RH versus EC, and the Figure 5.5 shows EC versus WC.

Figure 5.2. Upper Tail Wind Gust Speeds

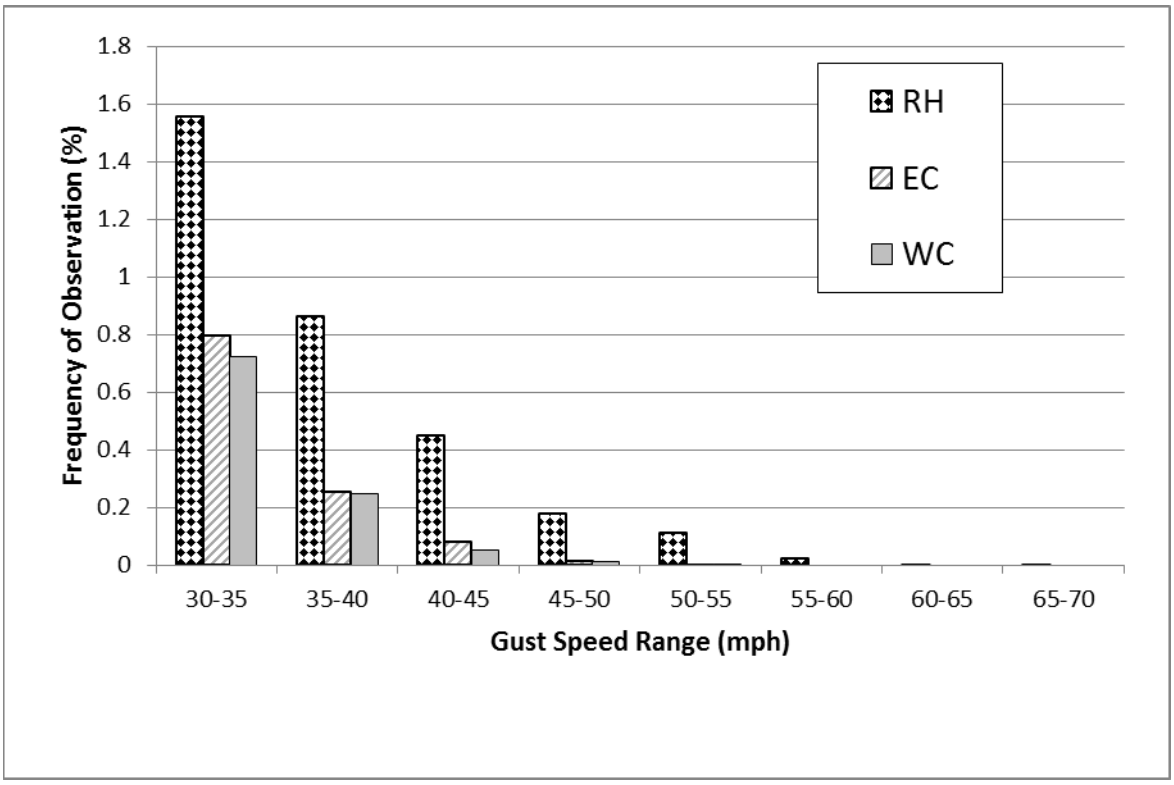

Figure 5.2. Histogram of the upper-tail of wind gust speeds, for gusts in excess of 30 mph.

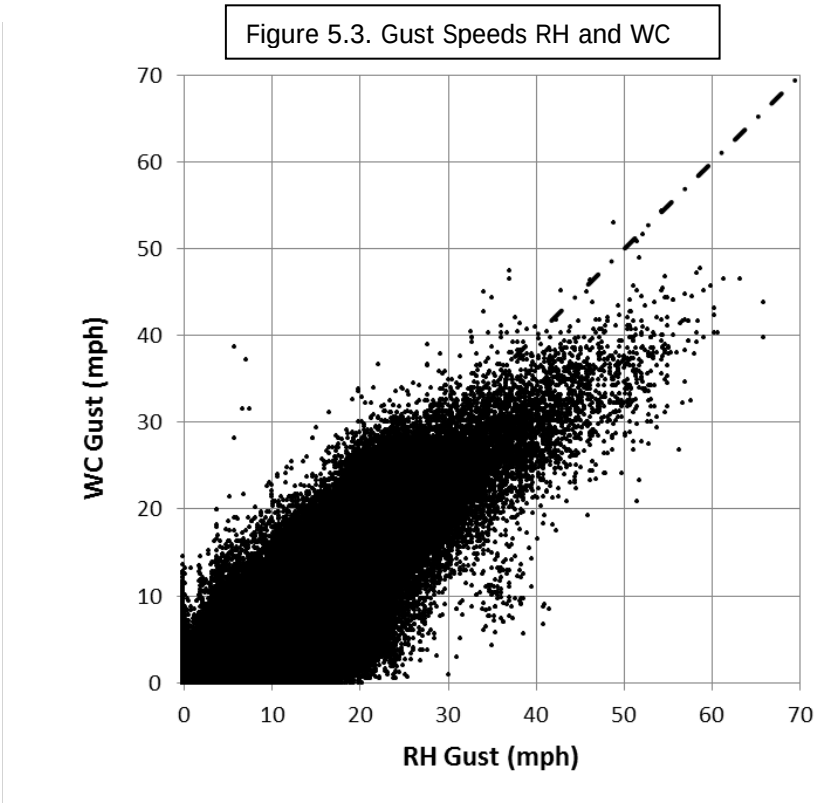

Figure 5.3. Scatter plot of gust speeds at RH versus WC.

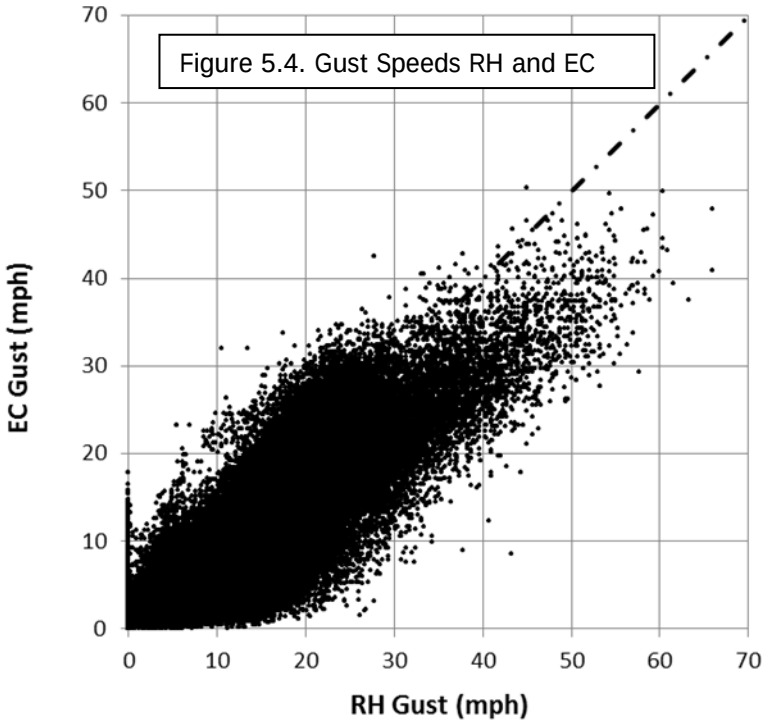

Figure 5.4 Scatter plot of gust speeds at RH versus EC.

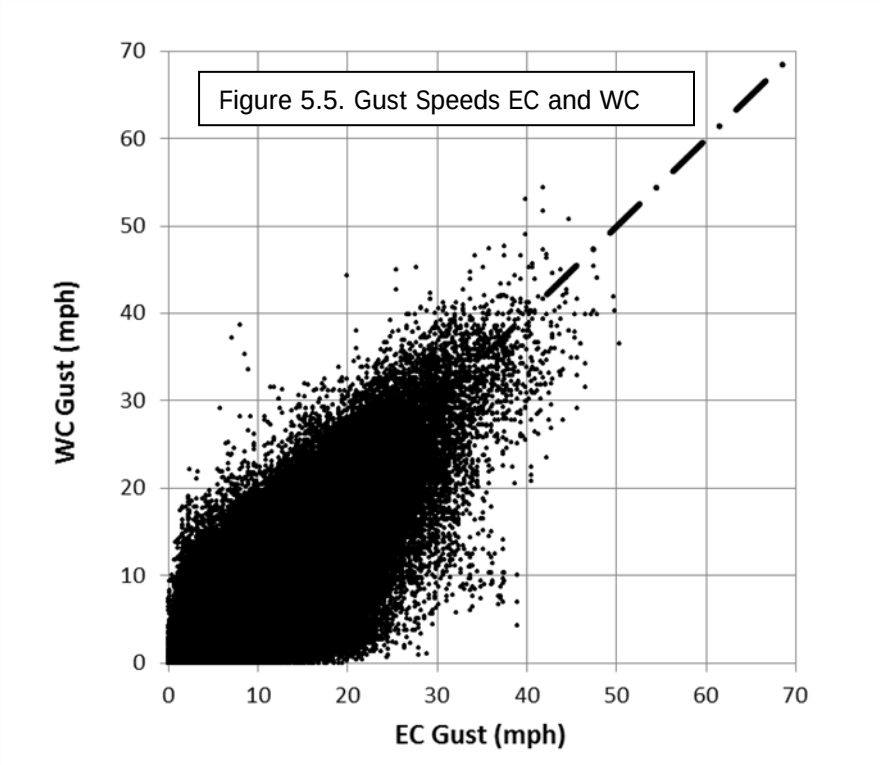

Figure 5.5 Scatter plot of gust speeds at WC versus EC.

Each data point on Figures 5.3 through 5.5 is an ordered pair consisting of the peak gusts measured at the two sites indicated on the axes of each graph during the same 5-minute interval. Each of these figures includes a diagonal line with 1:1 slope through the origin. Data points that lie above this line correspond to times when the gust speed at the site indicated on the vertical axis exceeded the gust speed of the site indicated on the horizontal axis. Conversely, data points that lie below the 1:1 line correspond to faster gusts measured at the site indicated on the horizontal axis compared to the site indicated on the vertical axis. The discussion which follows focuses on gusts in excess of 30 mph. Nearly all wind gusts in excess of 30 mph come from a westerly direction (centered on 250° at EC and RH, and 270° at WC), except RH has some gusts up to 38 mph which come from the east (80°). In Figure 5.3 (RH versus WC), the overwhelming majority of the points for which the gusts exceeded a threshold of 30 mph at one or both of the two sites, lie below the 1:1 line, indicating that above this threshold winds are almost always faster at RH than WC. Figure 5.4 shows a similar result in the comparison between RH and EC. Namely, above the threshold winds are almost always faster at RH than at EC. In both cases, RH gusts exceed the gusts at the other two sites, sometimes by as much as 20 mph, but never by much more than that. Figure 5.5 compares the gust speeds at EC and WC. At these two sites, when wind speeds exceed 30 mph, there is a slightly higher proportion of occurrences where the gusts at the WC site exceed those at the EC site, but generally not by more than about 10 mph.

The general characteristics of the three sites are as follows: RH is a highland site whose predominant wind patterns move around the southern end of Paradise Ridge, unobstructed by Paradise Ridge; EC is a highland bench which occupies a toe-of-slope position adjacent to the abrupt ascent up the western side of Paradise Ridge; WC is a lowland site which sits in a relatively flat drainage valley, near the toe-of-slope which begins the ascent up through the central corridor to the sloped bench of the eastern corridor.

Both WC and EC have predominant weather patterns which flow up over Paradise Ridge to the East, and both occupy "toe-of-slope" positions within the local topography. Toe-of-slope locations experience generally reduced wind speeds compared to the large scale mean wind speed. This is supported by wind speed measurements at EC and WC which are slower than at RH whose airflow moves around Paradise Ridge, as well as by Computational Fluid Dynamics modeling (Blackketter et al, 2006).

The data show EC and WC to be more similar to each other, and RH to experience faster wind speeds than either of the other two. Since RH represents the southern portion of the study area, through which the existing U.S. Highway 95 and any possible proposed alternatives must run, it appears that vehicles are already exposed to the most severe wind conditions of the study area, and all of the proposed alternatives will continue to be exposed to these same severe conditions in the southern portion of the study area. Consequently, the effect of wind on vehicles in general, and large trucks in particular, should be no worse than what is currently experienced. The effects of the depth of fill sections on travel lane wind speeds are addressed in Blackketter et al (2006). The conclusions of that study were that depth of fill should not pose a significant problem with regard to wind.

The Central Corridor (CC) lies on the beginnings of the upslope toward the EC bench and has the potential to exhibit "leading edge of shoulder" characteristics. Computational Fluid Dynamics modeling indicates that leading edge of shoulders can experience accelerated wind speeds (Blackketter et al., 2006). However, the presence of Paradise Ridge above the EC bench will likely buffer CC as it does WC and EC, so that its wind speeds are expected to be lower than those of RH to the south.

Toward the northern end of the study area, in the vicinity of Clyde Hill, all proposed alternatives begin to converge as they approach the South Palouse River Drive drainage plain. This plain is oriented roughly east-west, and lies to the north of Paradise Ridge. As the influence of Paradise Ridge to the east diminishes due to reduced elevation, the wind exposure of all alternatives including the existing US Highway 95 is expected to be greater than that of the central third of the study area (WC and EC).

Each of the proposed alternatives will be designed to have an elevated roadbed on fill material. This will produced localized acceleration of wind across the road surface

(Blackketter et al., 2006), which will help prevent accumulation of drifted snow on the road surface.

There may be specific features in this area which locally reduce the wind such as trees along the roadway, or deep road cuts. These can cause their own problems in terms of road ice and snow accumulation, and sudden exposure to wind gusts during transitions from road fill to cut sections, for example.

Measurements at the WC site indicate that portions of the road in low lying areas or valleys experience winds of similar magnitude as those on the bench of the EC site. Thus, the data support the conclusion that all alternative alignments in the Western, Central and Eastern Corridors would experience similar wind speeds among them.

6 Fog

The presence of fog produces considerable driving difficulty. Consequently, measurements of visibility distance were made at each of the three weather stations and are reported below.

Figure 6.1 Visibility Distance

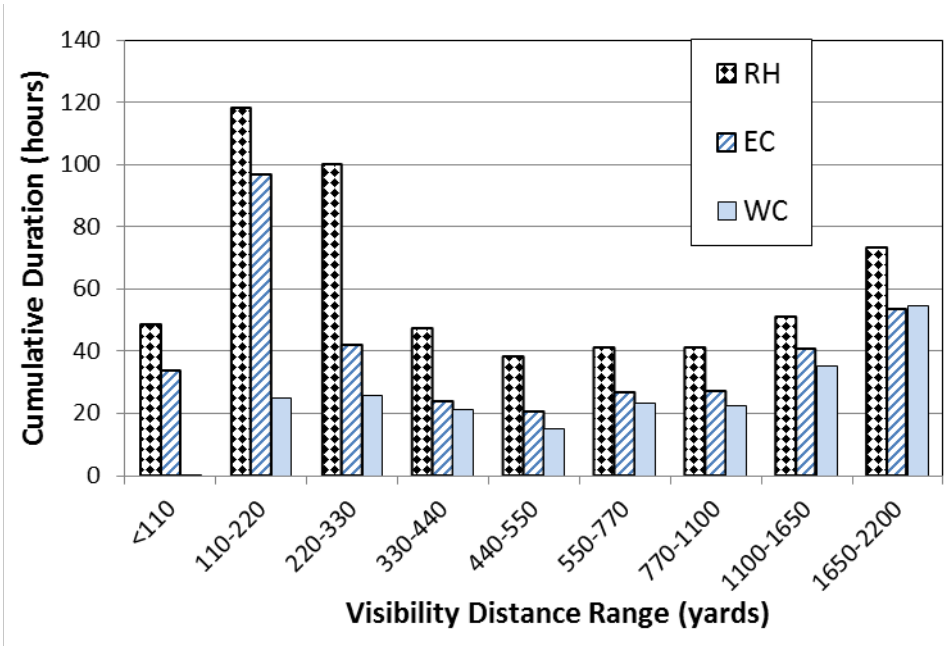

Figure 6.1 Cumulative duration of reduced visibility distance ranges at RH, EC and WC from January 2005 through July 2006. The cumulative time with reduced visibility represents less than 4% of the total time during the observation period.

Figure 6.1 shows visibility distance ranges measured at the three weather stations, RH, EC and WC in the study area. Only *reduced* visibility distance values are shown; values where visibility distance was measured to be 2200 yards or greater are not included on the figure as they represent more than 96% of the total time. The visibility distance ranges in Figure 6.1 show that RH has the worst visibility conditions, followed by EC, and then WC. Elevation likely plays a role in making visibility conditions worse at RH and EC than WC, however, RH has observably worse conditions than EC and these two were located at similar elevations. Thus, higher elevations and the southern portion of the study area were observed to have worse visibility conditions. These results are similar to the relative results reported for the three measurements sites in the original climate report (Qualls and Zhao, 2005).

Visibility distance is only a proxy for traffic accident potential due to fog. A better source of information is available: accident records related to fog. From 2001-2010, four accidents were reported during foggy conditions on US Highway 95 between Thorncreek Road and Moscow. One of these was due to tire defect, and occurred south

of Reisenauer Hill at a location before any of the proposed alternatives will deviate from the existing US HWY 95 No-build alternative. Because it was attributed to a tire defect, it is excluded from this climate discussion. The other three occurred while negotiating tight radii curves on portions of the existing US HWY 95, at low to mid-range elevations. The first accident was at elevation (Z) 2740 feet, radius (R) 955 ft. Plant Sciences Farm had recorded 1.3 inches of new snow on February 16, 2001, the day of this accident. The other two accidents occurred in different years at a single location with Z=2610 ft, R=1146 ft. At the time of the first of these, December 4, 2005, 10, 6 and 11 inches of snow were measured at the WC, EC, and RH, respectively; On December 13, 2007, when the second accident occurred, there was 4 inches of snow at PSF and snow also reported at Reisenauer Hill. Both of these latter two accidents list "Ice" as a road condition at the time of the accidents. With the exception of the accident caused by tire defect, none of the accidents during foggy conditions occurred at high elevations (i.e., near the top of Reisenauer Hill), where measurements show visibility conditions to be the worst within the study area, but rather in mid to low elevation areas of the study area. Thus, although fog was noted at the time of these latter two accidents, the location of the accidents cannot be correlated with the *magnitude* of reduced visibility on the basis of the existing accident records. This is because the few reported fog related accidents occurred in locations which measurements showed to have generally greater visibility distances (lower elevations) rather than at locations within the study area with lower fog-related visibility distances (top of Reisenauer Hill).

The portion of US 95 from the top of Lewiston Grade to Thorncreek Road (hereafter L-T) which has already been realigned provides information which may be used to infer the fog-related accident potential of the proposed alignment alternatives W-4, C-3 and E-2. L-T is a nearly 17-mile long segment which varies along its length within an elevation range of 2700 and 2900 feet above mean sea level. This corresponds to the elevation range designated as "highland" within the study area; that is it corresponds most closely to an elevation range between C-3 and E-2. The study area weather station at Reisenauer Hill (RH) was located just north of the L-T segment of US 95, and the worst fog-related reduced visibility conditions were observed at RH of the three weather stations within the study area, as noted above. Fog commonly occurs along the L-T segment and given its elevation range, together with the fact that it was designed in accordance with current AASHTO standards as are W-4, C-3 and E-2, L-T is the best available surrogate to represent these proposed alignment alternatives of US95 from Thorncreek Road to Moscow, especially the two higher elevation alternatives C-3 and E-2. For the five year, 3 month period from October 2007 through December 2012, only one fog-related accident occurred on L-T (Arnzen (ITD), May 7, 2014, personal communication). This corresponds to approximately 0.01 fog-related accidents per year per highway mile, which is very small.

Collectively, accidents were reported only a few times over a decade with fog listed as a weather condition at the time of accident. Those few which did occur on the existing US 95 from Thorncreek Road to Moscow all occurred at low to mid elevations on tight

radii curves, road ice was also listed in two of them, and weather records indicate that snowfall had also occurred recently preceding each accident. On the US 95 segment L-T which has already been updated to current AASHTO standards, fog-related accidents have been even less common. Thus, fog has not been observed to be a significant producer of accidents either on the existing old Thorncreek to Moscow US95, nor on the reconstructed AASHTO standard compliant Thorncreek to Lewiston segment. Consequently, fog should not be considered a primary factor in selecting a road alignment alternative, owing primarily to the limited number of accidents reported during foggy conditions, together with the fact that other contributing circumstances were reported, specifically negotiation of tight radii curves in the presence of ice. This indicates that the locations of the fog-related accidents were controlled by the location of challenging road characteristics (e.g., curve radii and slopes) rather than the spatial distribution of the severity of reduced visibility conditions. Furthermore, fog accident potential will be further reduced on proposed W-4, C-3 and E-2 alignment alternatives owing to adherence to modern design standards which eliminate many of the curves and lengthen the radii of remaining curves in the roadway, compared to the no-build alternative.

7 Historical Representativeness of Report

This report makes use of on-site weather station measurements within the study area collected from January 2005 through July 2006, satellite images of the study area and the surrounding region collected over the decade-long period from 2002 through 2012, principles of physics, thermodynamics, and published scientific studies, long-term weather measurements from a nearby climatological station, and vehicle accident records spanning the decade from 2001 through 2010. In order to answer whether this report is historically representative, it is important to define what "historically representative" means for the purpose of this study. To do this, the objective of this report is repeated below from the Introduction:

> Study Objective
>
> To characterize the general climate of the region using nearby long-term climatological measurements, to characterize spatial and temporal variability of important weather and climate elements across the study area using on-site weather data, satellite images, and principles of physics, thermodynamics, and other published studies, and to describe the relationship of this variability to relative safety of roadway alignment alternatives or groupings of roadway alternatives.

The long-term climate of the region can be established from the long-term measurements at the University of Idaho Plant Sciences Farm (PSF) station which has more than one hundred years' worth of data. However, variations of weather from one year to another (e.g., a snowy winter or a mild winter) will affect the entire region, so while the long-term climate is important, what is more important for this study is to describe the spatial variability within the study area of weather elements that would affect the relative safety of different highway alignment alternatives or groups of alternatives, particularly W-4, C-3 and E-2. ***Thus, this study may be considered historically representative if it adequately captures the general range of spatial variability across the study area that might be expected to manifest itself over time.***

The emphasis here is on range of local spatial variability across the study area rather than on the range of absolute conditions, the latter of which is a regional rather than local (study area) scale phenomenon. To illustrate this, consider two different winter conditions: one with 8 inches of snow at PSF, and another with 24 inches of snow at PSF. The latter is a more extreme absolute condition, but both would cover the entire study area sufficiently that driving conditions would be hazardous for all alignment alternatives within the study area, and the alignment characteristics themselves (e.g., distance, slope, curve sharpness and length, etc.) and would principally govern the safety of one alternative over another. Measurement of the spatial variability

associated with one of those snow depths would be sufficient to understand the spatial variability of the other, and their significance to driving safety.

As another example, consider two light snow events, one of which deposits a light snow at only upper elevations within the study area (EC and RH) and another which deposits a light snow at all three stations (EC, RH and WC). Conditions such as these were observed during the study period both with on-site weather station measurements and in satellite images, allowing the spatial variability of these conditions and their impact on different alignments to be considered.

Additionally, the spatial variability of many weather conditions (e.g., deposition of snow, melt-off snow, air temperature, wind speed) are influenced at the local scale by physics and thermodynamics (e.g., temperature lapse rate, cold air drainage, or variation of solar radiation loading on hilly topography affecting snowmelt,), behave in accordance with observed behavior from similar regions which has been published in scientific literature (e.g., peak precipitation on short uphill slopes occurs on the lee side of the hill), or can be observed using extraneous data (e.g, satellite images of the study area over a long time period). These principles are time-invariant when properly applied. Therefore, a limited number or period of observations can be made in order to verify adherence of the study area to these principles and studies, and then be used to generalize the behavior of spatial variability within the study area.

The foregoing sections describe observations, principles and other scientific studies which allow the characterization of a wide range of local-scale *spatial variability* of weather and climate conditions across the study area corresponding to a wide range of regional weather conditions, and the relationship of this spatial variability to relative safety of various highway alignment alternatives. Consequently, this study is historically representative.

The foregoing establishes the case that this study is historically representative for its intended purpose. Nevertheless, historical context is also useful. Historical context may be established using the long-term historical records from the Cooperative Observer Station located at the University of Idaho Plant Sciences Farm referred to as PSF.

The records from PSF contain daily data back to the early 1890s, however, Qualls and Zhao (2005) and the information presented below use the more recent 30 year climatological normal period, 1971-2000, according to standard climatological practice, and have included the 2001-2005 data. The daily data set includes precipitation depth, snowfall depth, snow depth on ground at time of observation, maximum air temperature, minimum air temperature, and air temperature at the 4 p.m. PST time of observation. The analyses of these data, and several other variables which may be

inferred from them, such as the number of days in a month with no snowfall, or no snow on the ground, are presented below.

In the analysis, the 2005 winter season PSF data are compared to the 35 year PSF historical record to determine how the 2005 PSF data ranks with respect to the historical record from the same location. Rank is defined as how a particular month places with respect to the corresponding month of the previous 34 years. For example, was February 2005 the warmest, 3rd warmest, 5th warmest, or 20th warmest month of the 35 year period? Since winter weather systems in the Idaho Panhandle generally have a spatial scale on the order of a 100 miles, as opposed to summertime convective thurnderstorms such as occur east of the Rocky Mountains which have a spatial scale on the order of 5 miles, the ranking of the 2005 season for various variables ought to closely correspond to the ranking at the three weather stations in the U.S. 95 Realignment Project study area with regard to their respective historical climatologies.

7.1 Snow

Snow data were recorded daily at PSF. These included depth of snow which fell on the current day measured to the nearest tenth of an inch, and snow depth on the ground at the 5 p.m. time of observation recorded in whole inches. The cumulative monthly snowfall depth for the months of November through March for the 35 years, 1971-2005, are shown in Figures –7.1.1-7.1.5 (one figure for each month). Cumulative monthly snowfall is calculated by adding up the values of daily snowfall depth. I have omitted the months of April and May from the snow analysis because historically they have little or no snow.

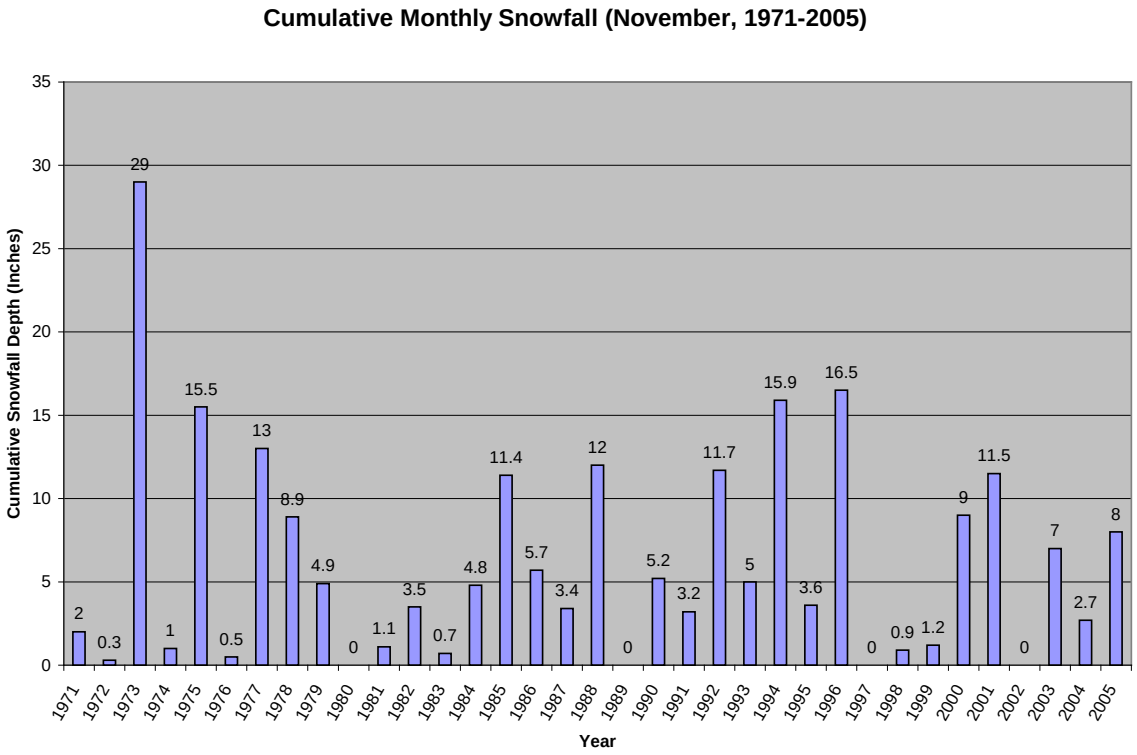

Figure 7.1.1. November Cumulative Monthly Snowfall, PSF. 1971-2005.

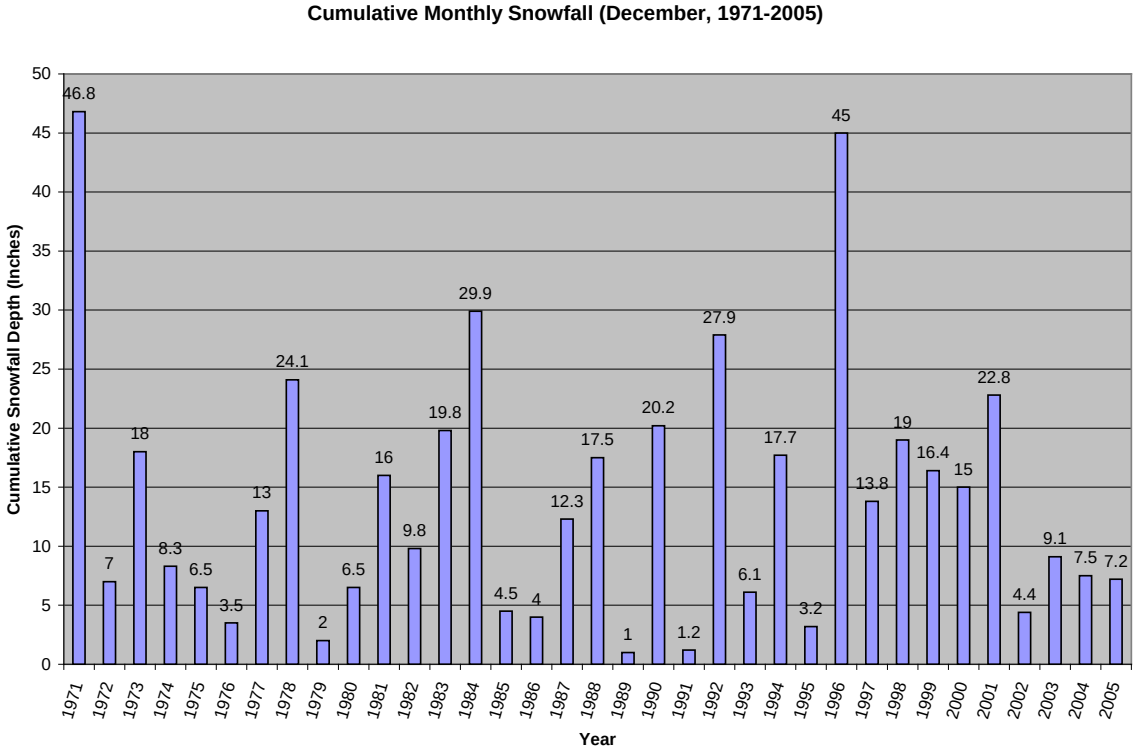

Figure 7.1.2. December Cumulative Monthly Snowfall, PSF. 1971-2005.

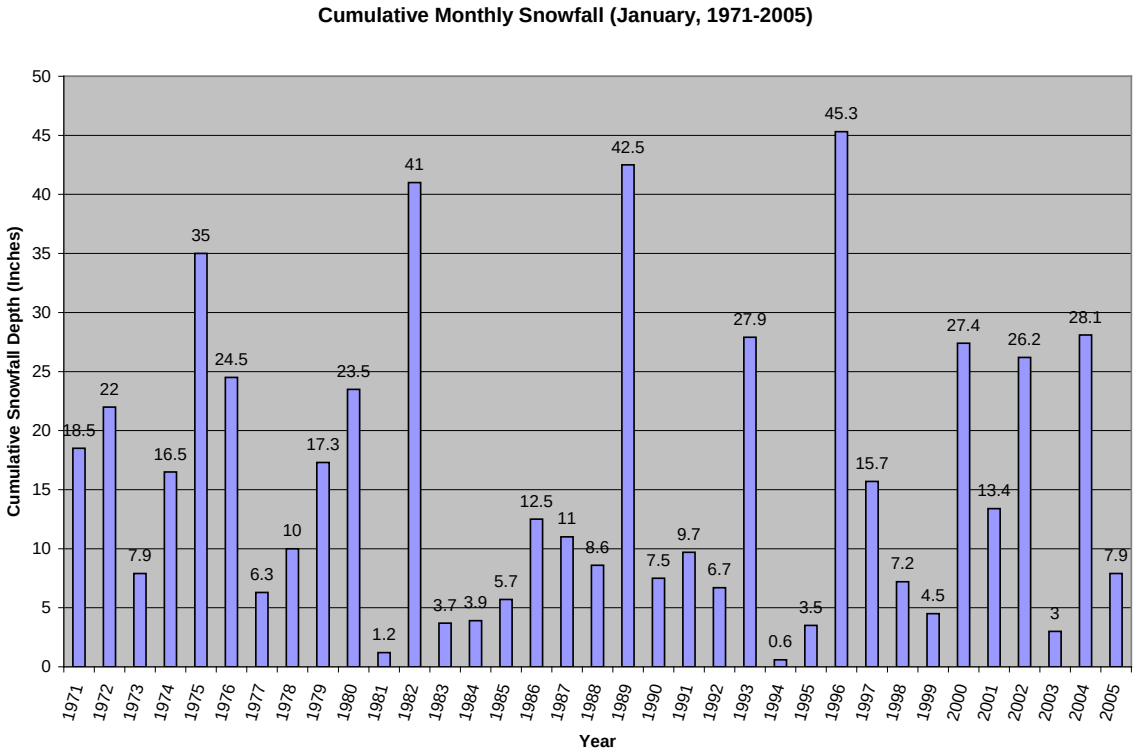

Figure 7.1.3. January Cumulative Monthly Snowfall, PSF. 1971-2005.

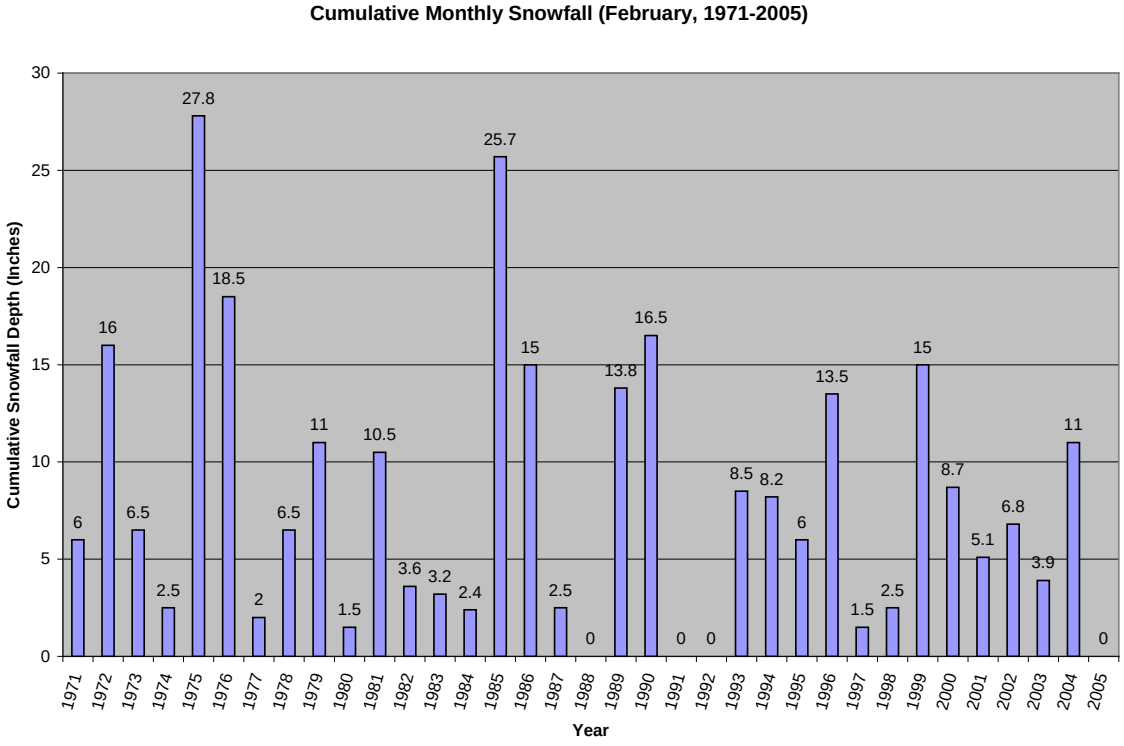

Figure 7.1.4. February Cumulative Monthly Snowfall, PSF. 1971-2005.

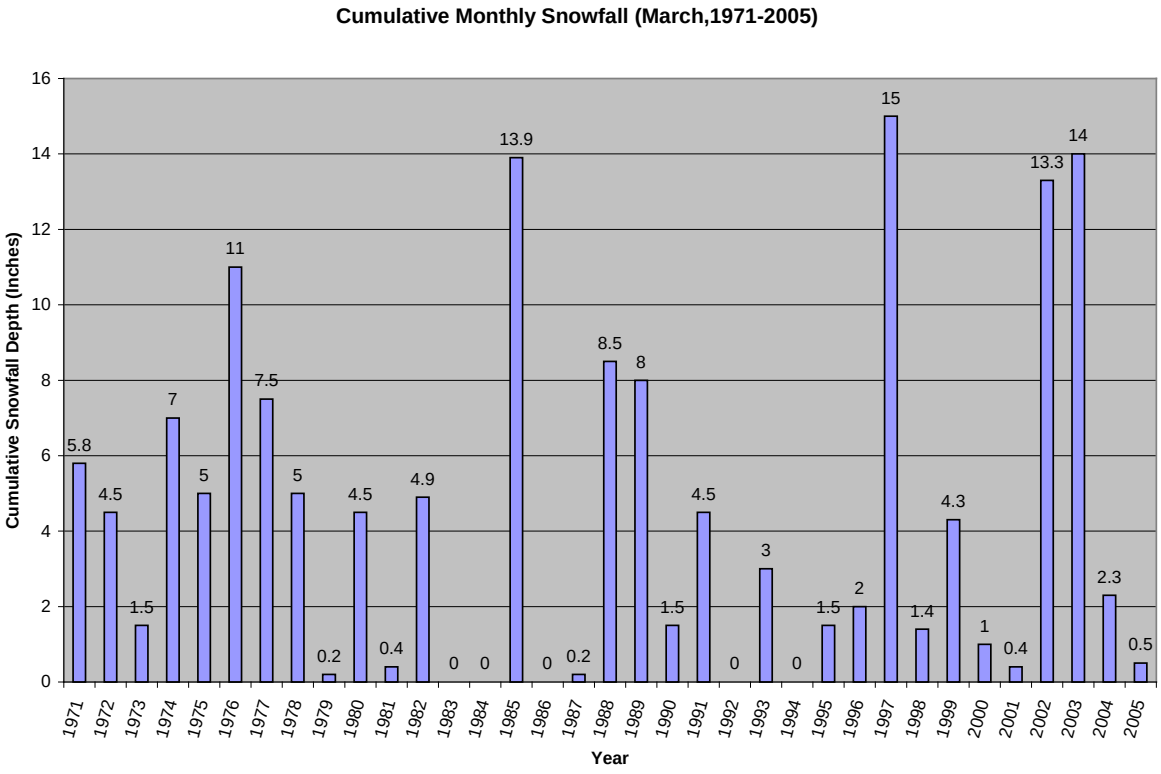

Figure 7.1.5. March Cumulative Monthly Snowfall, PSF. 1971-2005.

The November 2004 through March 2005 cumulative snowfall data can be compared to the historical data by counting the number of years from 1971 through 2005 for which the cumulative monthly snowfall was the same or less than the amount that fell each month during the November 2004 through March 2005 time period. The data are presented in the Table 7.1.1, by month from the 2004-2005 winter season.

Table 7.1.1. Monthly cumulative snowfall depth at PSF during the 2004-2005 winter season, and number of other years with the same or less monthly cumulative snowfall.

Month	Cumulative Snowfall (Inches)	No. of Years with same or lesser Cum. Snowfall	Non-Exceed. Probability (%)	Return Period (Years)	Median Snowfall 1971-2005 (inches)
Nov 2004	2.7	13	37	2.7	4.8
Dec 2004	7.5	14	40	2.5	12.3
Jan 2005	7.9	14	40	2.5	11.0
Feb 2005	0	4	11	9	6.5
Mar 2005	0.5	10	29	3.4	3.0

The non-exceedance probability column represents the probability in the corresponding month in any year of receiving no more snowfall than actually occurred during the same month of the 2004-2005 winter season. There is a 40% chance every January that 7.9

inches or less of snowfall will occur. Another way to express this is that about four years out of every ten, one can expect to receive 7.9 inches or less of cumulative snowfall in the month of January. The values in this column are calculated as the number of years with the same or lesser cumulative snowfall as the corresponding month during the 2004-2005 winter season, divided by 35 years. The return period, as I am using it here, represents the average number of years between years with cumulative snowfall depth less than or equal to that observed during the corresponding month of the 2004-2005 winter season. It is calculated as the inverse of the non-exceedance probability converted to a decimal. A non-integer return period implies that the return period brackets the number shown. For example, the return period for January snowfall less than or equal to the January 2005 value of 7.9 inches is 2.5 years, which means that the average is between 2 and 3 years. That is, based on the historical record, one would expect the average interval between years in which cumulative January snowfall was less than or equal to 7.9 inches to be 2 to 3 years. For comparison with the study period snowfall, the median snowfall over the 35 years record is provided in the final column.

In addition to cumulative monthly snowfall, the number of days per month with no snowfall provides a useful comparison of the 2004-2005 winter season to the 1971-2005 historical period (Table 7.1.2).

Table 7.1.2. Number of days at PSF with no snowfall during the 2004-2005 winter season, and number of other years with the same or greater number of days with no snowfall.

Month	Days with no snowfall	No. of other years	Probability (%)
Nov 2004	28	17	49
Dec 2004	26	14	40
Jan 2005	25	17	49
Feb 2005	28	5*	14
Mar 2005	30	12	34

*This number differs from the number of years with zero cumulative snowfall in the previous table because one leap year (1980) had 28 days without snowfall, so it was counted in this table, but not in the previous table.

Although this does not account for snow depth, the greater the number of days of no snowfall, the milder the winter. This is particularly relevant to winter highway maintenance; the fewer the number days of snowfall, the fewer the number of days of plowing are required. Table 7.1.2 reports the number of years with the same or greater number of days with no snowfall, in contrast to Table 7.1.1 which reports the number of years with the same or lesser monthly snowfall. Both of these conditions correspond to the number of years with conditions as mild or milder than the 2004-2005 winter season. The final column is the probability in percent of a winter month having the same or greater number of days of no snowfall as the same month of the 2004-2005

winter season. November and January were both near the median number of days with no snowfall; in both cases there were 17 years out of the previous 35 years with the same or greater number of days with no snowfall. This corresponds to a 49% probability in any given year of having the same or greater number of days with no snow. December and March also had high probabilities of having their respective numbers of days with no snow, 40% and 34%, respectively. Only February was a significant anomaly, with only 5 of the previous 35 years with the same or greater number of days with no snow, which in this case was 28 days, or the whole month without snowfall. This corresponds to a 14% probability. The return period for having no days of snowfall in February is approximately one year in seven. Conversely, on average six years out of seven will have at least one day of snowfall in February.

Depth of snow at time of observation accounts for the persistence or duration of snow on the ground even on days when no snow has fallen. Of particular importance in measuring how mild was the 2004-2005 winter season, is the number of days per month with snow depths of zero inches. Also of importance are the number of days with snow depths less than or equal to one, two, three and four inches. These numbers are presented in Table 7.1.3 along with the number of years from 1971-2005 which had the same number or more days, and the corresponding exceedance probability. The exceedance probability is the likelihood in any given year that there will be as many or more days with less than or equal to the specified depth of snow on the ground. As with the metrics reported above, the greater the number of days, the milder the winter.

Table 7.1.3. Number of days in 2004-2005 winter season with no more than the specified depth of snow on the ground (A Columns), the number of years from 1971-2005 with as many or more days as the number in the 2004-2005 season (B Columns), and exceedance probability (C Columns).

	Depth (inches)														
Depth (in)→	0*			1			2			3			4		
Month	A	B	C	A	B	C	A	B	C	A	B	C	A	B	C
Nov '04	29	17	49	29	20	57	29	23	66	30	23	66	30	25	71
Dec '04	9	15	43	10	16	46	10	14	40	11	13	37	11	15	43
Jan '05	14	20	57	20	16	46	26	12	34	27	13	37	31	12	34
Feb '05	28	8	23	28	11	31	28	15	43	28	20	57	28	21	60
Mar '05	30	20	57	31	21	60	31	24	69	31	25	71	31	28	80

*Note that some days have no snow on the ground at time of observation even if snow fell on that day. This resulted when the snow melted between the time it fell, and the time of observation.

For the purpose of defining how mild was the 2004-2005 winter, consider the number of days per month with zero inches of snow, and with one or less inches of snow. In the former case, the likelihood of having as many or more days as actually observed

with no snow on the ground, was in the 40 to 60% range for all months except February, for which the probability was 23%, or nearly one-quarter. For the month of February, nearly one year out of four has no measurable snow on the ground at the daily time of observation (5 p.m.). Similarly, for one inch or less, all months except February had probabilities of 46-60%, and February had a 31% probability, or nearly one year in three with one inch or less on all 28 days.

To summarize the snow information presented above, snow has been considered in terms of the categories of cumulative monthly snowfall, number of days with no snowfall, and number of days with no more than a specified depth of snow on the ground at time of observation. Probabilities have been assigned to the variables each of which indicates the degree of severity of the snow in the specified month compared to the same months in the 1971 to 2005 time period. The probabilities correspond to the likelihood of having had snow conditions in a particular category that were the same or milder than those observed during the particular month. For example, a 10% probability indicates there was only a 10% chance that year of observing values that mild or milder, meaning there was very little snow. Conversely, a 90% probability indicates that there was a 90% probability of observing the value that actually occurred or something milder, meaning that that the snow conditions in the 2004-2005 winter season were more severe than most of the years in the historical record. All months except February during the 2004-2005 winter season had probabilities in every category between 34% and 60% (except also March 2005 cumulative snowfall depth, which had a value of 29%). The probability ranges can be broken into thirds, where events with less than a 33% probability are considered mild, events with more than a 66% probability are considered severe, and those between 33% and 66% are considered normal. By this metric, all snow categories in all months except February (and cumulative snowfall in March) fell within the middle-third or normal range. February's conditions ranged between 11% and 23% probabilities, placing that month in the "mild" range with respect to snow conditions

7.2 Air Temperature

Both the maximum and minimum daily air temperatures need to be considered with respect to their values over the 1971-2005 historical period. Within any given month, there is a tremendous amount of variability in daily maximum or minimum temperature, so that the distribution of temperatures throughout the month tend to vary across most of the entire range of historical temperatures. To give an idea of how much these variables change from day to day, I have plotted the daily values as a connected line for each year in Figures 7.2.1-7.2.14. For a given month, the values for each year from 1971 to 2005 are shown. The tangle of lines illustrates how variable the temperatures are throughout a given month. The data for November and December 2004, and January through May 2005 are shown as heavier lines for emphasis.

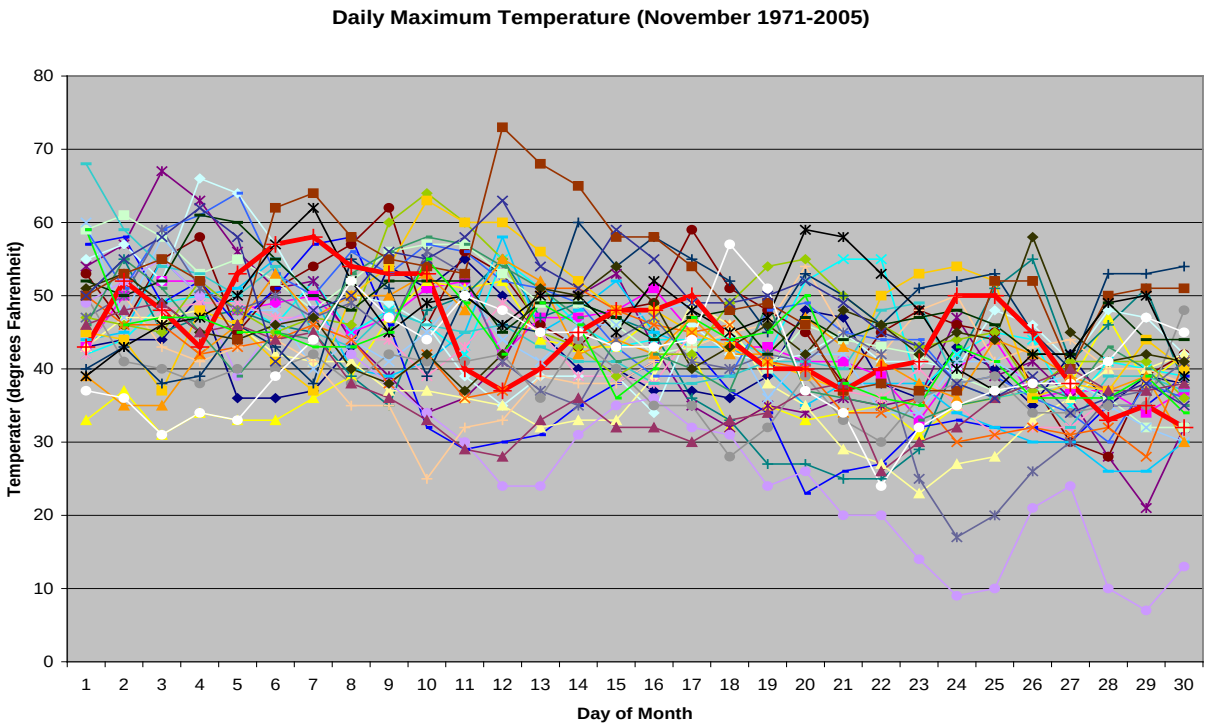

Figure 7.2.1. Daily Maximum Temperature for November from 1971-2005. Each line represents the days for a month in a single year. The highlighted red line was for the year 2004.

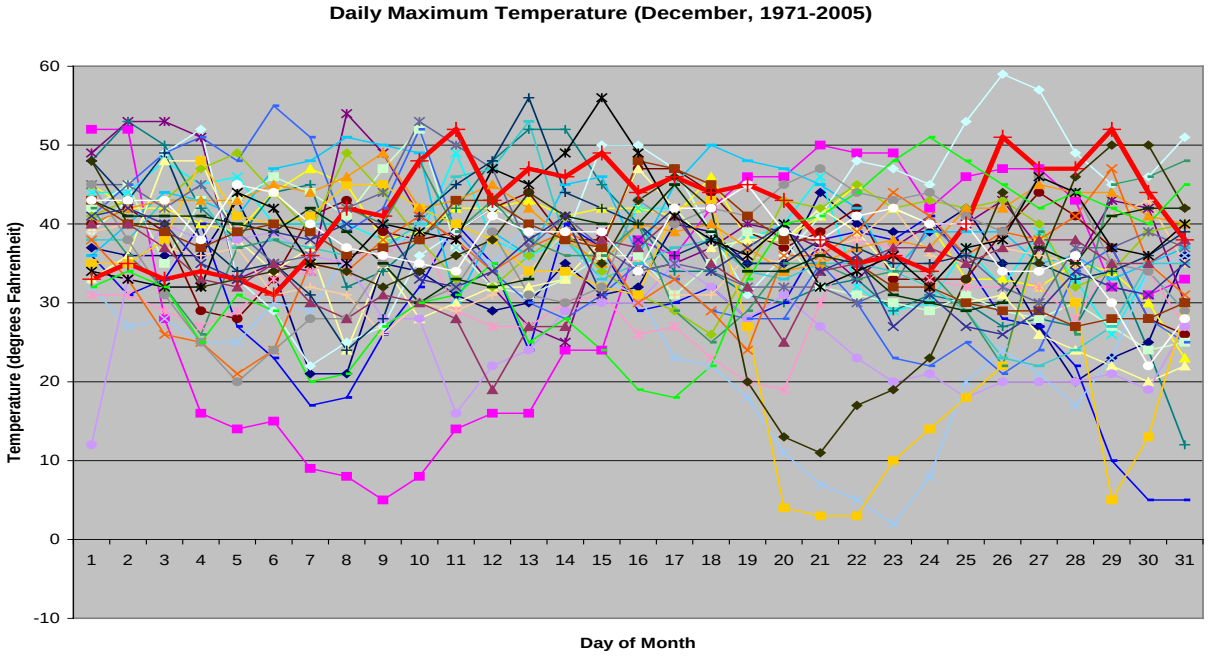

Figure 7.2.2. Daily Maximum Temperature for December from 1971-2005. Each line represents the days for a month in a single year. The highlighted red line was for the year 2004.

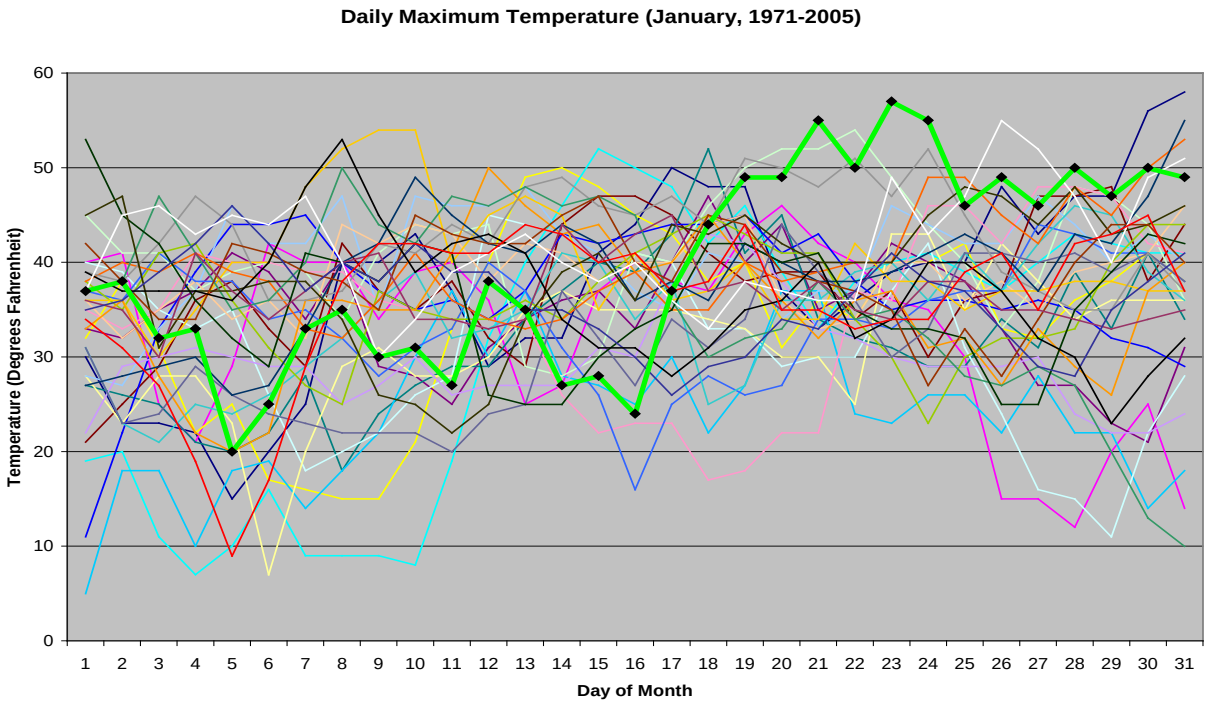

Figure 7.2.3. Daily Maximum Temperature for January from 1971-2005. Each line represents the days for a month in a single year. The highlighted green line was for the year 2005.

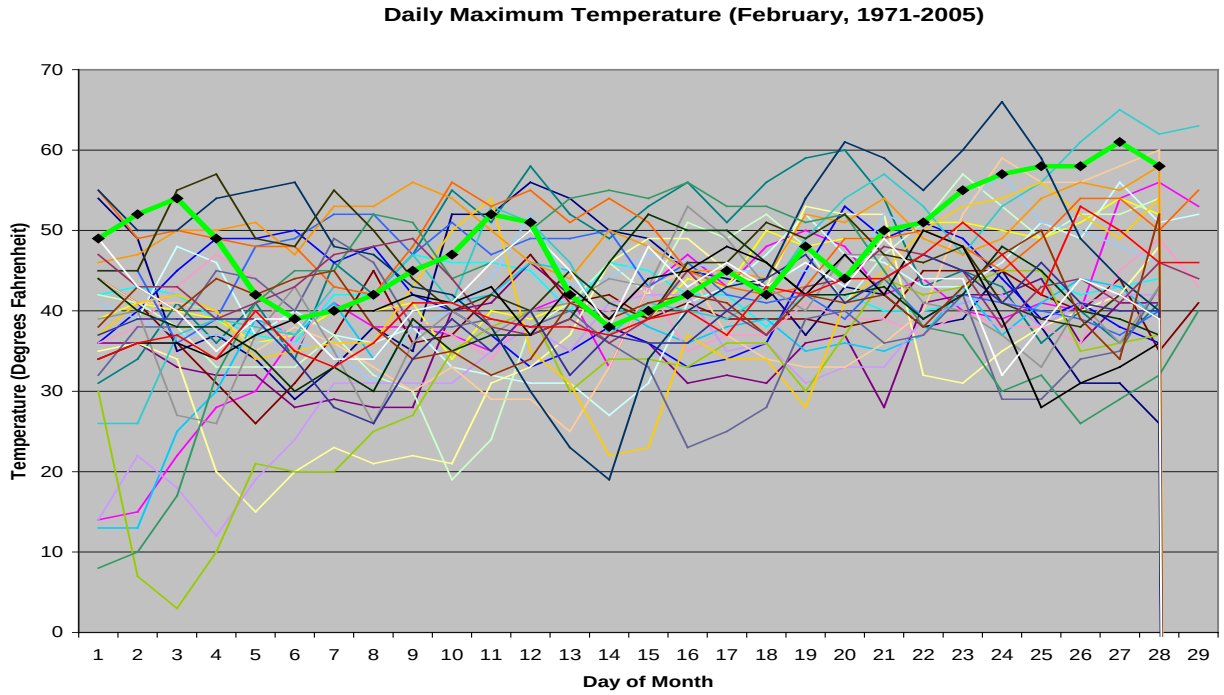

Figure 7.2.4. Daily Maximum Temperature for February from 1971-2005. Each line represents the days for a month in a single year. The highlighted green line was for the year 2005.

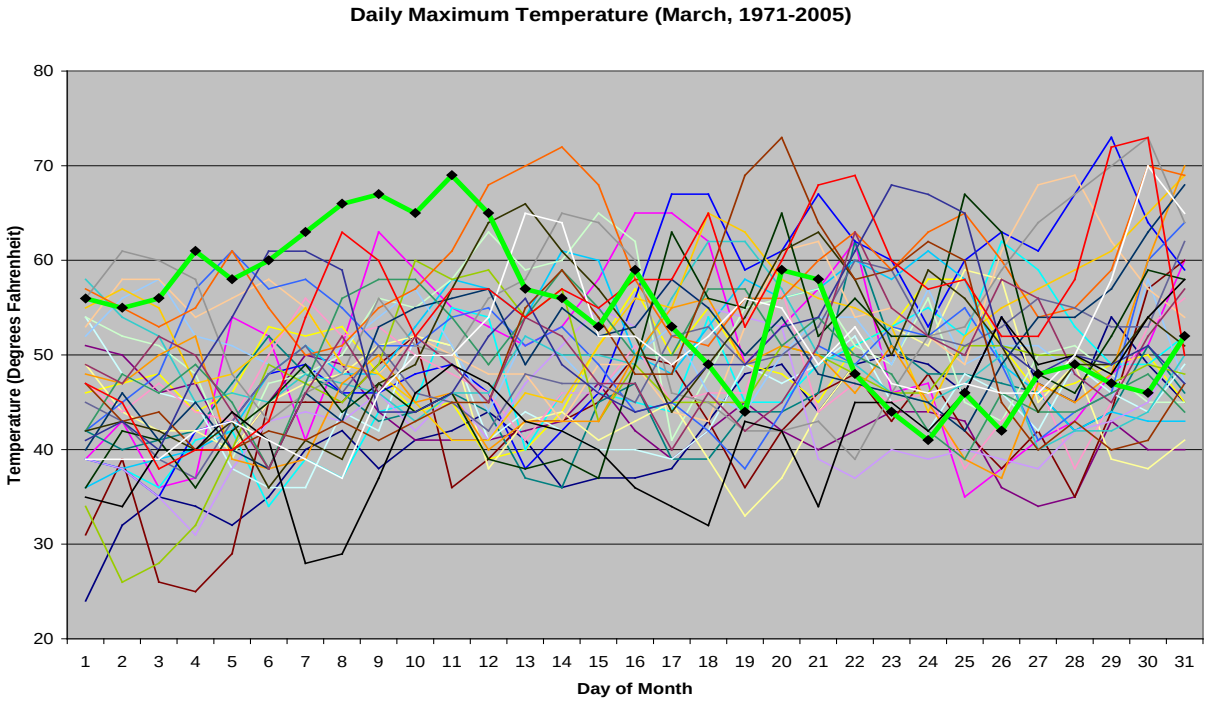

Figure 7.2.5. Daily Maximum Temperature for March from 1971-2005. Each line represents the days for a month in a single year. The highlighted green line was for the year 2005.

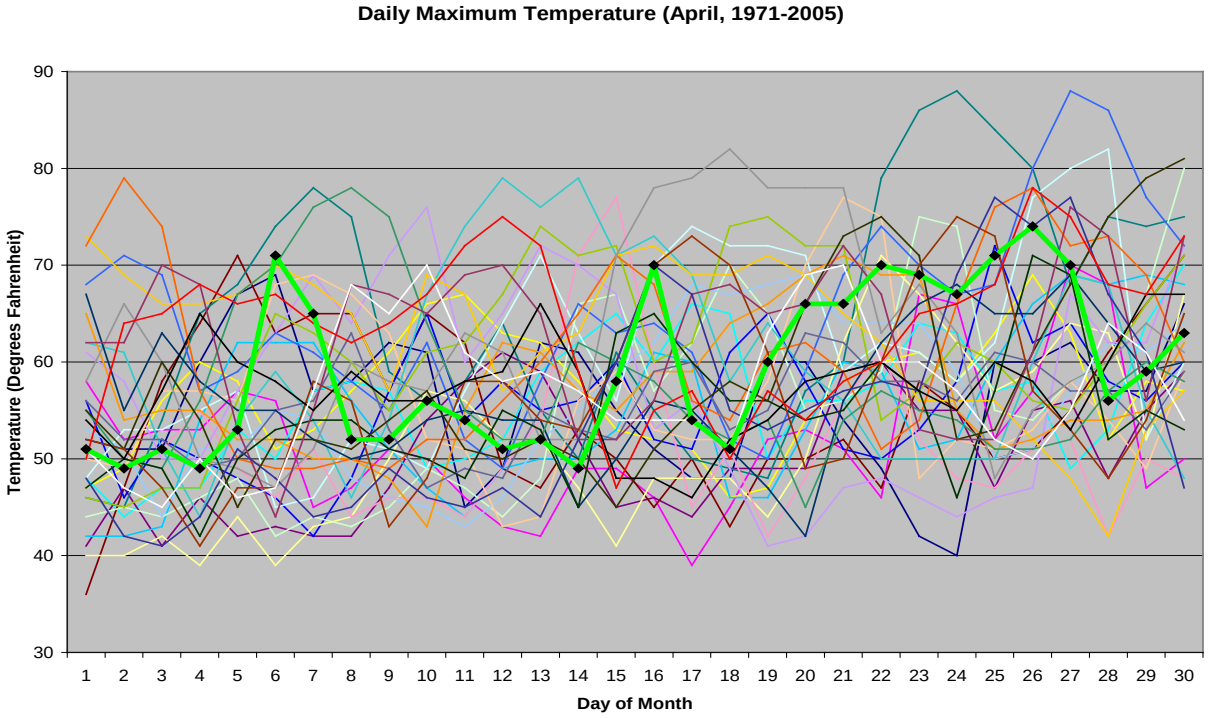

Figure 7.2.6. Daily Maximum Temperature for April from 1971-2005. Each line represents the days for a month in a single year. The highlighted green line was for the year 2005.

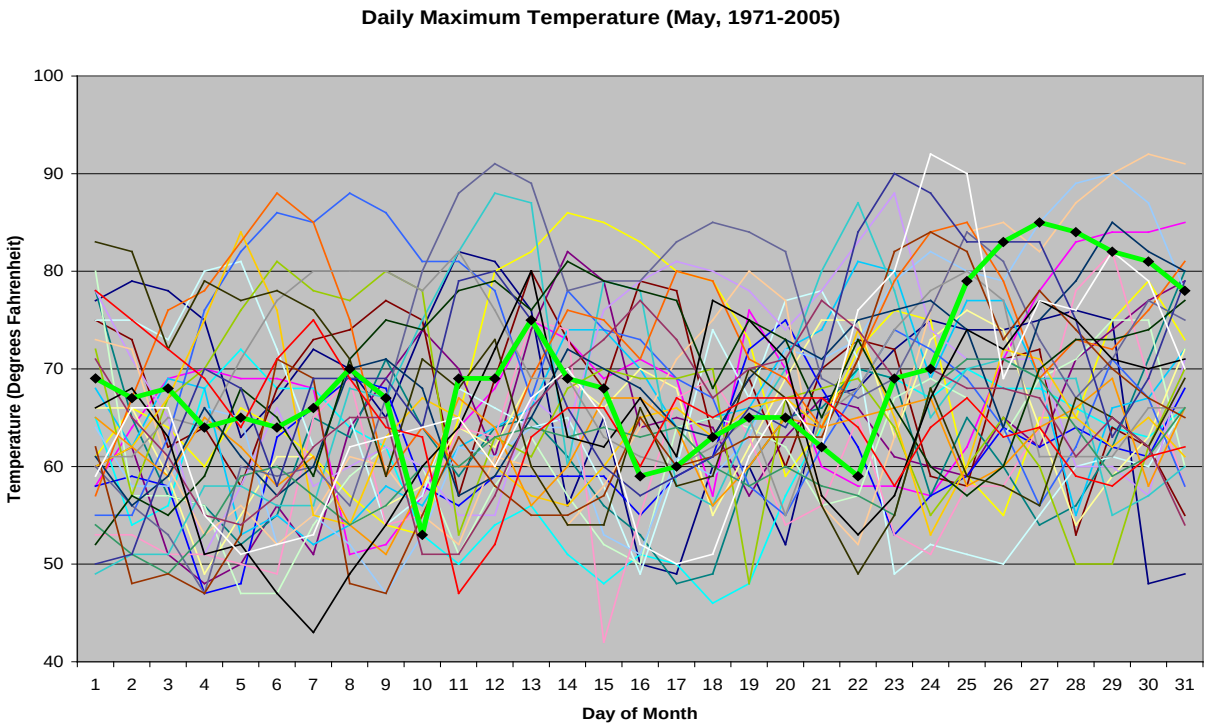

Figure 7.2.7. Daily Maximum Temperature for May from 1971-2005. Each line represents the days for a month in a single year. The highlighted green line was for the year 2005.

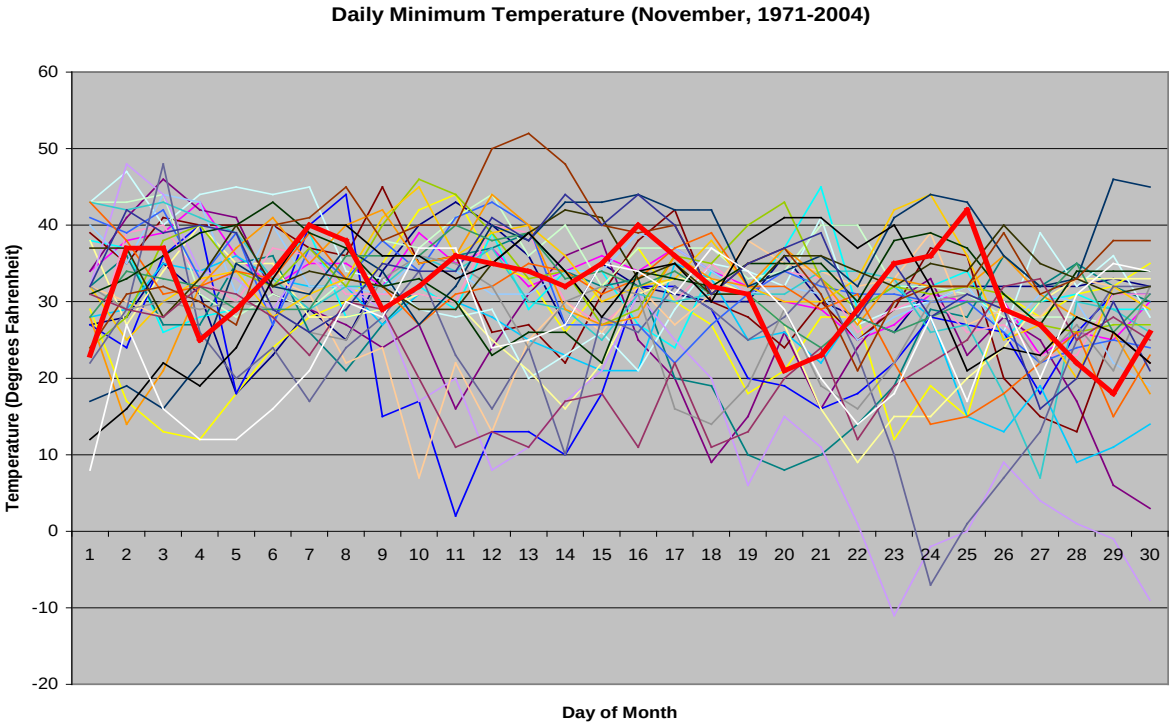

Figure 7.2.8. Daily Minimum Temperature for November from 1971-2005. Each line represents the days for a month in a single year. The highlighted red line was for the year 2005.

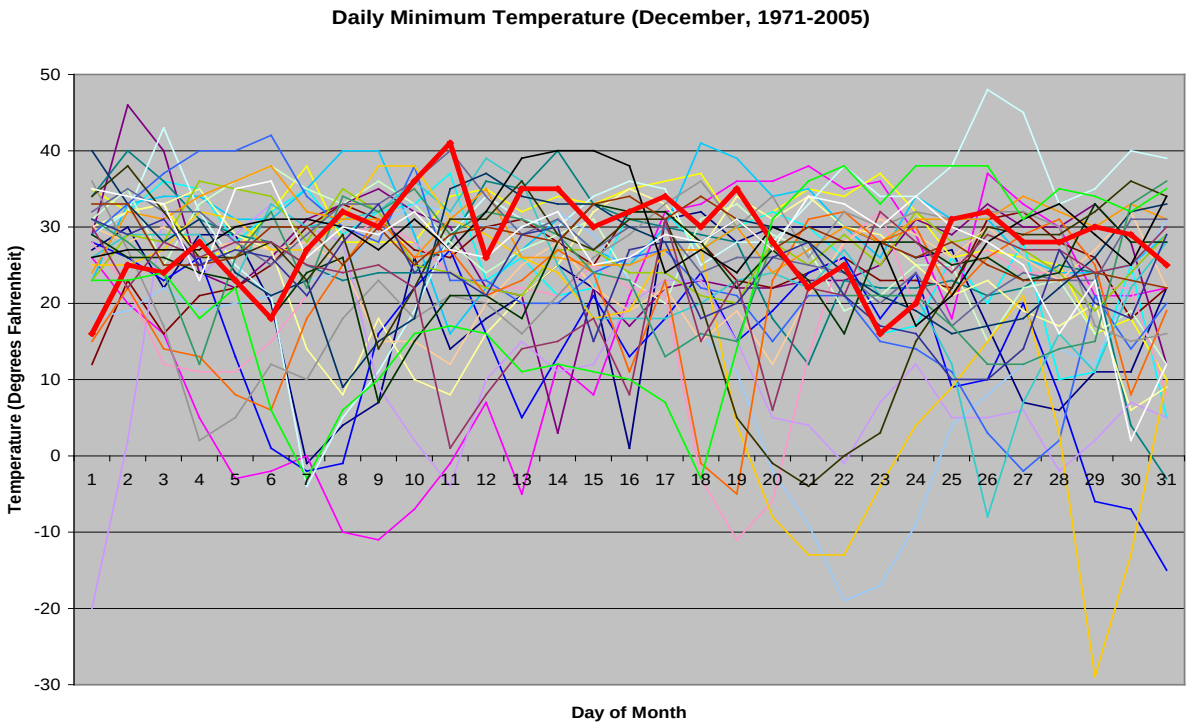

Figure 7.2.9. Daily Minimum Temperature for December from 1971-2005. Each line represents the days for a month in a single year. The highlighted red line was for the year 2005.

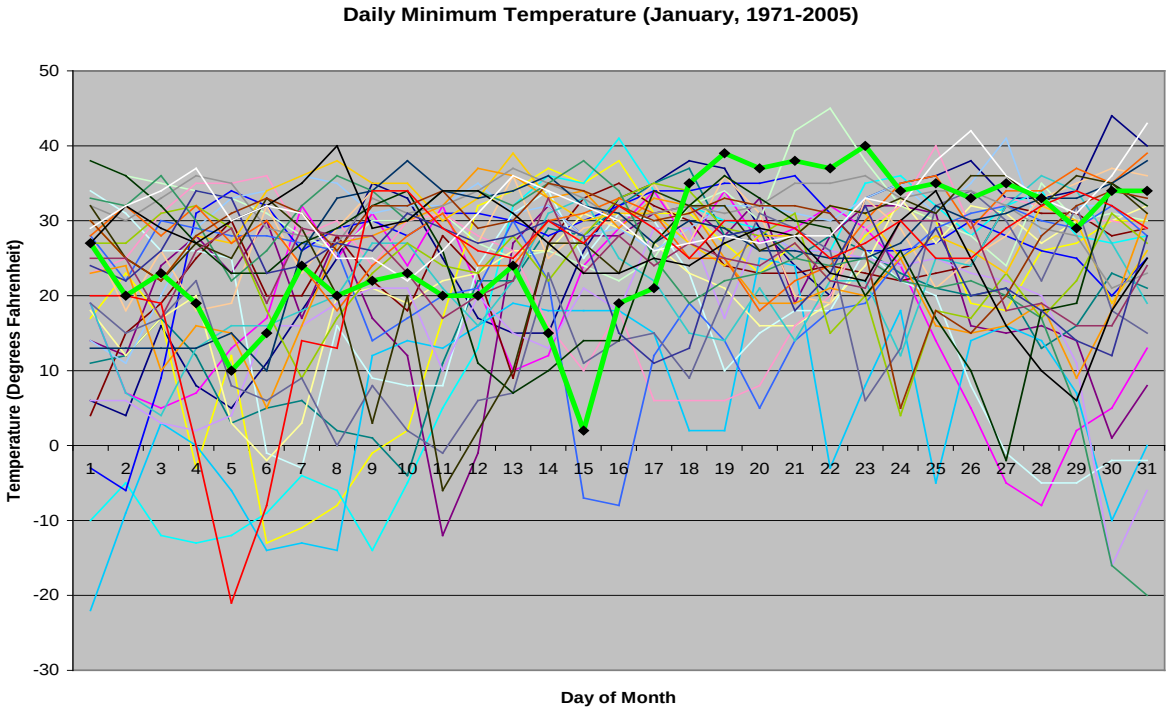

Figure 7.2.10. Daily Minimum Temperature for January from 1971-2005. Each line represents the days for a month in a single year. The highlighted green line was for the year 2005.

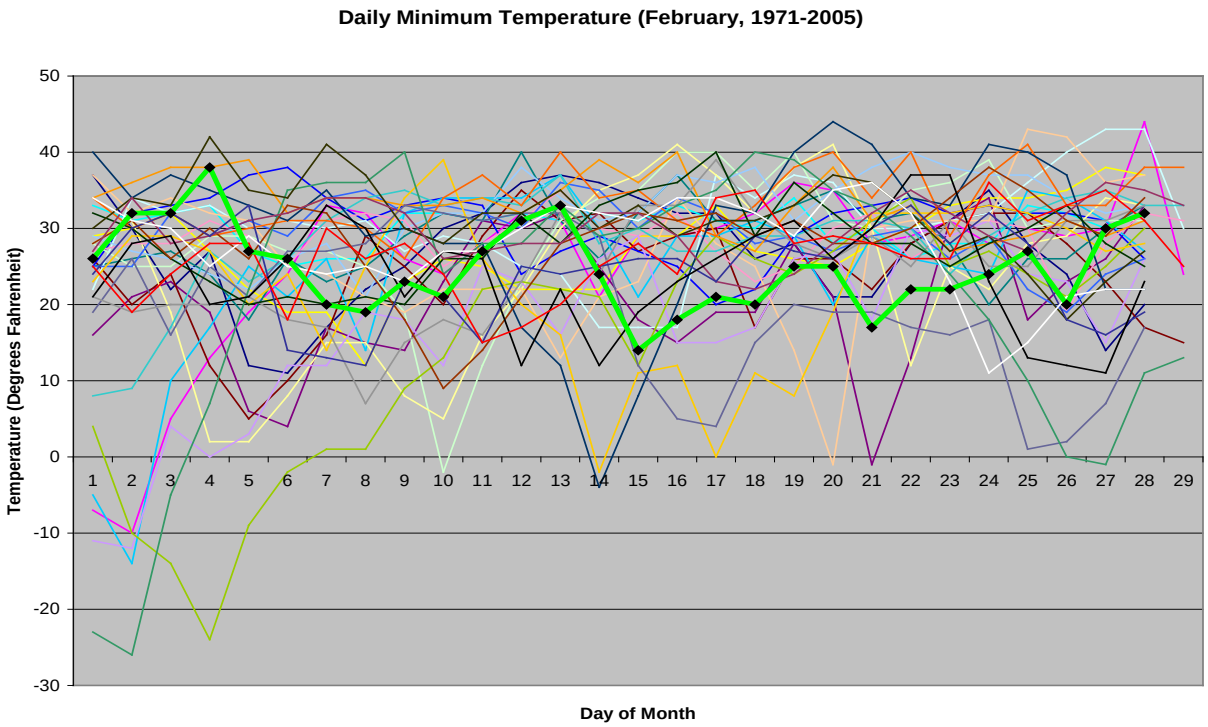

Figure 7.2.11. Daily Minimum Temperature for February from 1971-2005. Each line represents the days for a month in a single year. The highlighted green line was for the year 2005.

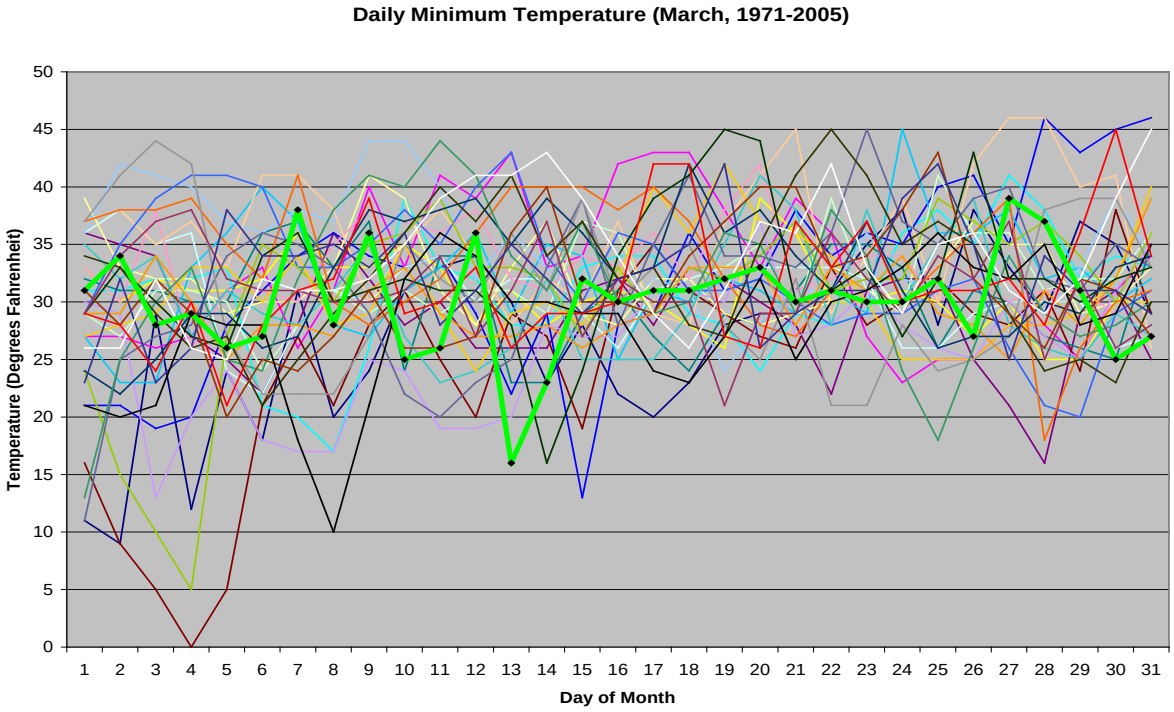

Figure 7.2.12. Daily Minimum Temperature for March from 1971-2005. Each line represents the days for a month in a single year. The highlighted green line was for the year 2005.

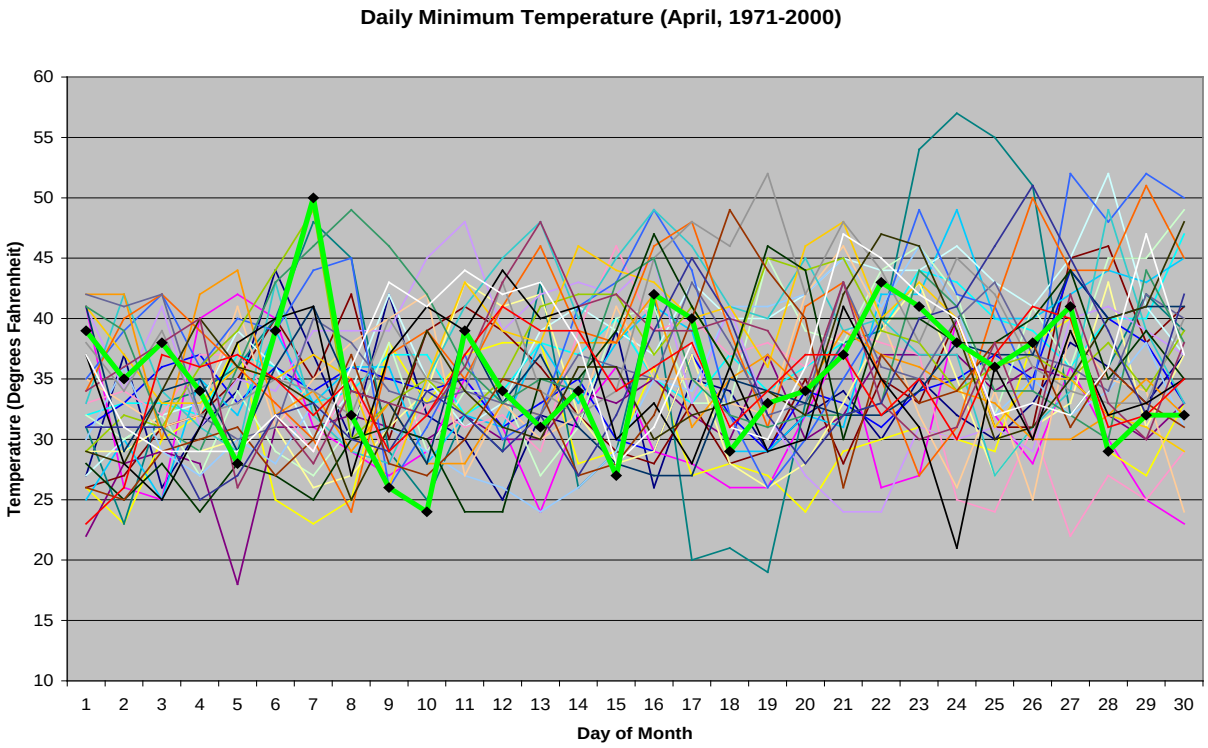

Figure 7.2.13. Daily Minimum Temperature for April from 1971-2005. Each line represents the days for a month in a single year. The highlighted green line was for the year 2005.

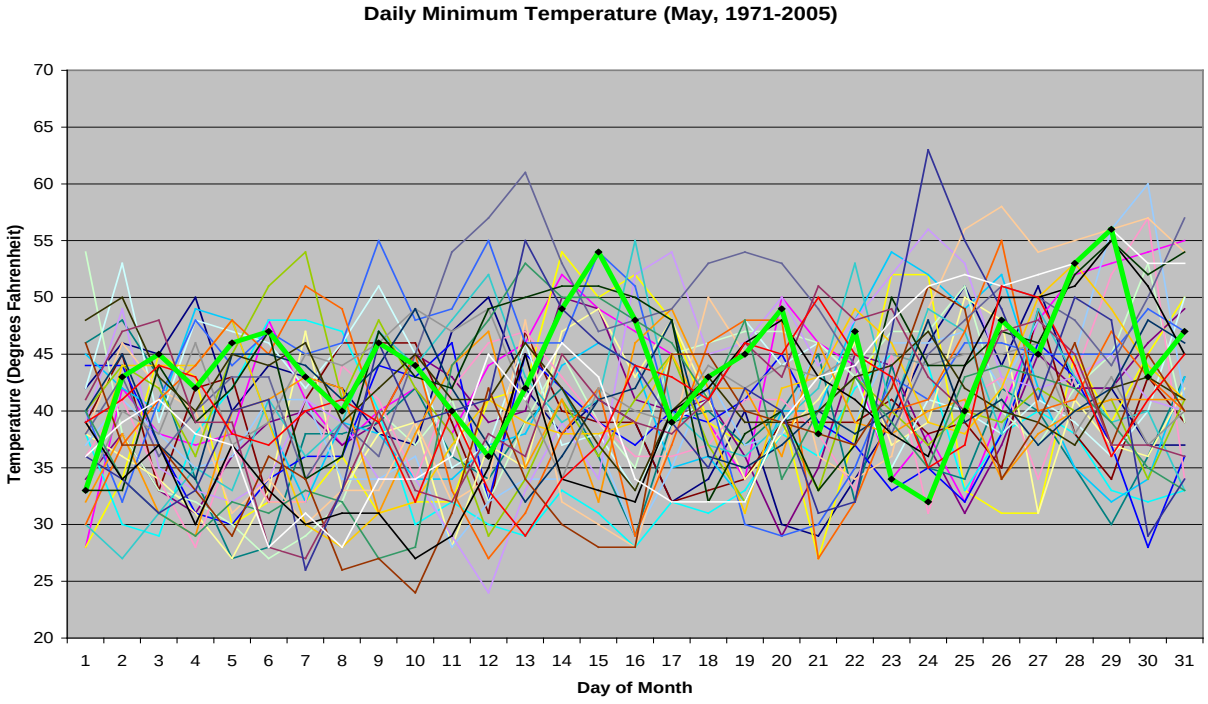

Figure 7.2.14. Daily Minimum Temperature for May from 1971-2005. Each line represents the days for a month in a single year. The highlighted green line was for the year 2005.

The data for each month over the 35 year period 1971-2005 can be ranked in order to calculate exceedance probabilities associated with the mean values of maximum temperature and minimum temperature actually obtained each month. Tables 7.2.1 and 7.2.2 show these exceedance probabilities by month for maximum temperature and minimum temperature, respectively.

Table 7.2.1. Exceedance probabilities for the monthly average of the maximum daily temperatures with respect to the 1971-2005 historical period.

Month	Tmax (Deg F)	35-Year Median Tmax	Rank	Exc. Prob. (%)	Return Period (Years)
Nov '04	44.9	43.3	14	39	2.6
Dec '04	35.1	35.6	24	67	1.5
Jan '05	39.5	36.1	7	19	5.3
Feb '05	48.3	41.0	3	7	13.4
Mar '05	54.6	49.5	3	7	13.4
Apr '05	59.3	57.0	11	30	3.3
May '05	69.3	66.2	5.5	15	6.9

Table 7.2.2. Exceedance probabilities for the monthly average of the minimum daily temperatures.

Month	Tmin (Deg F)	35-Year Median Tmin	Rank	Exc. Prob. (%)	Return Period (Years)
Nov '04	31.4	31.4	18	50	2
Dec '04	28.1	24.1	7	19	5.3
Jan '05	26.4	24.2	12	33	3
Feb '05	24.9	27.4	23	64	1.5
Mar '05	30.0	31.2	29	81	1.2
Apr '05	35.2	35.2	18	50	2
May '05	43.8	40.7	3.5	9	11.8

In Tables 7.2.1 and 7.2.2, the rank is the placement of the particular month's temperature in the 35 year record. The largest monthly average has a rank of one, and the smallest value has a rank of 35. The exceedance probabilities correspond to the likelihood in any given year of observing a value of the average maximum or minimum temperature that was greater than the value actually experienced. Low exceedance probabilities indicate that one is unlikely to observe a value as large or larger as that actually observed; the larger the exceedance probability, the more likely it is for that value or larger to be observed. The large amount of variability of temperature within each month, as shown in the daily maximum and minimum temperature figures, causes

them to have a large standard deviation, which creates some uncertainty in the ranking of each value with respect to the values from other years. This in turn produces some uncertainty in the actual values of the exceedance probabilities.

7.3 Precipitation

Cumulative monthly precipitation depth is the sum of the depths of all precipitation events, including frozen (i.e., snow or ice) and liquid precipitation, all reported in terms of their melted liquid depth. As with other meteorological variables, there is a large amount of variability across the years both within a specified month, and between months. The range of values over the 35 years for precipitation from November through May includes values close to or less than half an inch in every month except November, and values in excess of five inches in every month as well. The time series of monthly precipitation depths are shown in Figures 7.3.1 to 7.3.7 with each month collected in a single figure and displayed sequentially by year.

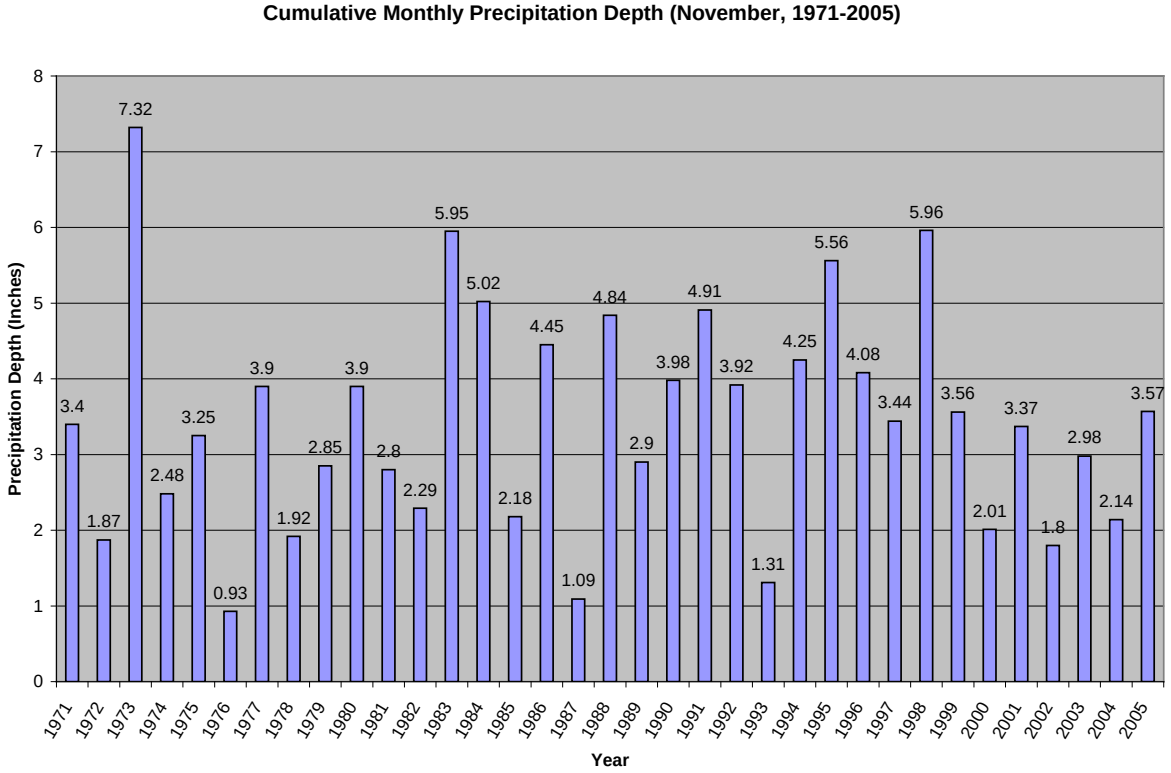

Figure 7.3.1. Cumulative Monthly Precipitation Depth for November (1971-2005).

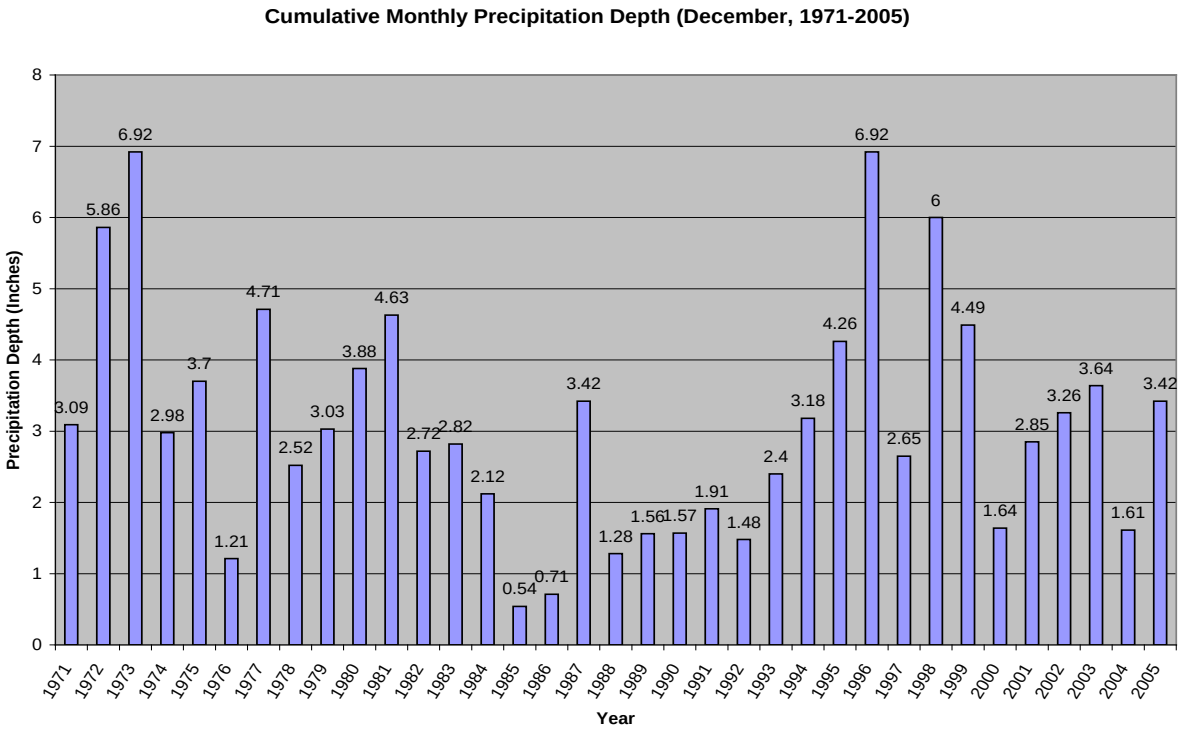

Figure 7.3.2. Cumulative Monthly Precipitation Depth for December (1971-2005).

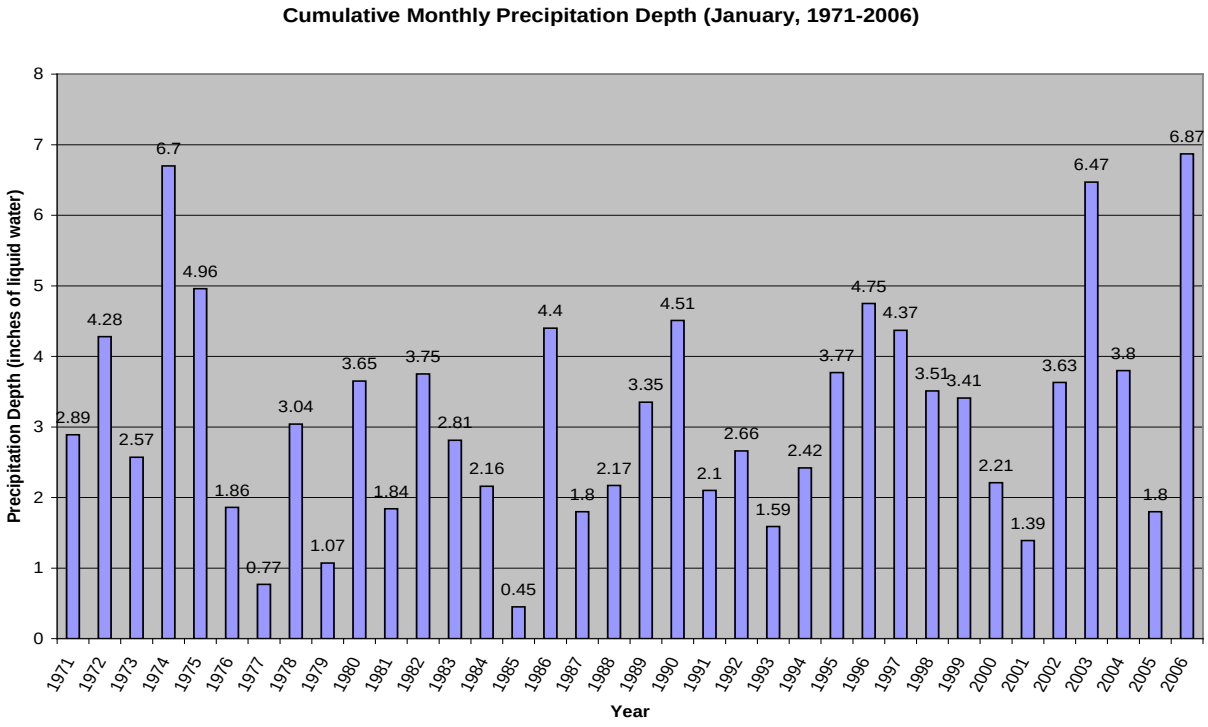

Figure 7.3.3. Cumulative Monthly Precipitation Depth for January (1971-2006).

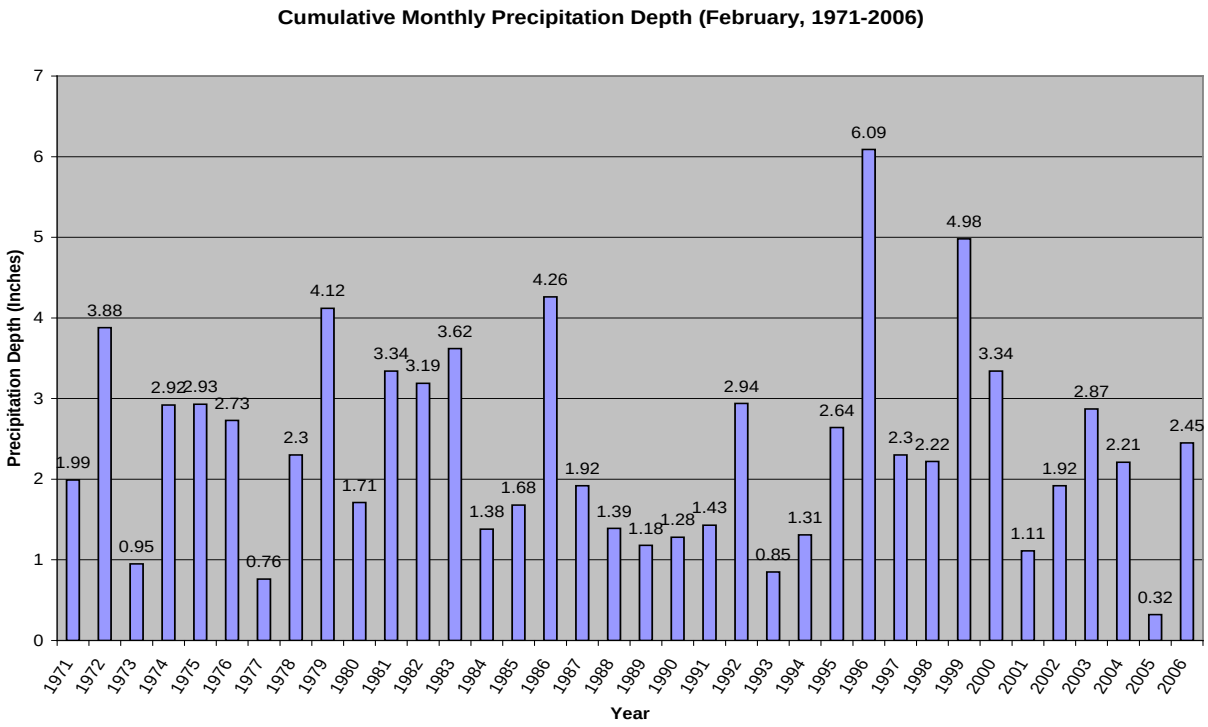

Figure 7.3.4. Cumulative Monthly Precipitation Depth for February (1971-2006).

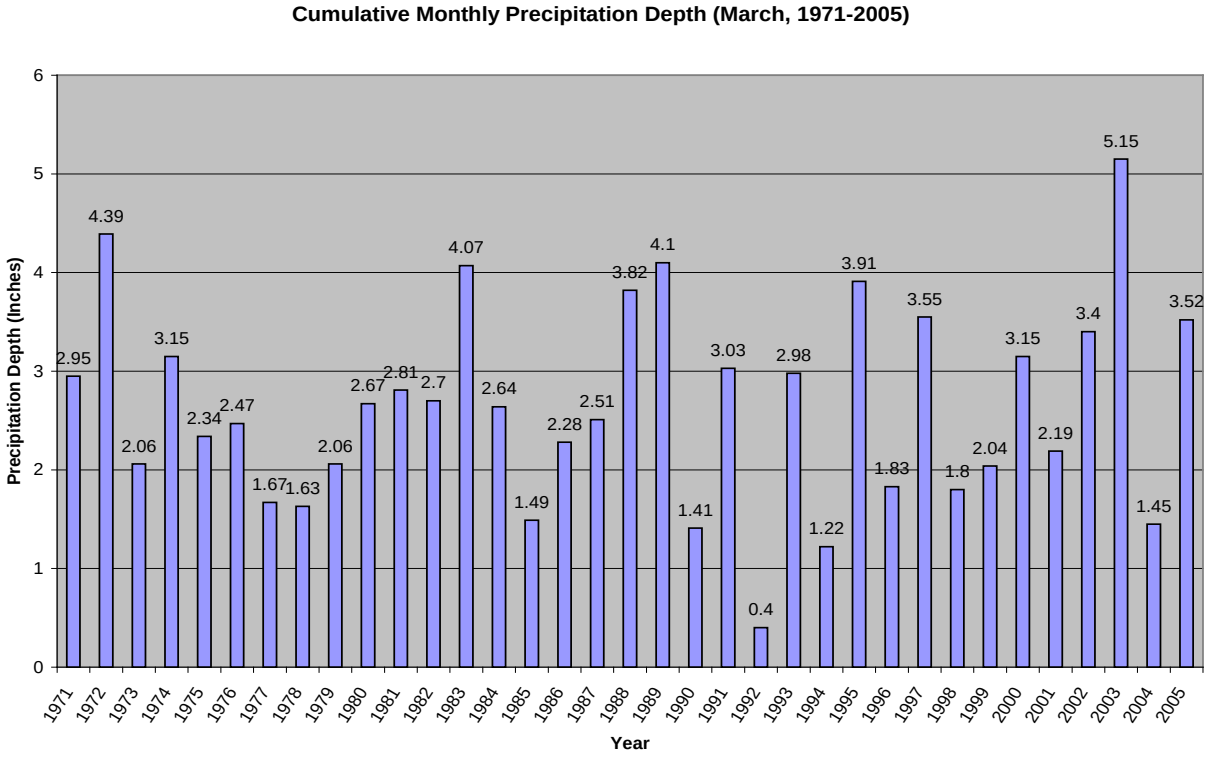

Figure 7.3.5. Cumulative Monthly Precipitation Depth for March (1971-2005).

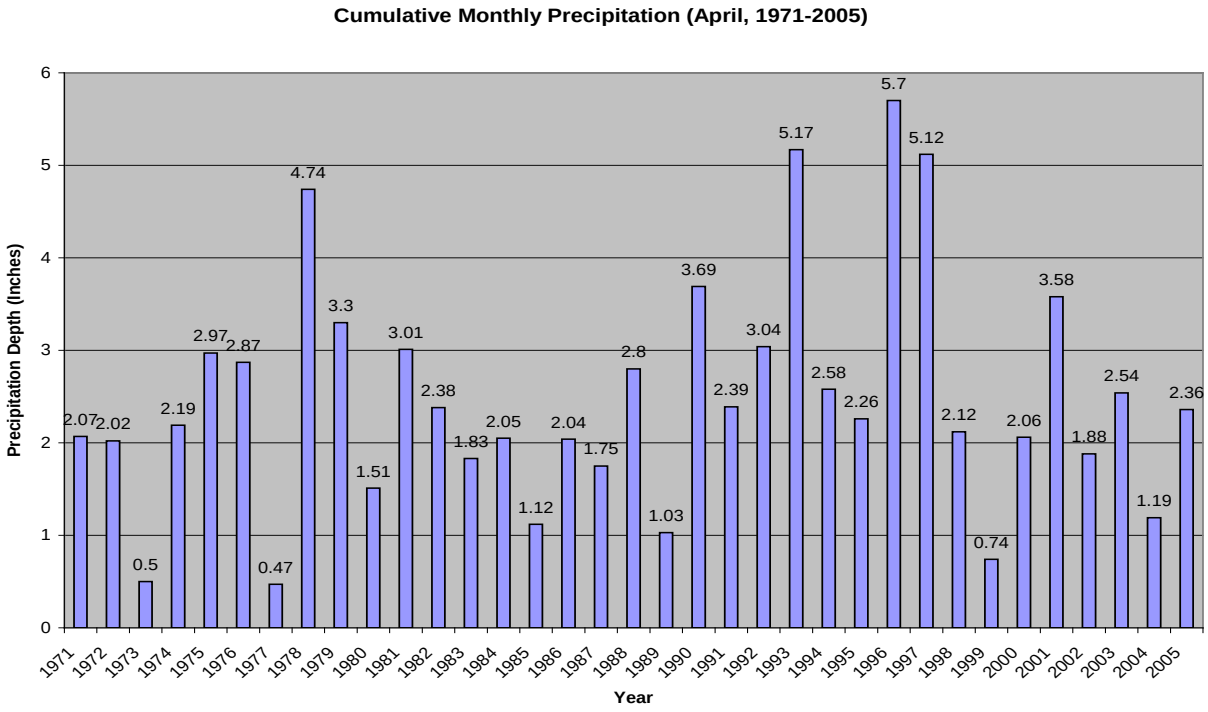

Figure 7.3.6. Cumulative Monthly Precipitation Depth for April (1971-2005).

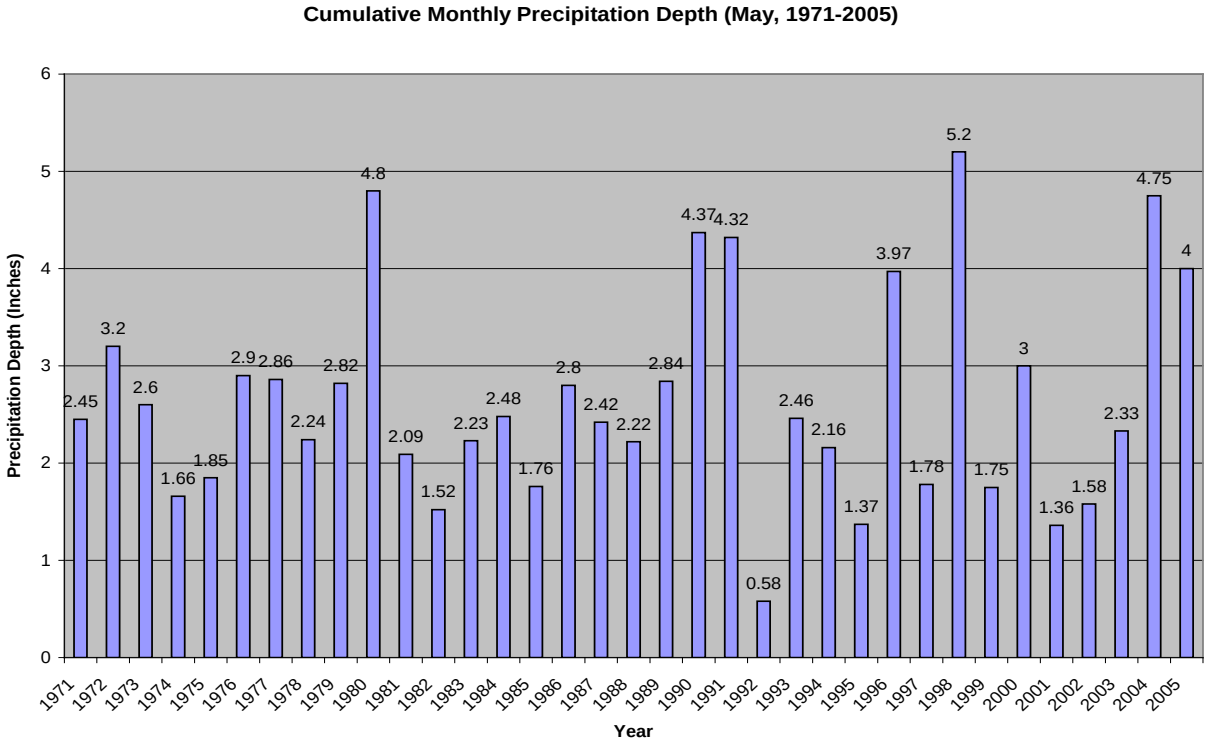

Figure 7.3.7. Cumulative Monthly Precipitation Depth for May (1971-2005).

The data for each month over the 35 year period 1971-2005 can be ranked in order to calculate exceedance probabilities associated with the values of cumulative monthly precipitation actually obtained each month. Table 7.3.1 shows the exceedance probabilities associated with each month.

Table 7.3.1. Exceedance Probabilities for the cumulative monthly precipitation depth with respect to the 1971-2005(6) historical period.

Month	Precip (in)	Median (in)	Rank	Exc. Prob (%)	Return Period (Years)
Nov '04	2.14	3.40	28	81	1.2
Nov '05	3.57	3.40	15	44	2.3
Dec '04	1.61	2.98	28	81	1.2
Dec '05	3.42	2.98	12	33	3.0
Jan '05	1.80	2.97	30	82	1.2
Jan '06	6.87	2.97	1	2	58.
Feb '05	0.32	2.26	36	98	1.0
Feb '06	2.45	2.26	16	43	2.3
Mar '05	3.52	2.64	8	22	4.6
Apr '05	2.36	2.26	17	47	2.1
May '05	4.00	2.45	6	16	6.23

In Table 7.3.1, the rank of a particular month's precipitation is its placement with respect to the same month in the 1971-2005(6) historical period, with the largest value for the period holding the rank of one, and the smallest holding the rank of 35(36). The rank indicates how many years of the historical period that the same-month precipitation was greater than the value measured in the month represented by a particular row in the table. Values of a climatological variable falling within the middle one-third of exceedance probabilities, (i.e., having exceedance probabilities between 33% and 66%, or falling within the middle third of measured values) are often considered to represent the normal climate, and values falling above or below this range are considered to represent climate realizations above or below normal, respectively.

Considering the measurements during the study period from January 2005 through May 2005, two months, January and February, had exceedance probabilities in the upper one-third, meaning they are likely to be exceeded, and therefore are "small" relative to the climatological norm. Two months, March and May, had exceedance probabilities in the lower one-third, and therefore represented high precipitation months relative to their climatological norms. April precipitation fell almost exactly on the median, with an exceedance probability of 47%. This was squarely in the middle of the climatological norm for that month.

This wide range of observations with respect to climatological normals, made the 2005 study period very useful to accomplish the established goals with respect to precipitation. There were two goals: one was to establish the relative magnitudes of monthly precipitation between the three stations in the study area; the other was to establish the climatological norm for each station with respect to the long term record at the UI Plant Sciences Farm. With regard to the relative magnitudes of precipitation within the study area, the different months brought a wide range of precipitation, yet the stations maintained their same relative magnitudes. This provides a high degree of confidence that the relative magnitudes of precipitation as measured during the study period will be maintained regardless of how large the precipitation depth is during a given month. Secondly, the wide range of monthly precipitation depths observed allowed us to assess the relationship of the precipitation at each of the study sites to that at the UI Plant Sciences Farm. Had all the values fallen at or near their median values, the tight cluster of points would have made it impossible to extrapolate outside that range with any certainty. As it was, between January and May, 2005, values of monthly precipitation between 0.32 inches and 4.00 inches were observed at PSF, and there was a strong correlation between the PSF values and those in the study area, as shown in Figure 7.3.8 below, which is a reproduction of Figure 10 from Qualls and Zhao (2005). This gives great confidence in the relationships established between monthly precipitation at PSF and the three measurements stations in the study region, which further allows us to estimate the climatological normal values for monthly precipitation at the individual stations based on the long term record at PSF with greater confidence.

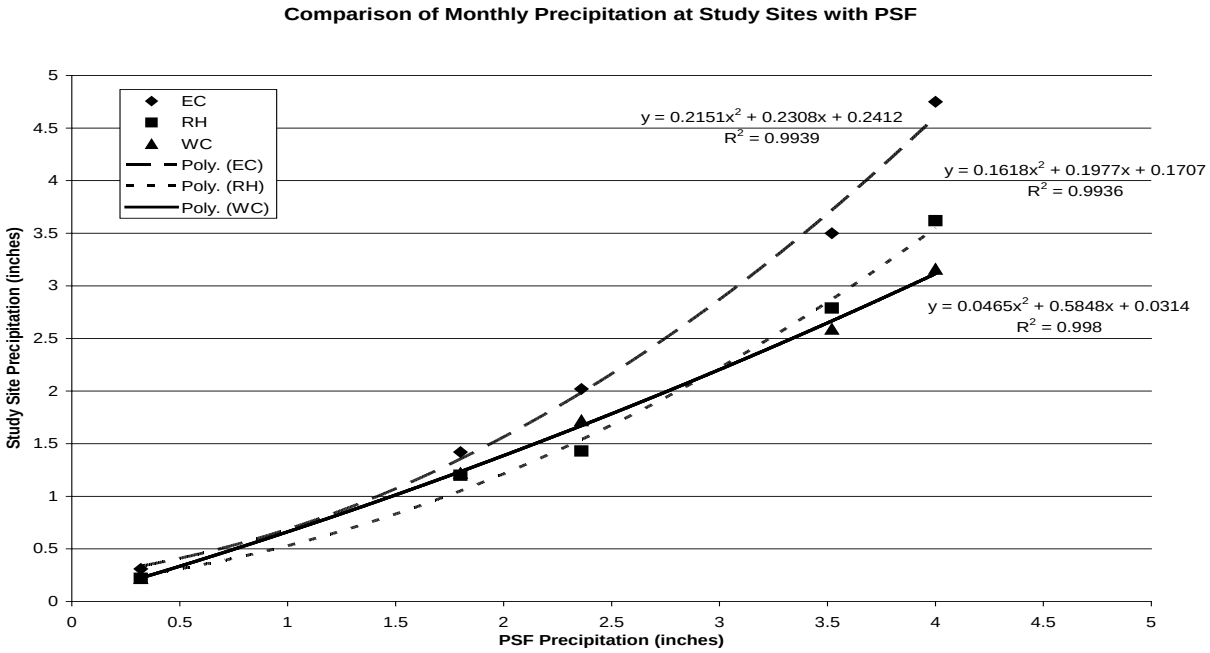

Figure 7.3.8. Monthly precipitation at each of the three study sites paired against precipitation depth at PSF for each of the corresponding months, January through May 2005 (symbols). The lines are polynomials fitted to the data from each of the study sites versus PSF. The fitted polynomial equations are shown next to their

corresponding lines, as are the R-Squared values (Appears as Figure 10 in Qualls and Zhao, 2005).

8 Summary

The objectives of this study were:

1. To characterize the general climate of the region using nearby long-term climatological measurements, 2. to characterize spatial and temporal variability of important weather and climate elements across the study area using on-site weather data, satellite images, and principles of physics, thermodynamics, and other published studies, and 3. to describe the relationship of this variability to relative safety of roadway alignment alternatives or groupings of roadway alternatives.

Associated with the general climate of the region, the study area can be expected to experience snow, wind and fog. The spatial distribution of wind and fog are discussed in sections 5 and 6 of this report, but for the decade 2001-2010, these two weather elements were reported in association with vehicle accidents only 3 times each, and half of those were also associated with ice or slush. Consequently, fog and wind have not posed significant historical accident risk in the study area.

Snow, ice, slush, or wet road conditions have contributed much more significantly to vehicle accidents than fog and wind. Nearly 44% of the total accidents involved snow, ice or slush, and together with wet road conditions, the percentage is greater than 56%. Seventy-five percent of these accidents were associated with road curvature, highly concentrated around sharp curves, especially sharp curves on roadway segments sloped greater than 2.5%. When the road surface was wet but not frozen, accidents tended to concentrate at ingress/egress locations such as road junctions and driveways rather than at curves.

Observations and theory indicate that precipitation increases modestly with elevation within the study area, but that owing to the short longitudinal distance of the rise to the crest of Paradise Ridge, that the precipitation maximum occurs downwind (i.e., primarily to the south and east) of Paradise Ridge. Within the study area, this produces the greatest persistence of snow in the vicinity of Reisenauer Hill.

Snowfall occurred at all three weather stations, WC, EC, and RH , around 80% of the time that snowfall was observed within the study area. Twenty percent of the time when snowfall was observed, it occurred only at EC and RH, the higher elevation stations within the study area, but for nearly all of these no ground snow accumulation occurred. A few percent of the time during snowfall, snow accumulations occurred at

RH and EC when no accumulation occurred at WC, but these were generally less than one or two inches.

Most often, when snowfall with ground accumulations occurred within the study area, the weather stations showed ground accumulations at all three stations. More importantly, satellite observations of snowcover presented in section 3.1 provide a view of the entire study area and the spatial distribution of snow. The most salient points from those images are: 1) any significant snow within the region provides complete spatial coverage of the study area; 2) large events (e.g., 6 inches of snow or more either accrued in a single event or in small increments over several days) virtually always, and small events (e.g., 1-3 inches) usually, provide complete spatial coverage; 3) as the snow begins to melt, south- and east-facing slopes predominantly in the middle portion of the eastern and central corridor containing the E-2 and C-3 alternative alignments, begin to melt off first; and 4) snow consistently persists longer around Reisenauer Hill.

Fog and wind have been shown to be of relatively minor significance with regard to accident potential. Slick roads, on the other hand, significantly affect accident potential. A large fraction of the historical accidents when snow, ice, or slush road surface conditions existed, were associated with short radii curves, and wet road condition accidents tend to cluster around ingress/egress locations associated with junctions and driveways. ***In spite of modest spatial variability of precipitation and other weather elements around the study area, the spatial distribution of accidents is predominantly influenced by the spatial distribution of road characteristics, rather than by spatial variability of weather.***

This dominating influence of road characteristics over spatial distribution of weather is most clearly demonstrated by the fact that most of the accident-concentrating road elements were located at relatively low elevations within the study area (see Figures 2.1-2.3), and in contrast, high elevations areas such as the summit of Reisenauer Hill exhibited few accidents. This may be partially due to the general tendency of snow, for example, to accumulate across the entire study area; there is only a limited amount of time when snow accumulates solely at higher elevations. This would make the weather influence on accidents more uniform across the study area, so that road characteristics would dominate the spatial distribution of accidents. Furthermore, plowing removes snow from road surfaces across the study area even when spatial variability due to differential accumulation or melt occurs. This also would tend to produce uniformity of the weather influence across the study area, again allowing road characteristics to dominate the accident locations.

Thus, given the significance of road characteristics over spatial distribution of weather in controlling accidents, the best metric for comparing the relative safety of different road alternative would be based on road characteristics alone. All of the proposed alternatives are designed in accordance with current AASHTO standards, with the exception of the “no-build” alternative, and therefore will improve the road alignment characteristics and significantly reduce weather and non-weather related accident potential relative to the existing US 95. An analysis of the relative safety of each alternative has been conducted in accordance with AASHTO criteria and is reported in the ITD safety analysis (Arnzen, 2013).

References Cited

Abramovich, R., M. Molnau, and K. Craine (1998), Climates of Idaho, University of Idaho Cooperative Extension System, College of Agriculture, Moscow, Idaho.

Arnzen, C. J. (2013), *US-95 Thorncreek Road to Moscow AASHTO Highway Safety Manual Analysis on Alternatives Carried Forward*, ITD, September 3, 2013

Barry, R. G. (1992), *Mountain Weather and Climate*, 2nd ed., Routledge, New York, 402 pp.

Blackketter, D.M., R. Qualls, and G. Corti, (2006), Wind Study for the Proposed Highway 95 between Thorncreek and Moscow Idaho, Final Report to the Idaho Transportation Department, January 15, 2006.

Carruthers, D.J. and T. W. Choularton (1983), A model of the seeder-feeder mechanism of orographic rain including stratification and wind-drift effects, *Q.J. R. Met. Soc.*, 109, 575-88.

Chow, V. T., D. Maidment, and L. Mays (1988), *Applied Hydrology*, McGraw-Hill, New York, 572 pp.

Day, R.L. (1968), A microclimate profile between the Snake River Canyon and Clearwater Mountains, Idaho, Research Technical Completion Report, Project A-012-Ida, Water Resources Institute, University of Idaho, Moscow, Idaho, September, 1968.

Draft Environmental Impact Statement (DEIS) and Section 4(f) Evaluation US-95 Thorncreek Road to Moscow (November 2012), FHWA-ID-EIS-12-01-D.

Dutton, J. A. (1986), *The Ceaseless Wind An Introduction to the Theory of Atmospheric Motion,* Dover Publishing, 617 pp.

Iribarne, J. V., and W. L. Godson (1981), *Atmospheric Thermodynamics*, Geophysics and Astrophysics Monographs, 2nd ed., D. Reidel Publ. Co., Boston, 259 pp.

Kattelmann, R. and K. Elder (1993), Accumulation and ablation of snow cover in an alpine basin in the Sierra Nevada, USA, in *Snow and Glacier Hydrology (Proceedings of the Kathmandu Symposium, November, 1992)*, Ed. G. J. Young, IAHS Publ. no. 218, 297-308.

Lauscher, F. (1976), Weltweite typen der Hohenabhangigkeit des Niederschlags, *Wetter u. Leben*, 28: 80-90.

Linacre, E. (1992), *Climate Data and Resources A Reference Guide*. Routledge, New York, 366pp.

Molnau, M. (1995), *Mean Annual Precipitation Map of Idaho, 1961-1990*, Idaho State Climate Services, University of Idaho, Moscow, Idaho.

Pomeroy, J. W. and D. M. Gray (1995), *Snowcover Accumulation, Relocation and Management*, National Hydrology Research Institute Science Report No. 7, Saskatoon, Canada, 144 pp.

PRISM Climate Group (2012), Oregon State University, Corvallis, OR (http://www.prism.oregonstate.edu/)

Qualls, R.J., and W. Zhao (2005), Final Report for Weather Analysis of Proposed Realignments of U.S. Highway 95, Thorncreek Road to Moscow, Prepared for the Idaho Transportation Department.

Qualls, R. J., (2006), Response to Public Comments on Qualls and Zhao (2005) "Final Report for Weather Analysis of Proposed Realignments of U.S. Highway 95, Thorncreek Road to Moscow", Prepared for the Idaho Transportation Department, March 29, 2006.

Qualls, R. J., (2012), *Safety Analysis of the Weather-Related Accident Potential for the Existing US Highway 95, Thorncreek Road to Moscow, and Three Proposed Alternatives, W-4, C-3 and E-2*, Report prepared for the Idaho Transportation Department, Project # DHP-NH-4110 (156), Key # 9294, Thorncreek Road to Moscow, Ph 1, January 10, 2012.

Smith, R. B. (1982), A differential advection model of orographic rain, *Mon. Wea. Rev.,* 110, 306-9.

Appendix A

Instrumentation

1. Solar Radiation ---- Kipp & Zonen QMS 101 SP *LITE* Pyranometer. http://www.kippzonen.com/pages/6/3/Pyranometers
2. Wind Speed & Direction ---- Vaisala WMS301 Combined Wind Sensors. http://www.vaisala.com/businessareas/instruments/products/wind/wm30
3. Temperature & Humidity ---- Vaisala HMP45D Humidity and temperature probe. http://www.vaisala.com/businessareas/solutions/roadandrailweather/products/roadandrailatmosphericinstruments/hmp45dhumidityprobe
4. Snow Depth ---- Campbell Scientific, Inc. SR50-L Ultrasonic Distance Sensor. http://www.campbellsci.com/sr50-l The snow depth sensor emits an inaudible sound pulse that bounces off the surface below the sensor and reflected back to the instrument. The travel time of the signal is used to measure the distance to the surface below the sensor. This distance can be subtracted from the distance between the sensor and the ground surface to calculate snow depth.
5. Precipitation and Visibility ---- Vaisala PWD12 Present Weather Detector. http://www.vaisala.com/businessareas/solutions/hydromet/products/sensors/sensorsformaws/presentweather/pwd Precipitation and fog were measured with a Vaisala Present Weather Detector (PWD12), which is a forward-scattering light sensor. The instrument emits light into a "detector volume" of air between its transmitter and its receiver. The direction of the beam of light is angled slightly off the axis between the transmitter and receiver. Under clear conditions, the beam of light passes through the detector volume unscattered and nothing is detected by the receiver. When water droplets from rain, snow, fog, etc., are present in the detection volume, light is scattered into the receiver. Signal processing algorithms distinguish between fog and precipitation, and together with ancillary measurements on the PWD12, the instrument distinguishes between different forms of precipitation. Output includes visibility distance (33 feet to 6560 feet) due to obstructions by fog or other particulate matter, precipitation type (slight, moderate, or heavy rain, snow, or frozen precipitation), intensity (in/hr, mm/hr), and liquid water depth accumulation (inches, mm).
6. Validation Raingage at WC---- Campbell Scientific, Inc. TE525WS-L Tipping Bucket Rain Gage. http://www.campbellsci.com/te525ws-l

Precipitation, Fog and Snow Description

Precipitation Rate (inch/hr, mm/hr) and accumulation (inch, mm) are given in equivalent liquid water depths (i.e., snow is converted to melted depth of liquid water). This measurement is made using the PWD12 visibility distance sensor described below. The sensor measures the scattering of light by hydrometeors (raindrops, snowflakes, etc.) and converts this to volume of droplets within the sensing volume, and then to precipitation rate. It is able to distinguish between liquid and solid precipitation and convert to equivalent liquid water depth. In order to verify the accuracy of this sensor, we installed a standard eight inch tipping bucket raingage at the WC site at the beginning of February and allowed it to run continuously throughout the data collection period. Figure 1 shows that the rainfall accumulation reported by the PWD12 exceeded that of the tipping bucket raingage by 0.4 inches out of a total accumulation of 7.7 inches, which was within six percent of the tipping bucket raingage accumulation after four months of operation. Within this time period, the PWD12 tracked the tipping bucket raingage well, demonstrating that the difference between the two instruments was consistent over time. Tipping bucket raingages are known to under-catch rain in windy conditions. Furthermore, since the tipping bucket records precipitation in increments of 0.01 inches, up to 0.01 inches of precipitation may remain in the tipping bucket at the end of each rain storm. This excess amount may evaporate out of the tipping bucket prior to the next rainfall, and therefore never gets recorded. This also results in the under-catch by the tipping bucket raingage, indicating that the true precipitation accumulation should be larger than what is recorded by the tipping bucket. The record of the PWD12 exceeds that of the tipping bucket raingage, which indicates that it differs from the tipping bucket raingage in the correct direction; the true value of precipitation should exceed that recorded by the tipping bucket raingage.

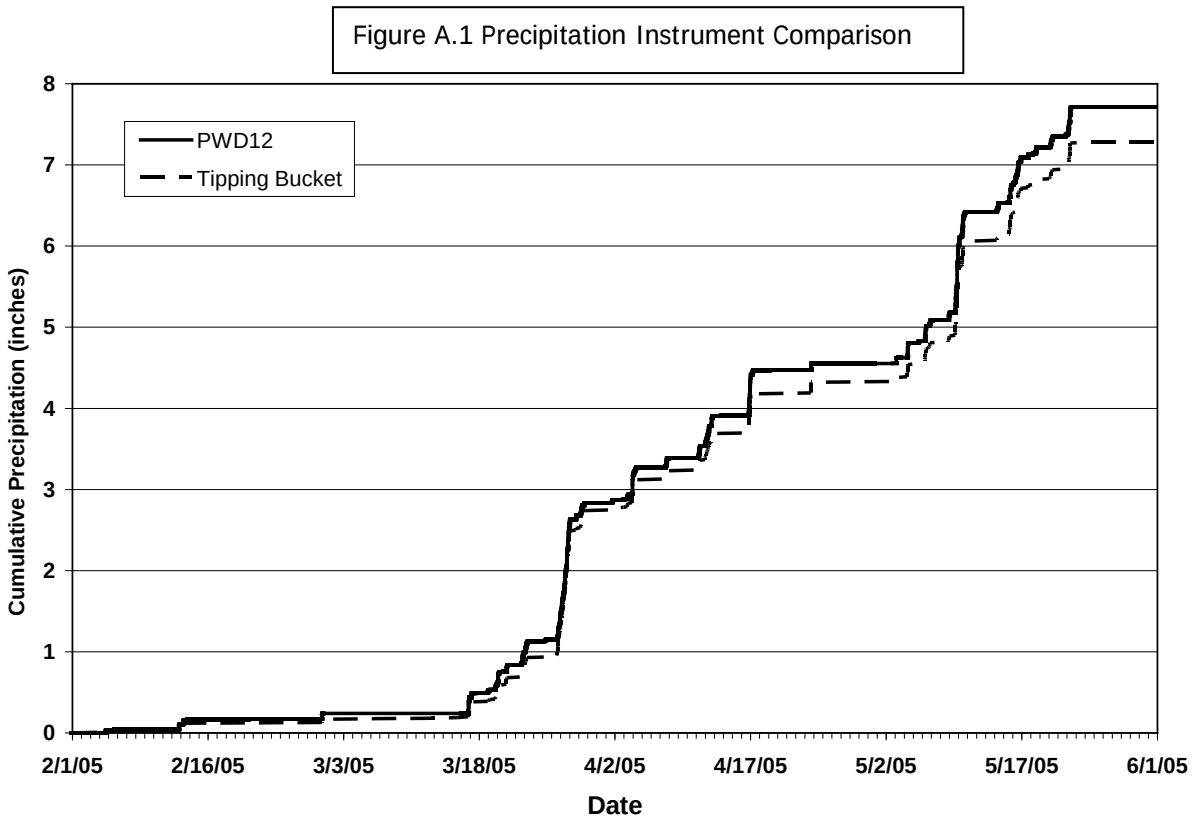

Figure A1. Comparison of Visibility and Present Weather Sensor (PWD12) with tipping bucket raingage at the WC site.

The visibility distance sensor measures the density of water droplet particles within a small volume near the instrument, by passing a beam of light through the volume, and then measuring how much light is scattered up toward a receiving sensor. Signal processing is used to convert this measurement to a visibility distance, reported in meters.

The snow depth sensor emits an inaudible sound pulse that bounces off the surface below the sensor and is reflected back to the instrument. The travel time of the signal is used to measure the distance to the surface below the sensor. This distance can be subtracted from the distance between the sensor and the ground surface to calculate snow depth.